Development and evaluation of a simulation-based adaptive shading control for complex fenestration systems

vorgelegt von
Dipl.-Phys.
Angelina Katsifaraki

von der Fakultät IV - Elektrotechnik und Informatik
der Technischen Universität Berlin
zur Erlangung des akademischen Grades

Doktor der Ingenieurwissenschaften
-Dr.-Ing.-

genehmigte Dissertation

Promotionsausschuss:

Vorsitzender:	Prof.Dr.-Ing.Stephan Völker
Gutachter:	Prof.Dr. Werner Osterhaus
Gutachter:	Dr. Bruno Bueno
Gutachter:	Dr. Jan Wienold

Tag der wissenschaftlichen Aussprache : 26. April 2018

Berlin, 2019

"Let's build robots with Genuine People Personalities, they said. So they tried it out with me. I'm a personality prototype. You can tell, can't you?"

Douglas Adams, *The Hitchhiker's Guide to the Galaxy*

Abstract

The necessity of solar control for the fenestration systems of commercial buildings has been extensively discussed over the past decades bringing forward issues such as energy efficiency, visual and thermal comfort, privacy, visual contact to the outside and aesthetics. However, a number of problems arising from manual control has been identified pointing towards the direction of automatized systems. Such systems continuously readjust the shading configuration in order to enhance comfort and energy efficiency during the day. To effectively address visual comfort, a balance between the two opposing aspects of daylight maximization and glare protection must be found; a task requiring a number of costly and sophisticated measurement devices. Therefore, driven by considerations of visual comfort, the implementation of automatic shading control systems presents difficulties which tend to increase with the sophistication of the system. The cost and the complexity of the commissioning process due to the extensive use of sensors inhibits the commercialization of multi-variate controllers. Additionally, the installation of multiple measurement devices in the office space leads to disturbance and low acceptance of the users.

A new control system for venetian blinds and electric lights focusing on office spaces, which substitutes the illuminance sensors and luminance cameras with real-time daylight simulations, was developed to explicitly address both daylight and glare aspects. By using the Radiance-based Three-phase-method the required computational time was substantially reduced. Additionally, an optimization engine based on the principles of Fuzzy Logic was developed to evaluate the visual conditions in the room and decide on the trade-off between the horizontal and vertical illuminance before applying a shading configuration. Considerations of view contact to the outside, thermal comfort in the sense of overheating prevention, and adaptation of the system to the user wishes were taken into account to improve the overall user acceptance. For periods of low occupation, the solar heat gains, selectively accepted according to time and season, contributed to the heating and cooling energy demand reduction.

Two controller prototypes were built and tested; one in a rotatable test facility at Fraunhofer ISE in Freiburg, Germany, and a second one in a real-life office in the same area. The purpose of the first prototype was to evaluate the accuracy with which the simulations predicted the horizontal and vertical illuminances in the room and to test and tune the overall operation of the controller. The second prototype was created to test the compatibility of the system with already existing components and to evaluate the user acceptance and the adaptation process under real-life operation conditions. An additional motivation was to identify weaknesses of the system perceived by a user unfamiliar to the control algorithm. To further investigate the potential of the controller a case study was conducted. Its purpose was to show the benefits of the new simulation-based controller over other shading control strategies and theoretically evaluate the reliability of the developed algorithm.

The prototype testing revealed a well operating open-loop system and a good agreement between the simulated and the measured illuminance values. Although during normal operation the positioning accuracy of the system was reduced, the overall visual comfort in the room, defined by glare control and daylight provision, remained within the acceptable limits. During the real life testing the performance of the controller was considered an improvement over the previously installed system and despite the shortcomings due to the age and restrictions of the existing components the defined conditions were fulfilled.
The theoretical comparison of the system showed the potential of important energy reductions in relation to other shading control strategies in combination with an improved glare control mechanism. However, the benefits of the glare control were found to depend greatly on the shading device used since perforated or specular reflecting systems were incompatible with the developed algorithm. By including any obstacles ain the surroundings of the installation site in the controller simulation the controller adjusted its operation in order to avoid any unnecessary window coverage and to improve the daylight admission in the room.

Kurzfassung

Die Notwendigkeit für Sonnenschutz im Fensterbereich von Geschäftshäusern wurde während der letzten Jahrzehnte umfassend diskutiert. Dies brachte wichtige Themen wie Energieeffizienz, visueller und thermischer Komfort, Privatsphäre, Sichtkontakt nach außen und Ästhetik hervor. Allerdings ergeben sich etliche Probleme aus der manuellen Steuerung der Sonnenschutzsysteme, wodurch automatisierte Systeme verstärkt im Fokus sind. Solche Systeme stellen das Sonnenschutzsystem im Tagesverlauf ein, um Komfort und Energieeffizienz zu verbessern. Um richtig auf den visuellen Komfort einzugehen, muss man das Gleichgewicht zwischen der Tageslichtmaximierung und dem Blendschutz bestimmen, die zwei gegensätzlichen Aspekte sind. Dies erfordert üblicherweise eine Vielzahl von teueren, anspruchsvollen Messgeräten. Daher gibt es, bei Berücksichtigung des visuellen Komforts, verschiedene Schwierigkeiten und eine zunehmende Komplexität automatisierter Systeme. Die Kosten und die Komplexität des Inbetriebnahme-Prozesses behindern die Kommerzialisierung von multivariaten Steuerungen, bedingt durch die umfangreiche Nutzung von Sensoren. Außerdem, führt die Installation von vielen Messgeräten in Büros zur Störung der Nutzer und eine geringe Akzeptanz .
Ein neues Steuerungssystem für Jalousien und künstliches Licht in Büros, dass die Messgeräte für die Beleuchtungsstärke durch aktuelle Tageslichtsimulationen ersetzt, wurde entwickelt, um die zwei Aspekte Tageslicht und Blendung direkt anzusprechen. Unter Anwendung der Radiance-basierten Three-Phase-Methode, wurde der Rechenaufwand erheblich verringert. Außerdem, wurde eine Optimierungs-Engine basierend auf dem Prinzip von Fuzzy Logic entwickelt. Damit beurteilte der Controller die visuellen Bedingungen des Raumes und entschied über den Kompromiss zwischen der horizontalen und vertikalen Beleuchtungsstärke, bevor er die Jalousieposition einstellte. Die Aspekte Sichtkontakt nach außen, thermischer Komfort, d.h. Überhitzungsschutz, und Adaptierung an die Präferenzen des Nutzers wurden berücksichtigt, um die Benutzerakzeptanz zu verbessern. Bei Abwesenheit des Nutzers trugen die solaren Wärmegewinne, die gemäß der Tageszeit und der Jahreszeit zugelassen wurden, außerdem zur Verringerung des Energiebedarfs für Heizung und Kühlung bei.
Zwei Prototypen wurden aufgebaut und überprüft. Ein Prototyp wurde in eine drehbare Testanlage am Fraunhofer ISE in Freiburg, Deutschland, installiert und der andere in einem echten Büro im selben Gebiet. Der Zweck des ersten Prototyps war die Genauigkeit der Simulationen zu beurteilen, mit dem die horizontale und vertikale Beleuchtungsstärke im Raum berechnet wurde, und den Gesamtbetrieb der Steuerung zu überprüfen und zu kalibrieren. Der zweite Prototype wurde aufgebaut, um die Kompatibilität des Systems mit bereits bestehende Komponenten zu überprüfen und die Benutzerakzeptanz und Adaptierung unter realen Bedingungen zu bewerten. Eine weitere Motivation war das Erkennen von Schwächen des Systems durch Nutzer, die nicht mit dem Regelalgorithmus vertraut waren. Um das Potential des Controllers weiter zu untersuchen, wurde eine Fallstudie durchgeführt. Ihr Zweck war die Vorteile des Controllers gegenüber anderen Regelstrategien zu zeigen und die Zuverlässigkeit des entwickelten Algorithmus theoretisch zu bewerten.
Die Erprobung des Prototypes zeigte eine funktionierende Steuerung und eine gute Übereinstimmung der Simulationsergebnisse und der Messwerte auf. Obwohl während des Normalbetriebs die Positioniergenauigkeit der Jalousien reduziert war, blieb der visuelle Komfort im Raum insgesamt, zusammengesetzt aus Blendschutz und Tageslicht, in akzeptablen Grenzen. Während der Erprobung im Büro, wurde das

System als eine Verbesserung gegenüber dem bereits installierten System bewertet. Trotzt des Alters und weiteren Einschränkungen durch die bereits vorhandenen Komponenten, wurden die festgelegten Bedingungen erfüllt. Der theoretische Vergleich der Systeme zeigte das Potential zur Energieeinsparung im Verhältnis zu anderen Regelungsstrategien zusammen mit einem verbesserten Blendschutz. Allerdings hingen die Vorteile beim Blendschutz in hohem Maße von den eingesetzten Jalousien ab, da die perforierte oder die spiegelnde Komponenten mit dem entwickelten Steueralgorithmus nicht kompatibel waren. Durch Berücksichtigung von Hindernissen in der Umgebung des Installationsorts in der Simulation, passte der Controller seinen Systembetrieb an, um die unnötige Fensterverdunkelung zu vermeiden und den Tageslichteinfall zu verbessern.

Acknowledgements

The current work has been conducted at Fraunhofer ISE which provided the scientific environment, the financial and the technical support necessary for the realization of this project. The controller presented in this dissertation thesis was designed within the Tageslichtverbund Project, financed by BMWi.
I want to thank Tilmann Kuhn for giving me the opportunity to do my PhD as a member of his group at ISE and my supervisor Bruno Bueno for his guidance and support during this time.
Many thanks to Jan Wienold and Martine Knoop for guiding and inspiring me, and for providing valuable insight into my work.
I also want to thank Stephan Völker for accepting me as a doctoral student at TU Berlin and Werner Osterhaus for joining my committee at such a short notice.
I would further like to thank ELERO for providing the SMI motors installed at the first test installation.
Special thanks to Peter Engelmann for offering measurement equipment used at the installations and for guiding me through its application.
Many thanks to Dennis Freiberger and Christof Wittwer for helping me set up the two installations and having them running in time.
Many thanks to Gernot Finselbach andUnmüssig for allowing me to test my second control prototype in their offices at Berliner Allee in Freiburg.
Moreover, I would like to thank all the colleagues and friends at ISE for supporting me with their feedback and their technical knowledge.
Many thanks to Simon Häringer for patiently reading and correcting my German.
My deepest thanks to Johannes Hanek who supported me not only with his technical knowledge and his resourcefulness but also with his optimism and cheerful disposition during the cloudy days.
Many thanks to Antonis Manousakis for helping me out with LATEX, without his help this document would have been just letters and pictures in random places.
I want to deeply thank Semina Angeli who was there for me at every step of the way and not only supported me psychologically but also gave perspective and a fresh view when I needed it the most.
Many thanks to Manolis Katsifarakis who was never too busy to answer my programming questions and un-stuck me at times of crisis.
Sophia, Nadine and Lukas, thank you guys for looking after me during this time.
Last but not least, I want to thank my parents who stood patiently by me, supported me in every possible way and inspired me to be the best I could.

Contents

List of Tables

Chapter 1

Introduction

From the antiquity to the dawn of the 21st century windows have always been an indispensable part of building design contributing to the regulation of indoor conditions such as interior lighting, ventilation, heating and cooling. Throughout the centuries the design of fenestration systems has changed significantly to address the needs of the users, often reflecting the sociopolitical and technological conditions of the era.
Such examples are found when looking back to the 19th century as the industrial revolution led a large amount of the rural population towards large cities. Due to the explosive growth of commerce the number of workers in clerical and administrative positions also increased introducing a new building classification; the *office buildings*. Although electricity was already available at the time, the high cost of light bulbs and energy made artificial lighting an exotic method of illumination. Looking back to the design of multi-occupant office buildings until the beginning of the 20th century one can observe large window areas combined with narrow office spaces to allow maximum penetration of daylight [1]. Over the following decades this trend changed promoting smaller windows; however, recent considerations of energy efficiency and welfare have influenced the architectural trends once more towards maximising daylight admission.
According to the European Commission, buildings in EU are responsible for 40% of the total energy demand in Europe. It has been further noted that by just improving the energy efficiency of the existing buildings a reduction over 5% of the total energy consumption is foreseen [2]. Several studies have shown a correlation between daylight utilisation and artificial light energy demand. Already in the '70s Ne'eman et al. [3], motivated mainly by considerations of visual comfort and wellbeing of the occupants, carried out a report for the British Department of Environment in which they developed a method to specify the daylighting requirements of four types of buildings; housing, schools, hospitals and offices. In their methodology considerations such as user activity patterns, geographical location, orientation, window geometry, and shading methods were taken into account in order to define the maximum and minimum sunlight penetration hours. Hunt [4] pointed out that the use of electric lighting in office spaces can be reduced by increasing the admission of daylight in the room. Choi et al. [5] investigated the potential of increased daylight admission in energy savings from reduced light energy demand in office buildings, also taking into account the probability of increased cooling demand due to excessive solar heat gains by varying the window apertures for different climates. Apart from the energy savings, many studies also described the positive physical, physiological and psychological effects of daylight. Among the multiple benefits of daylight admission in buildings is its contribution to the regulation of the circadian rhythm of the occupants [6] that common artificial lighting sources fail to offer. Moreover, a positive correlation between sunlit spaces and occupant performance in

schools, offices and retail stores has also been observed [7, 8]. Other benefits of sunlit spaces have been investigated in different works with the recent example of Choi et al. [9]. In their work they investigated the impact of indoor daylighting on a number of patients in a health care facility revealing a positive influence of daylight in the psychology of the patients resulting to further improvement of their physiology.

1.1 Shade control systems

Need for shade control - Limitations of manual control

Despite the many advantages of daylight admission in buildings, solar control is also necessary for various reasons. To begin with, and with our focus on commercial buildings, the unrestricted introduction of daylight into interior spaces can cause uncomfortable visual conditions of increased glare that induce the opposite effects on the satisfaction and, as a result, on the productivity of the users [10].
Rea [11] studied the patterns of manual shading control in offices and observed that the shades were more frequently used at the south oriented offices during the direct radiation hours. The assumption that the occupants used the shading device in cases of increased direct radiation in order to mitigate uncomfortable glare situations was further verified in a number of studies [12, 13].
Apart from the visual comfort, the selective acceptance of solar heat gains also improves the energy efficiency of the building offering substantial reductions in cooling and, potentially, heating energy demand. Coldicutt and Williamson [14] made a strong case for using solar heat gains to reduce energy demand in buildings and enhance user satisfaction. Santamouris et al. [15] studied over 186 representative offices in Greece and found out that heating, cooling and lighting accounted for over 70 % of the total energy consumption. In their conclusions they estimated that daylight admission can significantly reduce lighting and possibly also effect heating energy demand. Additionally, the use of appropriate shading could cause further reductions to the cooling energy demand of the buildings. Kuhn et al. [16] outlined the importance of sun shading systems for enhancing both visual and thermal comfort and developed a new method to evaluate the thermal performance of a shading system based on its Solar Heat Gain Coefficient (SHGC); otherwise known as g-value.
Despite the numerous benefits that shading systems offer, it has been proven that when the users apply shading inappropriately not only do they fail to increase the energy efficiency of the building but also sometimes induce to opposite effects. That comes as a result of the irregular manner in which the users tend to interact with the shading and lighting system. Such actions are often motivated by personal reasons like the need for privacy, mood or special requirements of room conditions, rather than visual comfort or energy efficiency.
It has been shown that users react with the shading system only under very uncomfortable situations such as high incoming radiation and leave the system unaltered the rest of the time. That is a result of a perception formed over long periods rather than a response to current conditions of weather or daylight [11, 12, 17]. Hunt [4] drew a similar conclusion concerning the users interacting manually with electric lights, according to which the users would switch the lights on upon their arrival, if necessary, but rarely switch them off when they were no longer needed.
Both of the assumptions above have been reinforced by a more recent work carried

out by de Silva et al. [13], who monitored 8 single occupied offices in Portugal in order to evaluate the shading and electric light usage habits of the occupants. According to their findings, daylight and glare metrics predicted in a better way the shading deployment patterns of the users, while quick changes in the illuminance did not often trigger manual reactions. However, most of the user reactions seemed to be motivated mainly by miscellaneous reasons and occupancy patterns rather than optimisation of the interior conditions. Finally, the electric light patterns seemed to agree well with the findings of Hunt, about the users reacting to low illumination by switching on the electric light and rarely reacting the other way round. To overcome the limitations of manual shading control, the idea of automatic control systems has become increasingly popular over the past few decades.

Automatic shade control principles

For the core definition of a control system one can consider the interconnection of components that can be characterised as a cause and effect relationship. In an automatic control a dynamic system model is described, in which a variable is controlled in a prescribed manner according to an actuating signal. The actuating signal can be a number of variables; the *inputs*. The controlled variable refers to the output of the control for specific inputs and will be hereafter referred to simply as *output*. Systems in which many variables can be controlled simultaneously based on a number of inputs are called *multivariable*.
The control systems can be classified in different ways depending on the relationship between their inputs and outputs, their dependence on time, and their structure. If the control output varies linearly with the input, the system is characterised as a *linear* control system. Although linear systems practically do not exist, many complex systems are idealised through assumptions for simplicity of analysis and design purposes. Moreover, if the magnitude of the inputs is within an area where the system exhibits linear characteristics, the system is also treated as a linear one. In an opposite situation, the system is characterised as non linear. Depending on its dependence on time the system can be either time dependent or time invariant. Finally, the automatic control systems can be categorised based on the process they follow to:

- open-loop control
- closed-loop control
- feed forward control

Open-loop control

Open-loop controls are the systems where the controller receives the inputs, processes them and returns the optimal output which is applied directly. The application of such systems requires that there is an excellent knowledge of the dynamic system model and that the control signals can be applied with high precision. The disadvantage of these systems is that they are susceptible to external disturbances and they are likely to fail in the case of unforeseen events. (Figure 1.1)
The electric clothes dryer is a typical example of an open-loop system. Depending on the amount of clothes or how wet they are, the operator sets the timer to say 30 minutes. After this time the drying process will stop regardless on whether the clothes are still damp.

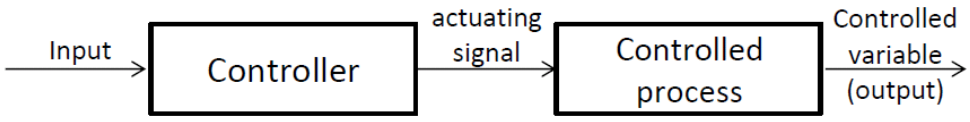

FIGURE 1.1: Open loop control flow chart

Closed-loop control

Closed-loop or *feedback controls* are the systems that correct their signal internally by receiving frequent measurements of the output and comparing them with a tracking reference. When the difference between the output and the reference grows to unacceptable levels the controller acts correctively and adjusts the control signal in real time. The closed-loop systems can be adaptive and very effective when there are many uncertainties connected to the system model or when unforeseen disturbances are anticipated. However, the system process itself is irrelevant and the controller only responds reactively at a single time-step basis to reduce the output deviation. (Figure 1.2)
As an example for a closed-loop controller let us consider again the electric clothes dryer from the open-loop controller. In this case a sensor is used to monitor the actual dryness of the clothes which is compared with the input reference. The error signal, defined as the difference between the required dryness and the actual dryness, is amplified by the controller. In this way the controller makes the necessary corrections in temperature or drying time to reduce this error.

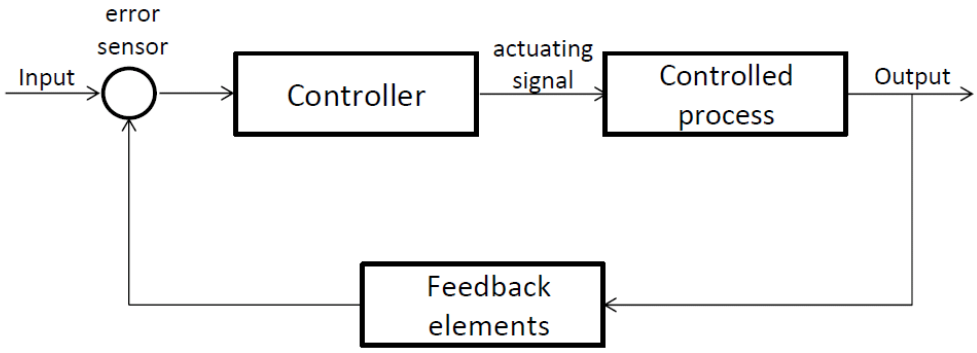

FIGURE 1.2: Closed loop control flow chart

Feed-forward control

Feedforward controls are the systems that at the introduction of the inputs, if external disturbances are measured, can react in a number of predefined manners to address the current situation. The feedforward controls are very similar to the open-loop controls in the sense that they receive no feedback from the output signal and are

therefore rather inflexible to unpredicted circumstances. However, when used in combination with a feedback control they can provide more reliable and flexible systems under conditions of high uncertainty.

A literature review to automatic shade and light controls

As mentioned earlier, the manual regulation of shading devices and electric lights fails to deliver in full the energy saving potential that the utilization of solar radiation can offer. To address this multivariate problem, numerous systems have been developed with focus on both comfort and energy efficiency. More specifically, the goals of systems addressing the shade and lighting can be distinguished in three categories:

- Visual comfort including sufficient daylight, glare prevention and view out
- Thermal comfort by rejection of excessive solar gains that might lead to space overheating
- Energy efficiency by utilising solar radiation in order to decrease heating, cooling and lighting energy demand

Although energy efficiency and visual comfort in buildings is in general a subject of high interest, the majority of the research work concerning automatic control systems focuses on commercial buildings; mainly due to the more strictly defined activity patterns of the occupants. Additionally, the visual and thermal comfort in the working space is a matter of great importance on grounds of both productivity and worker well-being. For all these reasons, the following review of research on automatic shading and lighting control focuses on commercial buildings.
The earliest attempts of automatising a shading control were made during the 80's. Inoue et al. [17] developed an automatic control for blinds with focus on visual comfort based on a series of observations of four high rise buildings located in Tokyo, Japan. Through these observations, the blind occlusion was for the first time correlated with the sunlight penetration depth in the room, for direct radiation on the window exceeding the threshold of 50 W/m^2.
Zhang and Birru [18], following the same idea of manipulating the depth of daylight penetration to maximise the daylight in a room, proposed an open-loop control for venetian blinds applicable to various shapes of slats. When the vertical illuminance at the exterior of the facade exceeded a prescribed threshold, the controller was activated and the position of the shading device was calculated based on an analytical solar angle model and on window geometry to block the direct solar component. Koo et al. [19] developed the concept a bit further by calculating the solar penetration at both the vertical and the horizontal plane. In this way, the daylight penetration into the interior space was optimised while glare due to direct solar radiation was prevented.
Although the above mentioned models allowed an efficient direct radiation control by blocking the direct solar component from office spaces, they required a high-precision commissioning for differently controlled spaces based on the detailed knowledge of the user sitting positions. To approach the problem in a different way, a number of control systems based on sensors has been developed over the years. Lee et al. [20] created an open-loop prototype shading control for venetian blinds synchronised with a dimming light system based on the measured average work plane illuminance. The system was installed in two private offices in California and was monitored over the course of a year in terms of electric lighting and cooling load. The

monitored performance was satisfying most of the time in terms of work plane illuminance measured by ten illuminance meters distributed around the defined work plane area. Additionally, substantial reductions were measured for the lighting and cooling energy demand. Lee and Selkowitz developed and tested a control system for roller shades combined with a dimming electric light for the Headquarters of the New York Times [21]. The controlled space was separated into two zones and two different shade control strategies were investigated; one based on the window glare and work-plane illuminance and one focusing on blocking the direct solar radiation. The shading control that was later installed at the site [22] aimed only to the reduction of the window glare based on the average window luminance measured by a high dynamic range (HDR) luminance measurement tool. The measurement positions were chosen in order to cover the worst case scenarios for glare in the open plane office. By monitoring the system a good performance in terms of both energy efficiency and glare control was observed.
The control of solar heat gains, on grounds of both thermal comfort and energy efficiency, has been often included in automatic systems like the one developed by Oh et al. [23] for double-sided internal venetian blinds. The system was developed and tested in Energy Plus to efficiently regulate the solar radiation through the window. The visual comfort was addressed by controlling the Daylight Glare Index (DGI) close to the window. The regulation of the solar heat gains in the building was achieved by dividing the system operation in two modes depending on the season, taking advantage of the different reflectance on the two sides of the blinds.
In his recent work, Konstantzos et al. [24] investigated the correlation of vertical illuminance at the eye level of the user with the Daylight Glare Probability (DGP) and the simplified DGP (DGPs). Based on that, they developed a model-based, real-time glare control for roller shades that would prevent direct radiation from reaching the work plane area while maintaining the work plane illuminance below a prescribed threshold.
Since comfort is a subjective feeling and cannot be easily quantified by measurement, its definition has been proven rather complicated. To address this problem, research has turned towards fuzzy logic for the optimisation of the control of systems taking numerous variables under consideration. Visual comfort has been addressed in different studies which developed fuzzy logic controllers taking irradiance and/or illuminance measurements into account for the control of shading devices [25, 26]. A more global approach for shading, lighting and HVAC control has also been adopted in a number of studies which developed fuzzy controllers combining illuminance levels, glare and thermal comfort parameters to address both visual and thermal comfort and energy savings [27, 28, 29].
Although the use of sensors ensures the accuracy of the inputs, their commissioning tends to cause problems not only due to the high installation costs but also due to aesthetic and functionality considerations. The installation of multiple sensors in an office space interferes with the interior design of the room and gives the impression of a test facility. Moreover, illuminance measurements on the work-plane might be influenced by the user's activities causing irregular readings, affecting the system's operation. Due to the above, interest has been taken in simulation based controllers. The calculation of indoor illuminance using numerical simulations has been a popular approach. By eliminating the need of expensive equipment such as HDR cameras for glare evaluation glare can be directly expressed through the DGP or the vertical illuminance. Ray-tracing methods have been used to calculate both metrics very effectively [30, 31].

Although the precision with which a controller manages a shading device to improve the visual comfort is of high priority, it is not certain that it can achieve the satisfaction of the users who might reject the system if they feel limited as to the control they have on their own working environment. As Vine et al. [32] concluded in their study with office workers at offices with automatically controlled blinds and lights, the workers were more satisfied in general when they could manually control the conditions in their workspace. Bakker et al. [33] reached a similar conclusion according to which users tended to judge the automatic system more favourably when they had influence over it. In the same study, the users also noted that the frequent readjustments of the shading device, no matter how smoothly they were applied, were distracting. Instead, more seldom and discrete transitions in the facade configuration were preferred.
Such findings led to the development of user adaptive systems to improve user acceptance. Guillemin and Molteni [34] developed a control system for roller shades which used genetic algorithms in order to adapt its function to the interactions of the users while remaining energy efficient. The controller stored every interaction of the user with the system and used them to adapt its process once per day based on a method simulating the gene mutation and propagation process. Another user adaptive controller for blinds and lights was developed and tested by Gunay et al. [35] based on a ceiling-mounted photosensor. The developed system used a recursive algorithm in order to develop discrete-time Markov logistic regression models and predict the user behaviour.
Lindelöf [36] used a different approach based on Bayesian probabilities to develop a user-adaptive system for small offices. The user adaptation was carried out by using an algorithm to estimate the visual discomfort of the user in a probabilistic manner. The algorithm used the illuminance distribution in the room before and after the user interactions, under the assumption that the conditions were uncomfortable right before the user took action and the desired conditions were set right after. In this way, the Bayesian algorithm inferred the probability of visual comfort or discomfort at every given situation.

Commercial systems

At the available commercial shading devices one can find a wide variety of types and shapes of shading systems for internal or external installation, residential or commercial application. These systems are usually accompanied by some kind of automatic control that ensures comfort and energy efficiency. Moreover, wrapped up to a user friendly interface, control systems are often available at the user's mobile phone to ensure user's acceptance and satisfaction. Additionally, a variety of sensors is available for supporting the shading control and monitoring the conditions inside and outside the installation. A market review of the available commercial shading control systems has been carried out with focus on the leading companies in the field. The available control systems are summarised in Table 1.1 for the two most popular shading devices; horizontal slat-type shades and roller shades. The additional features of each system are also included for a more complete overview of the automated system availability.

Feature	Slat-type shades	Roller shades
Programmed events (time-based, season based, occupancy-based)	✓	✓
On-off depending on sensor measurements (photo-sensors, irradiance, temperature etc)	✓	✓
Controlled daylight penetration depth (based on variable shade height)	✓	✓
Sun-tracking system (according to the solar profile angle)	✓	-
Building surroundings information (taking into account major obstructions around the building)	✓ (combined with the sun tracking system)	-

TABLE 1.1: Available features in commercial shade control systems

Limitations

The literature review conducted above, in combination with the results of the market research, offers a clear overview of the limitations of the existing automated shading controls explained in the following paragraphs. As far as daylighting is concerned, a lot of commercial systems use photosensors installed on the ceiling or on one of the walls in order to adjust the shading device according to the light availability in the room. Although such measurements offer an insight of the space illuminance, they do not explicitly account for the workplace horizontal or vertical illuminance that directly influences the visual comfort of the users. On the other hand, the placement of sensors on the working surface might interfere with the tasks performed and influence the measurements or cause discomfort to the user. Moreover, the excessive use of sensors reflects on the installation and maintenance cost and often interferes with the aesthetics of the office space giving the impression of a test facility.
In general, commercial systems address glare by blocking direct radiation from reaching the user. Although this approach would lead to a glare free environment the majority of the times, the glare caused by diffuse radiation, not being explicitly addressed, can in occasion also cause visual discomfort. To add to this, even if there are no direct light reflections, increased vertical illuminance on the computer screen creates haze and inhibits the visibility causing further discomfort [37]. The use of luminance meters or cameras to directly estimate glare conditions would be significantly costly and might raise privacy issues due to the camera use in working areas. As it has been already mentioned, the replacement of sensors with simulations has been successfully carried out using DGP as the metric to express glare. A strong disadvantage in this case is the necessity of an exact sitting position of the user along with one or more predetermined view directions which eventually limits the real life applications.
Finally, it is essential to address the user satisfaction since any oversight in this area might influence the user acceptance in a negative way leading to the rejection of the system. Two of the most common reasons of dissatisfaction are the user disturbance

due to frequent movements of the system and the repetition of unsatisfactory controller actions that do not take into account the subjective sense of visual comfort of the user. Furthermore, increased visual contact to the outside seems to have a generally positive influence to the user acceptance

1.2 Objectives of the thesis and methods

Within the current doctoral work, a simulation-based, self-adapting, open-loop controller applicable to various complex fenestration systems and electric lights has been developed in order to address the aforementioned problems in the following way:

- The sensors are replaced by daylight simulations to calculate horizontal and vertical illuminance at areas of interest, such as the working surface, in order to optimize the visual conditions in the room accounting for both glare and daylight penetration.
- The glare protection strategy is based on the simplified DGP which is proportional to the vertical illuminance. In this way, both glare from diffuse radiation and vertical illuminance on the computer screen are taken into account.
- The virtual sensors required for the calculation of horizontal and vertical illuminance can be assigned in a flexible way depending on the available knowledge of the room layout and the user's sitting position. If no prior knowledge of the room layout is available, the definition of the sensor grid can be based on a number of assumptions to significantly simplify the commissioning of the controller.
- Both the height of the shading device and the tilt angle of the slats are adjusted so that, for every control action, only the necessary window area is covered in order to favour view contact to the outside
- The controller calculates the optimal shade configuration internally before sending the signal to the actuators decreasing the unnecessary movements that disturb the occupants.
- Finally, the user interactions are used to adapt the controller reactions in accordance to the user preferences.

It must be noted that the structure of the system was designed in such a way as to remain transparent and to facilitate the monitoring and updating of the control process.
This thesis aims primarily to the development of a proof of concept controller based on real-time simulations and investigates the potential of an overall approach to visual comfort in a flexible and efficient way. Additional considerations of improved view out and overheating prevention are included to enhance the system functionality. Within this work, the developed controller is assessed based on its algorithm, its applicability as a real-life system and its total performance in order to determine whether it can be a viable alternative to sensor based systems.
Two prototypes are presented; one in a test facility with no pre-existing control system and one in a real life office with existing components. The objective of the former is to assess the algorithm and the simulation engine while the latter aims to the

evaluation of the system performance outside laboratory conditions by a user unrelated to system development. To add to the information received from the testing of the two prototypes, a series of simulations is used to determine the benefits of the system over other widely used control strategies. Finally, a sensitivity analysis and an evaluation of the developed glare control strategy are presented to identify the weaknesses of the daylight simulations upon which the system is based.
The overall goal of this thesis is therefore to create a solid theoretical background and a first application for the simulation-based control algorithm as a starting point for further research and for the potential development of a commercial product in the future. Based on the identified strengths, weaknesses and failing points within the existing work, clear targets and focus points will be provided to support follow-up projects in the future.

1.3 Thesis outline

In this section, the overall outline of the thesis is given chapter by chapter presenting an overview of how the presented work has been organised.
In the beginning, the control software is explained. The controller's architecture and workflow is presented followed by a detailed description of the algorithm's constituents and theory behind them (Chapter 2: System description).
The controller is described from the hardware point of view through two prototype installations built to test and evaluate the effectiveness of the control system, one in a test facility room at the headquarters of Fraunhofer ISE in Freiburg, Germany, and one in a real-life office in the same area (Chapter 3: Installation of two prototypes).
The results of the control installations are presented, organised in two sections. In the first section, the evaluation of the controller's features through measurements in laboratory conditions is carried out. In the second section, the beta-testing of the system by a user uninvolved in the system's development is described based on the questionnaires filled out by the user and on monitoring data collected during the testing period (Chapter 4: Experimental evaluation).
A comparison of the system in relation to two control strategies through annual simulations is carried out. The developed system is compared to a sun-tracking (cut-off) control and an on-off system based on global solar radiation on the building facade. The three systems are evaluated in terms of daylight provision, glare protection, average window occlusion and energy demand for heating, cooling and lighting as well as their ability to adjust to external factors such as obstructions at the site. Additionally, a sensitivity analysis of the controller's daylight simulations is presented (Chapter 5: Case study: Energetic and comfort potential).
For the evaluation of the glare control strategy, developed within the scope of the controller, a simulation-based comparison is carried out. Since the developed glare control is based on vertical illuminance, the vertical illuminance-dependent simplified Daylight Glare Probability (DGPs) is used as an indicator of the controller's performance and is compared with the enhanced DGPs for two shading devices; a simple white venetian blind system and a perforated venetian blind system. Through this comparison, the applicability of the glare control method is investigated and possible limitations related to different shading devices are identified (Chapter 6: Theoretical basis and evaluation of the developed glare control).
Closing, a general evaluation of the conducted work based on the previous chapters is presented combined with an overview of the future potentials of an improved, commercial version of the controller (Chapter 7: Conclusions).

Chapter 2

System description

2.1 Overall structure of the control algorithm

The overall structure of the control algorithm is primarily divided into two branches based on the occupancy status of the room. When the user is present the controller prioritises visual comfort, while still retaining energy-efficiency considerations by minimising the use of electric light. In situations when the threat of overheating is imminent, the controller reacts proactively to block additional solar heat gains. This action penalises view out without significantly affecting visual comfort. During the users' absence visual comfort is no longer important and the controller prioritises energy efficiency by selectively accepting or rejecting solar heat gains depending on the time of the day and the season of the year. A mid-season is additionally introduced referring to the periods when both the probability of heating and cooling demand exists. In the following bullet points the objectives of the controller are summarised for the two occupancy conditions:

Occupancy

- Visual comfort by:
  - Daylight maximization
  - Glare protection from both direct and diffuse radiation
  - Favouring view out
- Thermal comfort by:
  - Prevention of overheating
- Energy efficiency by:
  - Reduction of lighting and cooling energy demand by prevention of overheating

No occupancy

- Energy efficiency by:
  - Reduction of heating and cooling energy demand

Finally, to improve the user acceptance the controller adapts to the user preferences of visual comfort and electric light requirements expressed through interactions with the system.

2.2 Algorithm

The basic structure of the algorithm consists of four major parts: input measurements, rule-base algorithm, fuzzy logic based optimisation and output signals. The user adaptation is taking place once per day and the process is independent from the rest of the algorithm.
After receiving the inputs, the controller applies a set of rules to define the line of action that should be followed. For an occupied room with no immediate risk of overheating, determined by the room temperature and the global solar radiation on the facade, the tilt angle and height of the venetian blinds are defined based on the solar profile angle to prevent direct solar radiation from entering the room (Appendix A). The illuminance conditions in the room, under the defined window configuration in the current time-step, are calculated through the daylight simulation. The resulting values are then filtered through the optimisation engine based on fuzzy logic to evaluate the resulting visual comfort in the room. If the resulting illuminance is not in agreement with the prescribed visual comfort conditions, the daylight simulation is repeated for small variations of the blind configuration until the optimal position is found.
The entire iteration process takes place internally and only the optimised configuration is sent to the actuators to be applied on the shading device and lights. Throughout the day the user can freely interact with the system and re-adjust the shades or the light at any time. The newly defined conditions are indicative of the user's subjective sense of comfort. These interactions are saved and used in the adaptation process to change the controller's variables in order to better represent the user's preferences. The controller process is described in the form of a flow chart in Figure 2.1.

Inputs and outputs

As it has been already briefly discussed, the inputs of the controller consist of weather data, room temperature and occupation status of the room. The interior temperature is monitored to avoid using a thermal model which would introduce additional complexity and uncertainty at this early stage of the controller development.
The weather conditions include global and diffused irradiance on the horizontal plane, external temperature and wind speed. Wind speed is only used for safety purposes to avoid the damage of external shading devices if extreme weather phenomena occur. The required measurements can be taken on site, if a weather station is available, or can be downloaded from the nearest weather station. The outputs of the controller consist of two control signals for the venetian blinds; one for the extension length of the device, one for the tilt angle of the slats and one single signal for the electric light.
It is worth mentioning that in principle no illuminance measurements inside the room are necessary for the controller since they have been replaced by daylight simulations under the assumption that the accuracy of the simulated values is sufficient. However, the probability of reduced accuracy due to commissioning errors should not be ignored since it could reduce the effectiveness of the control and cause user dissatisfaction. To avoid any modelling errors, a short time monitoring or measurements on the spot could be used during the commissioning of the system.
On the other hand, a number of unaccounted external factors might also affect the daylight simulation, further reducing the required accuracy. Such factors can be

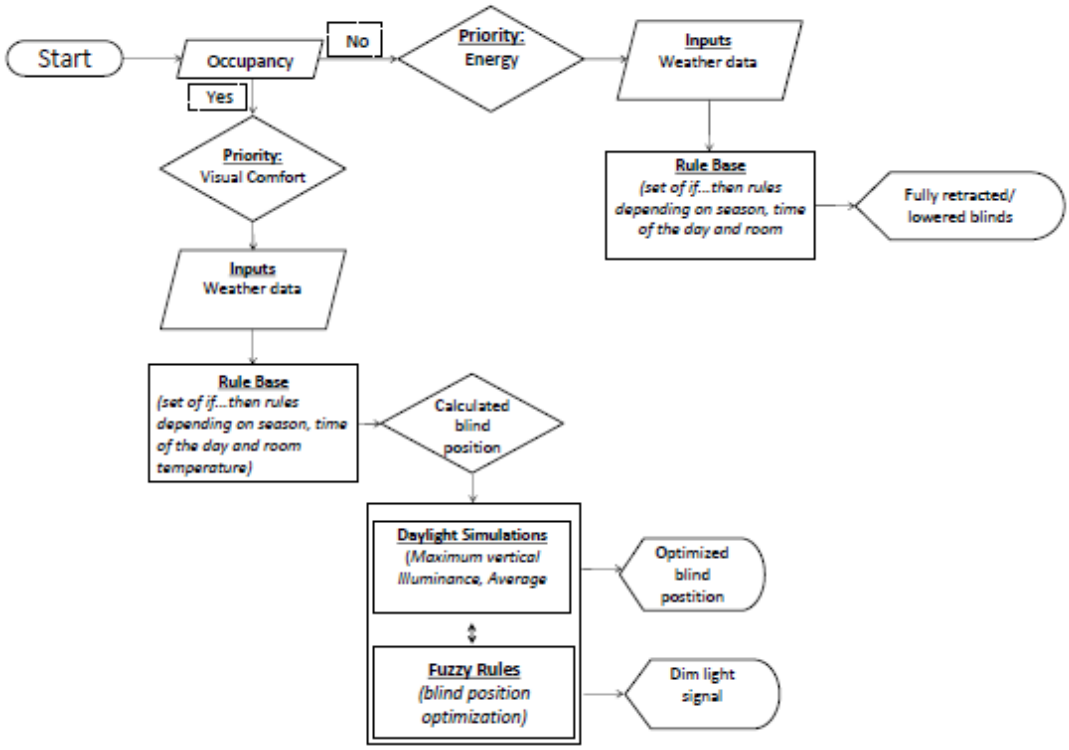

FIGURE 2.1: Work flow of the controller's process

weather related, e.g. intense snow cover increasing the ground albedo, or changes at the surroundings of the installation site, like seasonal changes of the trees or a new colour on the facade of the building across the street. Since such situations might occur after the commissioning of the system, it is useful to identify their effect on the daylight simulations in advance by conducting a sensitivity analysis and provide the possibility of further tuning for factors of high impact. Such a sensitivity analysis is carried out in the case study described in Chapter 5.

Case A: Rule-base algorithm for absent user

As shown in the workflow in Figure 2.1, the first level of control algorithm is a set of *"if ... then..."* rules dependent on room occupation, season of the year, time of the day, direct radiation on the facade and room temperature. These rules are used to define the current situation inside and outside the room in order to hierarchise the control priorities and decide on the following line of action.For an unoccupied room visual comfort is irrelevant so the energy efficiency of the building becomes first priority and the available shade positions alternate between fully closed and fully retracted blinds without any intermediate configuration. Initially, the controller defines the period of the year based on the 24-hour average external temperature. According to that, the year is separated into the heating period when the average temperature of the previous 24 hours is equal to or less than 8 °C, the cooling period when the average temperature is equal to or higher than 18 °C and the mid-period in any other case. This separation allows for a more effective rejection or acceptance of the solar heat gains to reduce the heating and cooling energy demand of the building. Although the temperatures used for the season definition can vary depending on the climate zone, the values used in this study have been chosen based on the monthly

mean temperature in Germany over the last 25 years (1991-2015), presented in Table 2.1. The prescribed temperature limits for the three seasons are defined based on the assumption that the heating season in Central Europe usually takes place between November and March while cooling is required during the summer months. In general, the temperature set-points can be set accordingly to address different climatic zones.

Jan	Feb	Mar	Apr	May	Jun	Jul	Aug	Sep	Oct	Nov	Dec
1	1.7	5.2	9.4	13.4	16.4	18.7	18.3	14.4	9.7	5.2	1.8

TABLE 2.1: Monthly mean historical temperature in Germany from 1991 to 2015 (source : sdwebx.worldbank.org/climateportal/)

After defining the season of the year, the daylight and non-daylight hours are calculated. For the heating and cooling, period the acceptance or rejection of solar heat gains is straightforward with fully retracted blinds in the heating period and fully closed blinds in the cooling period. The configuration reverses for each case during the nighttime in order to increase the insulation of the windows during the winter or allow the room to cool down during the summer. For the mid period, the behaviour of the controller needs to be flexible; therefore, the interior temperature is introduced as an additional condition in the rule-base algorithm. Under this condition, for room temperatures below 25 °C, the controller reacts according to the heating period settings, otherwise the cooling period settings are used. According to DIN V 18599 [38], the cooling set-point temperature for the working time in an office is 26 °C. Based on that, the criterion of 25 °C is used to signify that the probability of the room temperature rising at a cooling level is high and that the controller must block any additional solar heat gains to prevent any further temperature rise.

Case B: Rule-base algorithm for present user

When the room is occupied the comfort of the occupant becomes the controller's first priority and the optimisation process for the improvement of the interior visual conditions is used. The thermal comfort of the room is addressed only by prevention of overheating. The rule-base algorithm proceeds as above by defining the hour of the day and the time of the year which in this case is reduced to only two periods by merging the heating and the mid period. Since in this case the selective acceptance of the solar heat gains is not the first objective, the necessity of a mid-period becomes secondary. Instead, the cooling period is treated as a time of high overheating risk which allows the controller to react in a proactive way when the room temperature increases in the presence of high global radiation on the facade.
During the heating period, the overheating risk is low and the temperature indicating overheating is 26 °C according to the cooling set-point defined in DIN V 18599. If the room temperature rises above this point, the controller reacts directly by fully lowering the blinds and readjusting the tilt angle for optimal visual comfort. In this way, the horizontal and vertical illuminance in the room is maintained within comfort levels, while any direct radiation is prevented from entering the room in expense to improved view to the outside. On the other hand, during the cooling period the controller anticipates such situations as soon as the room temperature rises above 24 °C at conditions of high solar irradiance (global radiation on the facade exceeding 500 W/m^2) and reacts in the same way to prevent any further temperature

rise. As mentioned in 2.2.1, the room temperature is a measured value and therefore accounts for any influencing factors such as ventilation or internal gains which are therefore not explicitly addressed.
For daytime hours with no risk of overheating, the controller calculates the minimum height of the blinds to prevent direct radiation on the work surface and the cut-off angle of the slats, and optimises the final position through the iterative process described in detail in the following section. The full rule base of the controller is summarised in the matrix included in Appendix B.

2.3 Daylight Simulations

The controller incorporates a simplified version of the **Fener** simulation platform developed at Fraunhofer ISE by Bueno et al. [39]. Although one of the innovative characteristics of **Fener** is the coupling of the daylight and thermal simulations in a time step basis, for the needs of the controller, a version supporting only daylight and glare analysis is used. However, the possibility of further developing the controller in order to also take into account thermal variables remains open.
The model used in the daylight simulations is a rotatable, single-zone "shoebox" generated in a Radiance geometry format. The complexity of the scene inside the room can be in principle minimised taking only the work station into account. The surroundings of the building are also taken into account in the same geometry format if they affect the direct radiation on the facade. The degree to which the obstructions at the exterior of the building can influence the daylight simulations is discussed in Chapter 5.
The daylight simulations use the Radiance-based Three-Phase-Method [40] to estimate the solar transmission to the inside and the indoor illuminance. The Three-Phase-Method separates the light transport between the sky and the illuminance sensor points in the room into three phases, each of them simulated independently and stored in a matrix form. These three phases are: the exterior transport, expressed by the daylight matrix (D), the fenestration transmission, expressed by the transmission matrix (T) and the interior transport, expressed by the view matrix (V). At every time step the illuminance inside the room is calculated by multiplying the three matrices as expressed by the following Equation 2.1:

$$I = VTDs \tag{2.1}$$

The last term s symbolizes the sky vector which for a given time and sky condition contains the average radiance of each sky patch (Figure 2.2).

The transmission through a fenestration system is expressed by a Bi-directional Scattering Distribution Function (BSDF) dataset expressing the light scattering off and through the investigated surface. The BSDF data can refer to either individual fenestration layers or to the entire window system and is based on the method proposed by Klems [41, 42] relating all incident light directions with reflected and transmitted light by direction. The BSDF uses the Klems coordinate system that consists of 145 patches arranged hemispherically in such a way that each patch corresponds to almost the same cosine-weighted solid angle. Such a hemispherical formalisation is considered for each side of the fenestration surface to express both the input and output directions (Figure 2.3). The BSDF of a fenestration system can be generated in various ways such as the *Radiance* tool genBSDF [43], the program Window, developed in Lawrence Berkeley National Laboratory (LBNL) or through photogoniometric measurements. The View matrix describes the light reaching each prescribed

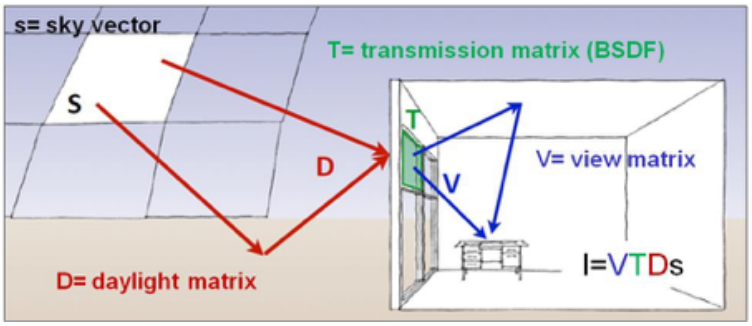

FIGURE 2.2: Three-Phase-Method schematic representation (Source: McNeil, Radiance Workshop 2014, https://www.radiance-online.org)

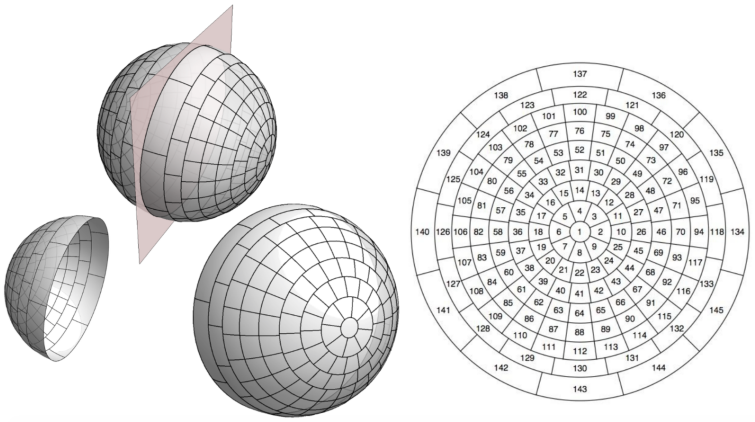

FIGURE 2.3: Schematic representation of a BSDF as two hemispheres at each side of a window (left) and the Klems 145-patch hemispherical basis with numbered subdivisions (right) .(Source: McNeil, Radiance Workshop 2014, https://www.radiance-online.org)

view point in the room taking into account the contribution of each Klems' patch of the window and it has dimensions 145 x the number of virtual sensors.
The sky hemisphere is described by the sky vector and it is discretised according to the Reinhart angle basis of 2305 divisions. The high resolution subdivision is preferred in order to reduce inaccuracies occurring when peaks of solar radiance are spread over large solid angles [43]. The Daylight matrix describes the luminous flux transfer from the sky divisions to the window at each incident direction defined by the Klems' patches and therefore, has dimensions 2305 x145 (Figure 2.4). The generation of the sky is based on the Perez all-weather-model [44]. The contribution of the ground is also included as one coefficient of the Daylight matrix.

The Three-Phase-Method has been selected over other daylight simulation softwares using DAYSIM [45] and classic Radiance [46] in the core engine due to its capability of calculating the three daylight transmission phases separately. While DAYSIM and classic Radiance calculate the light transfer from the exterior to the interior in a single phase, the Three-Phase-Method allows the dynamic simulation of the shade control in one time-step by alternating between different transmission matrices. The pre-calculation of the BSDF, corresponding to various window configurations, reduces the computational time of the simulations substantially. Additionally, since the transmission matrices are produced during the commissioning

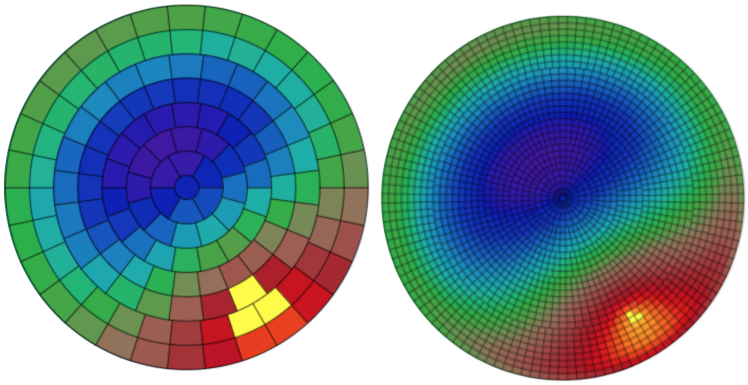

FIGURE 2.4: Comparison of the sky luminance distribution for a discretization of 145 divisions (Tregenza sky) (left) and for a discretization of 2305 divisions (Reinhart MF:4)(right) (Source: McNeil, Radiance Workshop 2014, https://www.radiance-online.org)

process, they can be obtained experimentally maintaining all the complexity of the fenestration system. In this way, the Three-Phase-Method allows the simulation of complex fenestration systems which can not be easily simulated in classic Radiance. Despite its benefits, there are situations where the Three-Phase-Method fails to accurately predict the indoor illuminance. The Perez model, on which the daylight simulations rely, is based on the reproduction of the sky luminance distribution for different weather conditions. Although the Perez model is in general physically accurate and recognised as an industry standard, its accuracy decreases for non-uniform cloud patterns of overcast skies. In general, days with dynamically changing cloud patterns are a common problem for automatic shading controls which must either keep up with the frequent daylight changes risking the user discomfort due to the frequent movements of the shading devices, or occasionally allow high glare conditions in the room.

The simulation based control approaches the specific problem in two different ways. First of all, on a level of simulation accuracy, the effect of small discrepancies between simulated and actual values is reduced due to the use of fuzzy logic at the optimisation process as long as the illuminance values correspond to a similar perception of comfort (see Section 2.4.2). Additionally, the irradiation measurements can be averaged over a short time period of a few minutes to mitigate any sudden changes caused by moving clouds. However, it must be noted that this can be the case only when the irradiance measurements are received on time intervals shorter than the time-step between the controller reactions.

Within the control algorithm the daylight simulations are used to calculate the indoor horizontal and vertical illuminance for a prescribed virtual sensor grid. The virtual sensors are characterised by their three dimensional position in the room and their direction. The horizontal illuminance sensors look always upwards while the vertical illuminance sensors can have any direction parallel to the plane on which they are defined. This allows the sensors allocated for the calculation of vertical illuminance to refer to both the user's eye level and the computer screen. Since the view point height for both cases is fairly the same height and the view direction is flexible, it is not necessary to specify the exact purpose of each vertical illuminance sensor.

To evaluate the visual comfort in the room based on the horizontal and the vertical

illuminance measurements at multiple positions, two conditions must be fulfilled; the light in the room is sufficient and no position is highly affected by glare. Moreover, it is important to ensure that the representation of each position in the defined conditions is equivalent. Therefore, instead of examining each position separately, the average value of all the horizontal illuminance sensors and the maximum value of all the vertical illuminance sensors are used. In this way, it is ensured that the horizontal illuminance at positions away from the window does not become too low and that at positions adjacent to the window it remains bellow uncomfortably high values. Additionally, the maximum vertical illuminance ensures that the glare protection is effective at any position independently from its proximity to the window.
As mentioned in Chapter 1, a weakness of the control systems that explicitly address glare is the requirement of detailed knowledge on the user's sitting position and looking direction. The controller offers a more flexible definition in the sense that the virtual sensor grid can be specified based on a series of assumptions depending on the room specifications, in the cases that no previous knowledge on the user's position in the room is available. Although there are no strict rules for these assumptions, the basic idea lies on the identification of the most affected positions in the room, provided that they can accommodate the work surface.
For example, in a large multi-person office one can assume a number of sitting positions and view directions in order to address the situations when the user faces the window or is turned parallel to it. When areas of high interest are represented in the sensor grid, for example sitting positions away from or adjacent to the window, the controller will act in order to maintain the areas of high glare risk below disturbing limits while still allowing the daylight reach deeper into the room. Additionally, by defining vertical illuminance sensor pairs of opposite facing directions to also address glare on the computer screen every sitting position can refer to two possible scenarios. For example, a user sitting at a work station in front of to the window can be either directed towards it or have the back turned to it. In cases when the desired vertical illuminance limits vary for different positions, the lowest limit available would define the prescribed set-points leading to more conservative controller reactions. In a similar way, in cases of limited knowledge of the room the controller's performance is also expected to be more conservative than in the cases when more information is available. It is therefore evident that the controller can perform to its full potential when a detailed knowledge of the room's set-up is available.

2.4 Fuzzy logic based optimisation

Fundamentals of fuzzy logic

While it is a common belief that most situations in the physical world can be precisely characterised by analytic functions or numerical values, one often encounters systems where the ambiguity of the measurements or the imprecision of the defined criteria makes their characterisation in a classical way difficult.
Consider, for example, having to separate a group of people based on their age in two groups, young and old and set the age of 45 as the boundary between the two categories. One can easily characterise a person of 90 years as old but following this strictly defined criterion, an athletic person of 46 would also fall under the same category. Therefore, such a categorisation is inadequate since it doesn't really provide sufficient information about the population it characterises. In such cases, fuzzy

logic provides a framework that allows the definition of physical processes with continuous grades of membership rather than strictly defined values. The application of fuzzy logic is especially useful in the two following cases:

1. Situations involving highly complex systems whose behaviour can not be fully understood or whose large number of inputs and outputs cannot be conventionally controlled

2. Situations where a rather fast and approximate solution is of more use than a very precise and time consuming analysis.

Fuzzy sets and membership function

As mentioned above, classical sets are characterised by strictly defined (crisp) values whereas; fuzzy sets are characterised by degrees of membership which indicate the degree to which an element belongs to the set.
According to the definition that Zadeh introduced [47], if we consider X as a set of generic elements and $x \in X$ an element within the universe X, then for a fuzzy set A within X there is a membership function which associates uniquely every x with a real number within [0,1] indicating the degree that it belongs to A. The highest degree of membership to the fuzzy set is expressed by 1 while the non-association is indicated by 0. If the same definition is expanded to ordinary sets, the membership function of an element can only have the value 0 or 1 belonging or not belonging to the set. The membership function is the most important element in the theory of fuzzy logic since it defines the relationship of each element in a space with the fuzzy set. Different shapes of membership functions can be used according to the posed problem, such as triagonal, trapezoidal, gaussian etc. Some examples are presented in Figure 2.5.

Implementation of fuzzy systems

The implementation of a fuzzy system consists of three steps; *the fuzzification*, *the rule base definition* and *the defuzzification*. The process of turning a crisp value into a fuzzy one is called *fuzzification*. Values that are not clearly deterministic but instead are characterised by an uncertainty that rises from ambiguity or vagueness can be fuzzified. As soon as a variable is selected, it can be represented by two or more membership functions attributed by a qualitative category; e.g. high, medium, low. The Rule-base refers to a set of linguistic *"if...then..."* rules characterising the dynamic behaviour of the fuzzy system. The number of membership functions defines the potential number of rules in the rule base. The membership functions in combination with the defined rules are also referred to as *knowledge base* of the fuzzy system. The rules are in principle experiential and their outputs are also fuzzy sets which result from applying logic operators on the fuzzified inputs corresponding to the defined rules. Operators such as Union, Intersection, Complement and Containment, normally used for numerical sets, are also applicable on fuzzy sets. The resulting output is an array of as many fuzzified output values as rules.
The reverse process of the fuzzification, in which a fuzzy quantity is reversed to a single scalar quantity, is called *defuzzification*. Several methods have been proposed in the literature depending on the shape of the output function. However, the most popular way is the *centroid method* which calculates the centre of gravity of the output fuzzy function and uses the horizontal coordinate as the single crisp output.

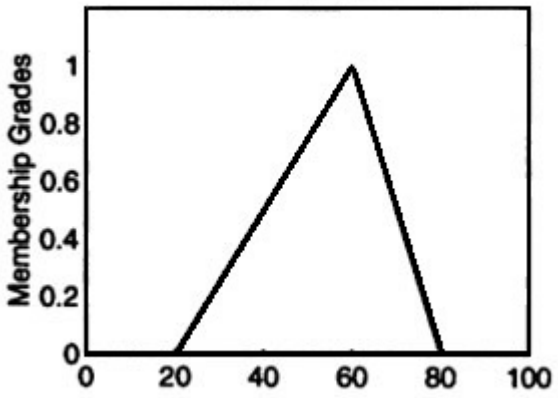

(a)

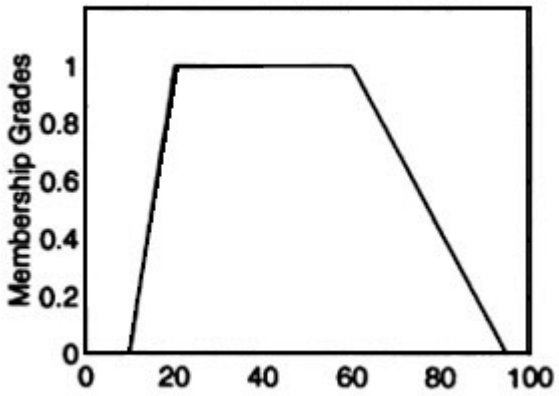

(b)

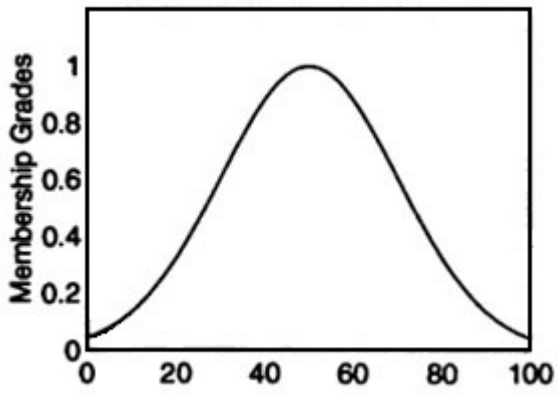

(c)

FIGURE 2.5: Common shapes of fuzzy functions: (a) triagonal, (b) trapezoidal, (c) gaussian

Fuzzy logic in the controller

As mentioned above, after the controller has calculated the average horizontal and maximum vertical illuminance for a specific window configuration, it evaluates them in terms of visual comfort. The concept of visual comfort in the room in the presence of natural light is in principle rather difficult to pinpoint since it depends on both vertical and horizontal illuminance; two interconnected and opposing quantities. As the controller acts in order to increase the daylight admission in the room, expressed as horizontal illuminance, the vertical illuminance rises as well increasing the glare probability. Since the application of strict rules on either value influences the other in the opposite way compromising visual comfort, a fuzzy approach has been developed instead.
The optimization system is characterized as *"fuzzy-logic-based"* because it borrows the fundamental principles of fuzzy logic but the full process deviates substantially from the classical fuzzy systems. Since the purpose of the developed process is the evaluation of a specific window configuration as to the resulting glare and daylight in the room and not the determination of a configuration from the scratch, the defuzzification process can be omitted. Unlike the classical approach of a fuzzy system, the controller only uses the rule-base outcome as a switch for the optimization process. For every shading configuration introduced at the process, the output of the rule-base gives the controller a signal to apply the configuration if it fulfils the conditions of visual comfort or to continue testing alternative solutions that would improve the daylight conditions.
The two variables under evaluation are the average horizontal illuminance on the work surface and the maximum vertical illuminance at both the eye level of the user and at the screen level to address both the glare at the eye level of the user and the haze on the computer screen. Each of them is described by two membership functions corresponding to the uncomfortable and the comfortable situation. Each variable is characterized by three values; two constant ones, expressing the illuminance for which the membership function of comfort and the membership function of discomfort are equal with the unity, and an adjustable one for which both membership functions are equal to zero.
The fuzzy functions for the maximum vertical illuminance describe how the degree of discomfort increases with the illuminance. Therefore, the membership function expressing comfort is equal to 1 at 0 lux $(x_{V,comf})$ and decreases monotonically with increasing illuminance values until the 2000 lux $(x_{V,sp})$ where the function is equal to zero. At the same point the membership function representing discomfort starts increasing monotonically until 3000 lux $(x_{V,uncomf})$ to which point it becomes equal to 1 and remains so.
Since the vertical illuminance refers to both the eye level and the computer screen, the value of 2000 lux represents the transition point between comfort and discomfort for both cases. According to Schierz et al. [37], the value that vertical illuminance starts affecting the visibility of the computer monitor is about 1500 lux, depending on the screen. On the other hand, Wienold [48] concluded through user surveys that the users tended to prefer high illuminance levels of around 3000 lux and being allowed to adjust their own shading device, an average vertical illuminance of about 2500 lux at the eye level was measured. In order to express both situations, 2000 lux has been chosen as the mean value. The point where the membership function representing discomfort becomes equal to 1 has been set again to 3000 lux. According to Schierz et al., this is the threshold at which the vertical illuminance produces haze at the computer screen and compromises the visibility on the computer monitor.

In the case of the average horizontal illuminance, the degree of comfort is assumed to increase with the amount of light. The discomfort membership function becomes equal to 1 for 0 lux ($x_{H,uncomf}$) and decreases monotonically until it becomes 0 at 500 lux ($x_{H,sp}$) at which point the comfort membership function begins. This value has been chosen according to EN-12464-1 [49] where 500 lux is the recommended value of horizontal illuminance at the work area. As mentioned earlier, user surveys have shown that office workers in a sunlit office prefer to work under high illuminance levels and would, in average, start experiencing glare problems for work plane illuminance above 3000 lux [48]. According to this assumption and given that the membership function of comfort begins at 500 lux, the illuminance value for which the comfort function becomes and remains equal to 1 ($x_{H,comf}$) has been set at 1000 lux. In this way, the comfort membership function remains within the acceptable limits and is still considerably flexible to daylight changes. It is worth noting that no upper limit has been assigned to the horizontal illuminance although very high values of average horizontal illuminance would in fact lead to glary situations. Under the assumption that such a case would be prevented by the application of a high limit on the vertical illuminance, for the sake of simplicity, the upper limits of the horizontal illuminance have been omitted.
The shared point representing the transition between comfort and discomfort can be reset according to the user's subjective sense of comfort. In both the case of horizontal and vertical illuminance, one membership function has a triangular shape and one a trapezoidal, as shown in the examples given in Figure 2.6. To simplify the procedure and preserve the transparency of the system actions, no overlapping between the comfortable and uncomfortable functions of each element was allowed. Since only the basic principles of fuzzy logic are applied in the described method and no de-fuzzification takes place, this simplification has no significant impact on the optimisation results. To avoid unequal value representation, the normalised values of illuminance are used instead of the actual values. In the normalised axes the $x_{H,uncomf}$ and the $x_{V,comf}$, corresponding to the lowest illuminance values of both cases, are equal to zero while the $x_{H,comf}$ and the $x_{V,uncomf}$, corresponding in turn to the highest limits, are equal to one. The $x_{V,sp}$ and the $x_{H,sp}$ can be readjusted by the users to better fit their subjective sense of visual comfort and are calculated by the following formulas:

$$x_H = \frac{E_{Hor} - x_{H,uncomf}}{x_{H,comf} - x_{H,uncomf}} \tag{2.2}$$

$$x_V = \frac{E_{Ver} - x_{V,comf}}{x_{V,uncomf} - x_{H,comf}} \tag{2.3}$$

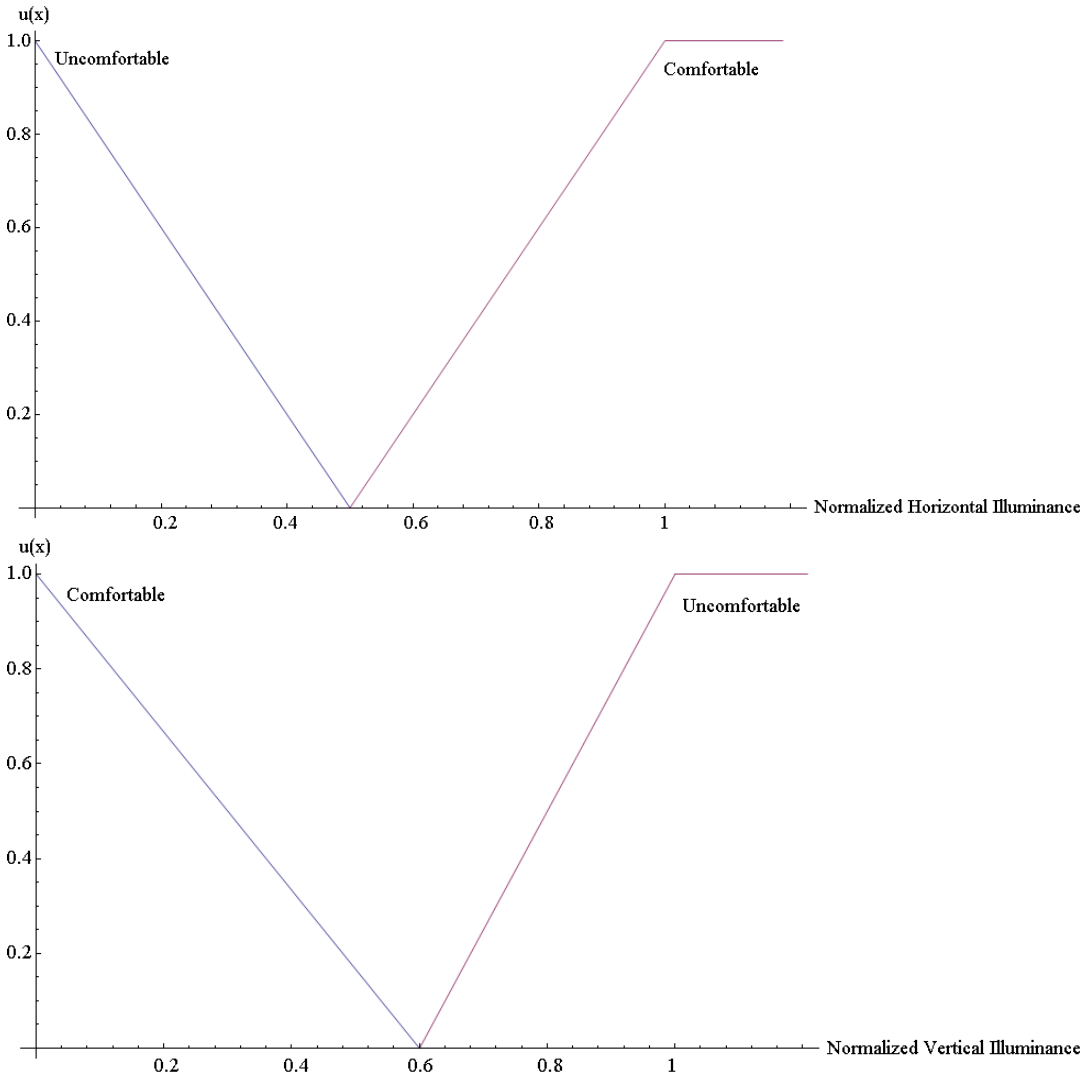

FIGURE 2.6: Fuzzy functions of horizontal (up) and vertical (down) illuminance. For a more even representation of the two functions, the x-axis of the illuminance has been normalised.

Fuzzy rules and evaluation of visual comfort

The rules based on which the algorithm evaluates the visual conditions that occur from a specific window configuration are based on two sets of fuzzy functions. The set of functions corresponding to horizontal illuminance is annotated with (F_{Hor}) and is comprised of the $(f_{Hor_{uncomf}})$ and the $(f_{Hor_{uncomf}})$. The vertical illuminance set, annotated as (F_{Ver}), is comprised of $(f_{Ver_{comf}})$ and $(f_{Ver_{uncomf}})$. It is reminded here that, for the sake of simplicity, both functions characterising a value can not be at the same time larger than zero. The entire set of rules is summarised bellow.

1. If F_{Vert} is *completely uncomfortable* and F_{Hor} is *not completely uncomfortable* then blinds close one step
2. If F_{Vert} is *uncomfortable* and F_{Hor} is *comfortable* then blinds close one step
3. If F_{Vert} is *not completely uncomfortable* and F_{Hor} is *completely uncomfortable* then blinds open one step
4. If F_{Vert} is *comfortable* and F_{Hor} is *uncomfortable* then blinds open one step
5. If F_{Vert} is *uncomfortable* and F_{Hor} is *uncomfortable* then:
   (a) If $f_{Vert_{uncomf}}$ is larger than $f_{Hor_{uncomf}}$ then blinds close one step
   (b) If $f_{Hor_{uncomf}}$ is larger than $f_{Vert_{uncomf}}$ then blinds open one step

In any other case, the configuration is considered appropriate and applied to the shading device in the room.
The characterisation *'completely'* for comfortable or uncomfortable situations refers to the corresponding fuzzy functions being equal to one, while the characterisation *'not completely'* refers to every case excluding only the area where the corresponding functions equals one.

2.5 Electric light control

The electric light control is activated when two conditions are fulfilled:

1. The room is occupied
2. The average horizontal illuminance of all the specified virtual sensors is reduced below the prescribed set-point and the blinds have been completely retracted.

As in the case of the shading control, the current illuminance levels in the room are calculated with the daylight simulations; however, the workflow of the electric light control is considerably simpler with no additional processes. If the available electric light supports a dimming function, the controller requires three variables; *the switch-on set-point*, *the switch-off set point* and *the required illuminance level*, all of which refer to the average horizontal illuminance on the work surface. As soon as the average horizontal illuminance due to daylight falls bellow the *switch-on set-point* the controller switches the lights on and dims the system to the point that the total illuminance due to both daylight and artificial light reaches the *required illuminance level*. If the user leaves the room or the illuminance due to only daylight reaches

the *switch-off set-point*, the electric light will automatically switch off on grounds of energy efficiency. For traditional on-off lighting systems, the required illuminance level is omitted since the user has no control over the light output and the control signal is limited between the values 0 and 1, to simply indicate the status of the electric light as on or off.
The *switch-on set-point* of the system as well as the *required illuminance level* are flexible variables and can be eventually adjusted to the users' preferences. On the other hand, the *switch-off set-point* is constant and will not be affected by any user interaction. The prescribed value of 500 lux is based on EN 12464-1 as explained at the previous section. The default values of the two adjustable variables of the system have been chosen, like in the case of the shading control, so that the controller will address both visual comfort and energy efficiency. For the default *switch-on set-point*, a very low value has been chosen in order to prevent unnecessary energy consumption. Since the user's interactions with the lights will eventually influence the switch-on value, 100 lux has been arbitrarily chosen as a starting point. The *required illuminance level* is by default also set to 500 lux for the same reasons as the *switch-off set-point*; however, this value is expected to rise since the users working under high daylight levels tend to also require higher illuminance levels by artificial light sources [50].

2.6 User adaptation

Shade control adaptation

Recognising the reasons that cause the user to interact with the system is very important for the adaptation of the shading control algorithm. Since the controller already acts in an energy-efficient manner, it is assumed the user interventions are motivated by visual comfort, the need for view to the outside, or other exceptional circumstances (e.g. a presentation, privacy etc). As the last case cannot be accounted for in an analytical manner, the controller excludes actions leading to radical shade positions that result to extremely high vertical or extremely low horizontal illuminance. User interventions resulting to more open shade configurations are treated as being motivated by the need for additional daylight adapting the fuzzy function set-points to higher values. Although the actual motivation of a user uncovering the window is often the need for increased view out, when higher illuminance values are allowed more open window configurations are applied which indirectly improve the visual contact to the outside as well.
When the user interacts with the controller there are four values that need to be investigated; the average horizontal and maximum vertical illuminance preceding the user interaction and the corresponding values following the adjustment of the shading device. For every interaction, the controller calculates the four values and uses them to re-adjust the fuzzy functions.
The user adaptation takes place once per day at midnight. It readjusts the values for which both comfort and discomfort membership functions become zero for the vertical and the horizontal illuminance. The adjusted $x_{H,sp}$ and $x_{V,sp}$ remain always at the area between the non-adjustable points for which the two fuzzy functions become equal to 1. This adjustment essentially changes the perception of the controller concerning desirable and undesirable situations.
For example, if the user acts in such a way that the horizontal illuminance on the work plane increases above a value that before the interaction was considered comfortable, the controller assumes that the user requires more light and moves the $x_{H,sp}$ to a higher illuminance value, as shown in Figure 2.7. As a result of the user opening

the blinds, the vertical illuminance will also increase. If the new value belongs to the uncomfortable membership function, the $x_{V,sp}$ is also expected to move to the right signifying that the user is willing to accept conditions of higher glare in exchange to additional daylight in the room.
On the other hand, a user sensitive to intense daylight is expected to react to increased vertical illuminance at the eye level by lowering the venetian blinds. In this case, $x_{V,sp}$ is expected to move to the left towards lower illuminance values (Figure 2.8). If the reduction of the horizontal illuminance is not too large, the set-point will remain unchanged. However, if the value after the user interaction falls under the uncomfortable horizontal illuminance fuzzy function, the $x_{H,sp}$ will also move to the left.
To avoid that the controller learns extreme or random values which do not really represent the average visual comfort of the user, the horizontal and vertical illuminance values are aggregated before the adaptation. For every interaction, the stored values before and after the user interaction are compared to clarify the motivation behind the action and to decide on their usability. The registered user wishes of a day are discarded in the following cases:

1. The interaction is leading to changes lower than 5% of the interior illuminance.
2. Multiple interactions are taking place within a time frame of five minutes. In this case the intermediate interactions are assumed to be part of a single action with its beginning before the first input and its end after the last.

After the data has been sorted out, the remaining pairs of illuminance values before and after the user's input are averaged per interaction, leading to two 1-D arrays of average horizontal and maximum vertical illuminance values with as many elements as valid user interactions. The mean value of each array is finally used for the adaptation of the $x_{H,sp}$ and the $x_{V,sp}$.
If the resulting values correspond to the areas in which the fuzzy functions are equal to one, the applied value corresponds to a 10% increase of the current configuration. This condition is applied in order to avoid that the system learns non representative values. In this manner, randomly occurring, very high vertical illuminance values can not significantly influence the fuzzy functions. For this reason, 10% has been asigned to express a very small change. However, if this is an explicit user preference, the $x_{V,sp}$ will continue increasing until it reaches the desired levels.
At this point, it is worth taking a more critical look at the adaptation process used in the controller. As the main purpose of such a function is to enhance the user satisfaction, the preferences of the users introduced through their interactions with the system are evaluated and used to readjust the controller's perception of visual comfort. However, the history of these preferences is not explicitly used for cross-reference and is only reflected on the current set-point values of the fuzzy functions. The reason for that is on the one hand to allow a new occupant to readjust the system's behaviour in a simple and effective manner. On the other hand, it is assumed that the user preferences are not static over time and a correlation between the season of the year and the daylight requirements of the users might be possible. However, this assumption is not investigated further within this thesis.

Electric light adaptation

For the electric light control, the adaptation also takes place once per day at the same time as the blind control adaptation and is also based on stored user interactions

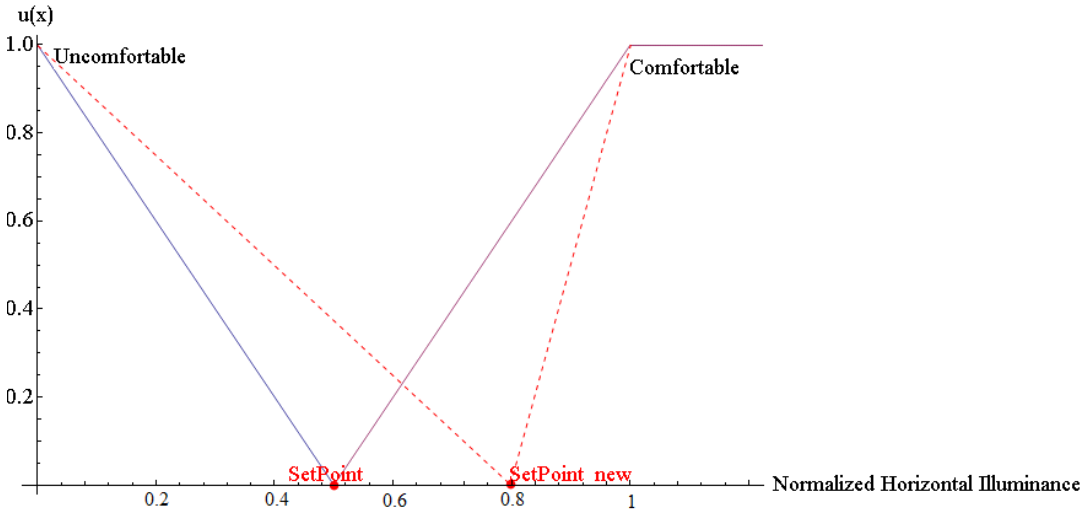

FIGURE 2.7: Adaptation of the horizontal illuminance fuzzy function for a user who requires additional light. The set-point of the horizontal illuminance is moving towards a higher value.

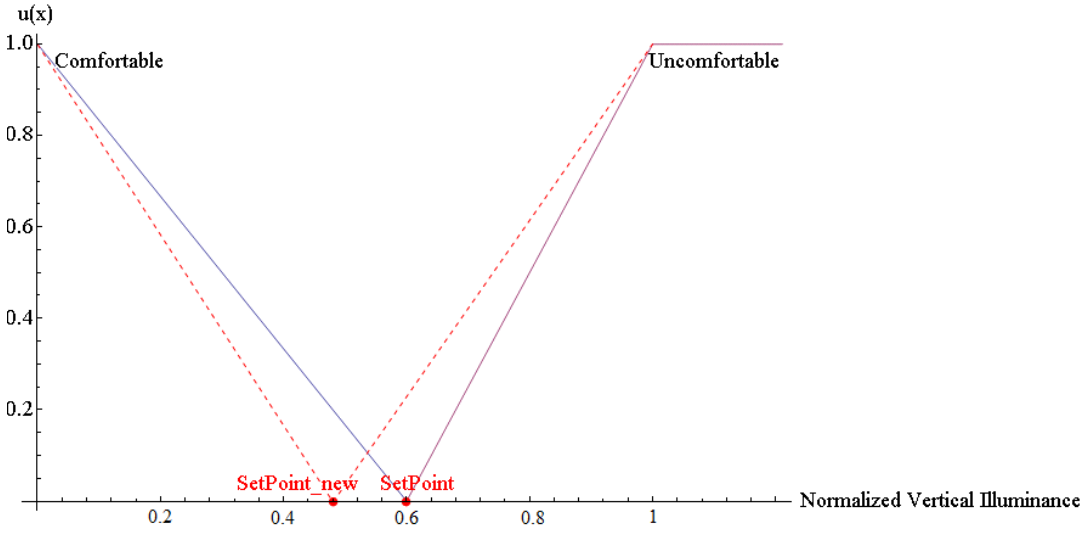

FIGURE 2.8: Adaptation of the vertical illuminance fuzzy function for a user sensitive to glare. The set-point of the vertical illuminance is moving towards a lower value.

from the previous day. The new *switch-on set-point* can never exceed the *switch-off set-point* and is adapted based on the value of the average horizontal illuminance on the work surface at the moment that the user switched on the lights. If such an action occurs more than once in the day, the average value of all horizontal illuminances is used instead. If this value exceeds the *switch-off set point*, it is not taken into account. For example, if the user switches the lights on manually when the average horizontal illuminance on the work surface reaches 200 lux, after the adaptation process, the controller will automatically switch the lights on as soon as the illuminance reaches this value.
For the adaptation of the dim level, all actions collected during the day are averaged and compared with the value. If the average preferred value is lower than the current one, it is directly set as the new dim level. In the opposite case, the percent difference of the existing dim level with the preferred value is calculated. If the increase remains below 25%, the averaged value is directly used; otherwise, the current value is increased per 25%. This quota is used to prevent the controller from learning wasteful wishes which would lead to very high energy consumption. Continuous requests for higher lighting output will eventually raise the dim level to the maximum value available.

Chapter 3

Installation of two prototypes

3.1 Laboratory testing

The daylight laboratory

The first controller prototype was installed in the daylight laboratory (Figure 3.1), an office-like facility which consisted of two identical rooms, located at the roof of Fraunhofer ISE in Freiburg, Germany (latitude 48.01° N, longitude 7.84° E). The laboratory was sited on a platform that allowed it to fully rotate to re-orient the facade at will. For the needs of the controller testing the facade orientation was facing south during the entire testing period.
Each room had dimensions 3.65 m x 4.6 m, with a suspended ceiling 3 m above the ground and its facade was fully covered with solar control glazing of 54% visible light transmission, SHGC (or g-value) of 29% and a U-value of 1.1 W/(m^2K). Identical luminaires and white, internal venetian blinds, 80 mm wide, were installed in both rooms.
During the testing period, all installed components were controlled with simultaneous control signals in order to both maintain the same interior conditions. One room served as an office in the centre of which a single work station with a computer was set up to simulate real life conditions for debugging and testing the controller. The other room accommodated an illuminance measurement setup for monitoring and validation purposes. Hereafter, the room serving as an office will be referred to as *"the test room"* while the other one will be referred to as *"the measurement room"*.
About 13 meters away from the east side of the daylight laboratory an obstructing building rose higher than the ceiling of the test facility. Additionally, an obstacle was found 7 meters away from the facade with about half the height of the laboratory when mounted on the rotation platform. This external geometry was also included in the simulation model.

Inputs

The weather data required for the operation of the controller was received from the Fraunhofer ISE weather station located beside the daylight laboratory, providing measurement values through the ISE network with a 5-second time-step. The incoming data consisted of: global and diffuse horizontal illuminance measured with an SPN1 sunshine pyranometer (Delta-T devices, UK). The received data was averaged within the controller over three minutes to avoid false controller reactions due to sudden irradiation changes. The outdoor temperature was measured and averaged over 24 hours within the control algorithm. Finally, although not necessary in this case, the wind speed was also included in the weather data.
The updated values were saved in a data-logger at the test facility along with the

FIGURE 3.1: The daylight laboratory

interior measurements of temperature (Pt100) and occupancy monitored by an infrared presence detector at the centre of the room.

Hardware set-up and system architecture

The controller prototype installation was based on an industrial network which was chosen over commercial automation systems such as KNX and LonWorks on grounds of modularity, flexibility and cost (Figure 3.2).
The fieldbus is in principle a two-way communication link between a controller and the analogue or digital inputs and outputs and it serves as a Local Area Network (LAN) for high speed automations. An important benefit of such a system is the easy maintenance and monitoring of all modules connected.
The main computer in the test installation worked on Linux environment and served as both a controller and a data logger. The measurements and signals within the room and from the ISE weather station were stored in the computer during the day. The control algorithm was written in Python and was based on the **Fener** simulation platform [39]. The communication between the controller and the hardware was managed by a script written in C. The computer was connected to the fieldbus while also being connected to the Fraunhofer ISE network at all times via two independent Ethernet connections.
The motors used for the setting of the venetian blinds were compatible with the Standard Motor Interface (SMI) which allowed the positioning of both the height and angle of the venetian blinds. The SMI allowed the bilateral communication between the controller and the actuator and reported back the position status of the shading device. The SMI interface remained connected to the computer hosting the controller via a serial port and reported back to the system about the current height

of the shading device and the tilt angle applied on the slats at the previous time-step which was used by the controller to calculate internally the current tilt angle.
Independently from the controller configuration, the venetian blinds could always be reset manually through two switches; one corresponding to the height of the shading device and one corresponding to the tilt angle of the slats. The user interactions were stored in the data logger and were used later for the adaptation process.

Electric light

The lighting system of the first prototype was installed particularly for the needs of the testing. It was designed in order to contribute to the visual comfort of the test room under the notion that the installation should simulate an average office space with a work station and a visual display unit (VDU). The installed pendant luminaire was direct/indirect (75/25) with louvre optic and two T5 lamps with a total nominal power of 98W and a colour temperature of 4000K. The lights were installed at the centre of each room and could be dimmed using 1-10V ballasts. In both rooms, the systems were connected with a **Hager** light actuator compatible with the dimming system which applied the control signal simultaneously to both luminaires. Just as in the case of the shading control, the user could always intervene by adjusting the illumination in the room manually according to his/her subjective sense of visual comfort. The interactions with the system were stored in the data logger and were used later by the user adaptation algorithm.

Dimming curve

To accurately evaluate the illumination in the room without the use of sensors, it was necessary to correctly simulate the dimming of the electric light. In order to do that, an array of illuminance sensors was placed on the work surface, right underneath the luminaire, to measure the dimming of the electric light before the testing of the installation began. Based on the actual horizontal illuminance measurements, the output illumination on the working surface was represented by a dimming curve expressing the relationship of applied voltage with light output.
The measurements took place overnight to avoid any interference from external light. The illuminance sensors used were specified for the measurement of the installed light source. The applied voltage increased per 0.5 Volt every half an hour via a signal generated by a short computer script and the illuminance sensors took a measurement every 10 seconds. The dimming steps were kept relatively small, to 0.5 Volts or to the 5% control input, to provide a better resolution to the dimming curve. The time between the dimming steps was 30 minutes to allow for the electric light to stabilise at each applied voltage and the frequent measurements during this time prevented errors due to unforeseen events such as external lights. The exact procedure was repeated for three consequent nights. Since no large deviations were observed between the three datasets, the measurements of each time step were averaged over the three nights. Finally, the measurements corresponding to each dimming step were also averaged to give an estimation of the illuminance output for every voltage.
In Figure 3.3, the dimming curves of two sensors are presented to correlate the horizontal illuminance output and the voltage signal at the luminaire. Only two sensors are examined on grounds of relevance and to avoid repetition. The upper illuminance curve corresponds to the illuminance sensor number 1 at the centre of the room and the lower curve corresponds to the illuminance sensor number 2, placed

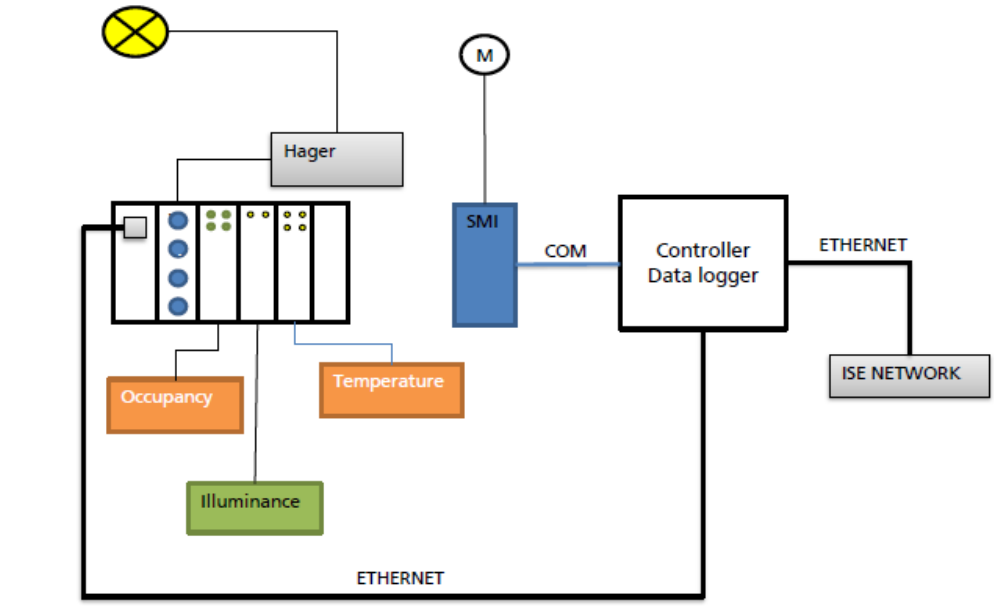

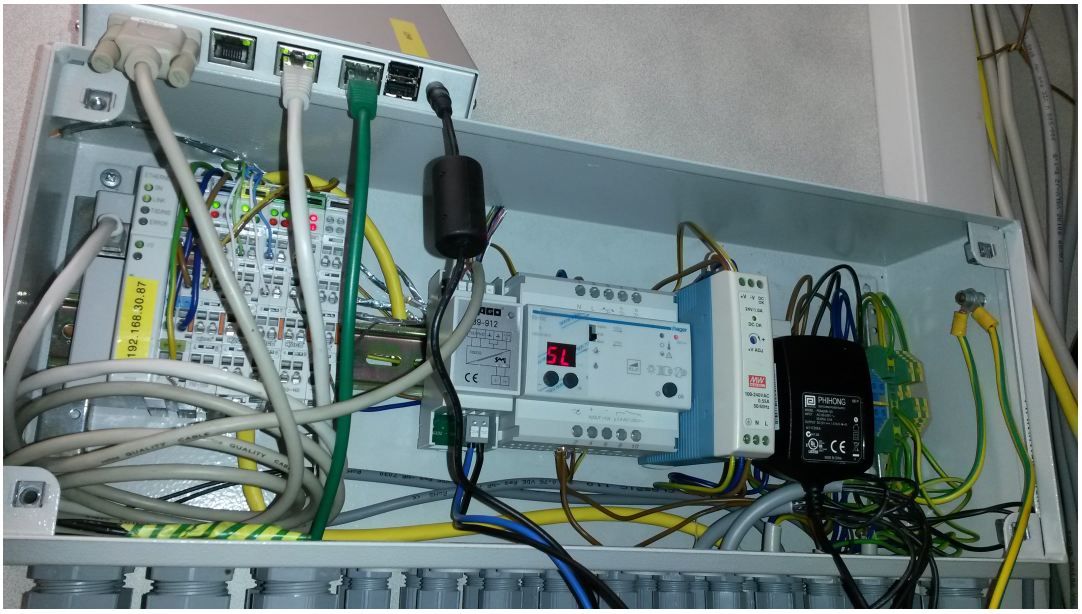

FIGURE 3.2: Schematic representation of the component set-up of the first prototype (up), the electric installation box of the first prototype (down)

1.5m further, closer to the window as shown in Figure 3.4. The dimming curve of the light output in respect to the applied voltage increases linearly until 6 Volt and then the light output is saturated to the maximum. The curve was fitted using the least square method as shown in Figure 3.5. The fitting was made only for Sensor 1 since it was directly under the luminaire and closer to the user's sitting position. The resulting Equation 3.1 was then incorporated in the control algorithm for the prediction of the electric light output.

$$E_{horizontal}(lux) = 317.08 \cdot V(V) - 456.91 \tag{3.1}$$

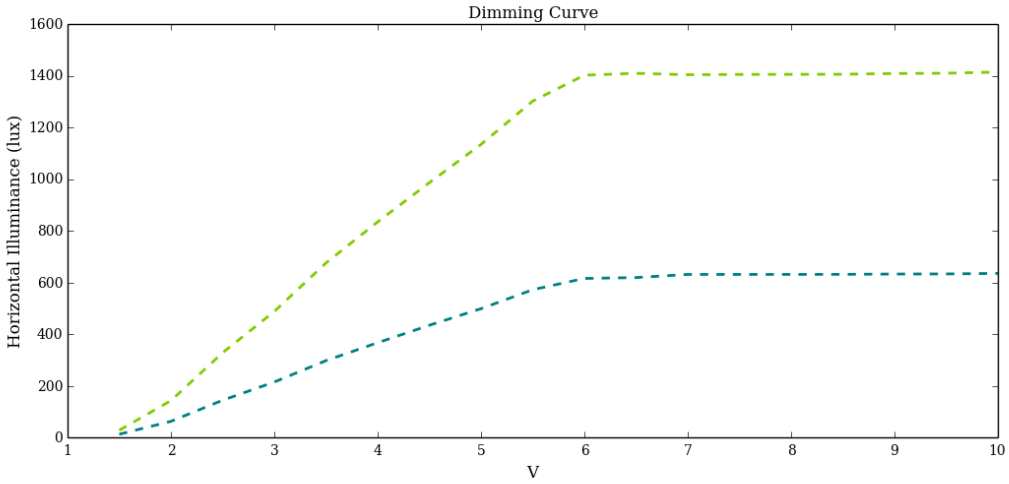

FIGURE 3.3: Correlation between input voltage and horizontal illuminance for two measurement positions. The green line corresponds to Sensor 1, positioned directly under the luminaire and the blue line corresponds to Sensor 2, positioned closer to the window as can be seen in Fig. 3.4.

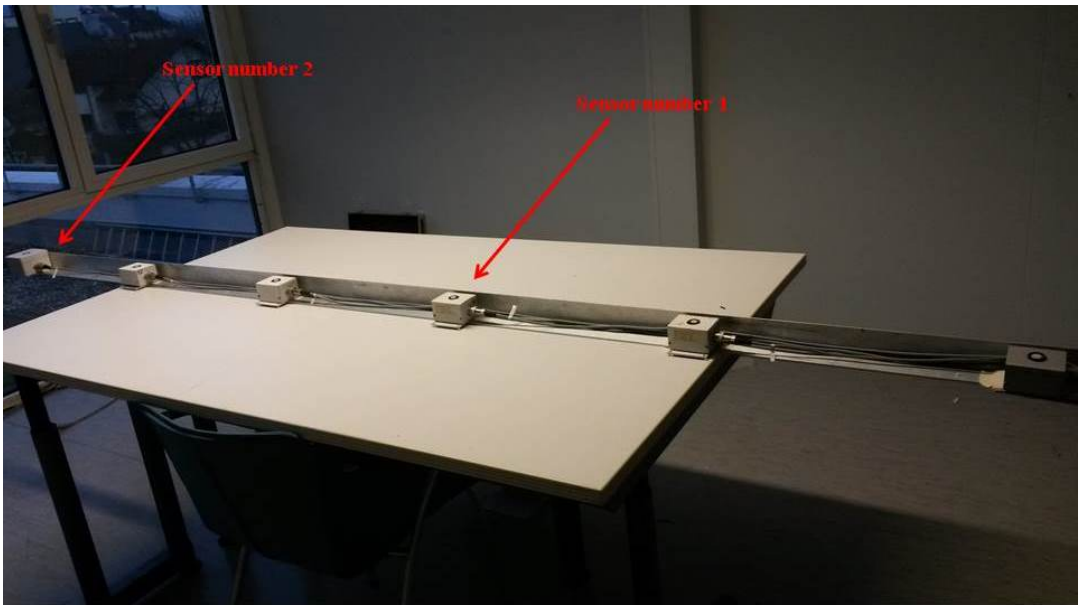

FIGURE 3.4: Illumuminance sensor layout. The array is positioned directly under the luminaire for the monitoring of the light dimming process

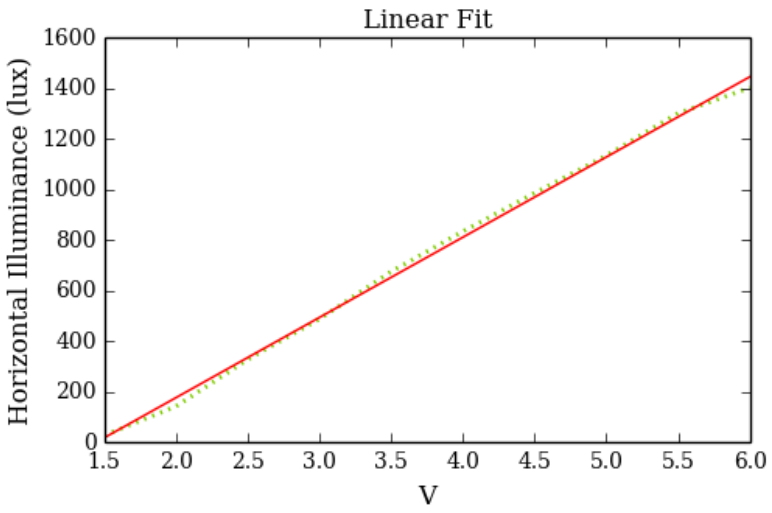

FIGURE 3.5: Linear fit of the illuminance output in relation to the applied voltage

3.2 The second prototype installation

The office

The second prototype of the controller was installed at a real-life office to allow the evaluation of the system by a real user who had not been previously involved in the development of the controller (Figure 3.6). The office was located on the fourth floor of a commercial building located at Berliner Allee in Freiburg, very close to the location of the first test installation, but not associated with Fraunhofer ISE in any way other than locality. The building facade was facing south-east and the office was occupied by one or occasionally two people, working on VDUs looking at opposite directions. The facade of the office was 50 % covered by with low-E double glazing of 80% light transmission, U-Value of 1.4 W/(m^{2}K) and a SHGC of 60%.
The shading device installed at the office was an external, white venetian blind system, with 80mm-wide slats and 70mm distance between them, very similar to the one used at the first installation. In this system, the tilting of the slats was not uniformly applied. Instead, the blinds at the upper part of the window remained more open than the blinds at the lower part in order to increase the daylight admission in the room. The default angle difference between the two parts was 35°, as shown in Equation 3.2, although the system allowed the blinds of the upper part to also completely close, provided that the slats of the lower partition were also fully tilted. When the blinds of the lower part of the window were completely horizontal the blinds of the top part were tilted to their minimum position at -35°.

$$\text{tilt angle}_{top} = \text{tilt angle}_{bottom} - 35^{\circ} \tag{3.2}$$

For the positioning of the shading device, the conventional motors installed at the windows were used and, unlike the SMI motors used at the first prototype installation, allowed no bi-lateral communication with the system. Therefore, they could not account for the current positioning of the shading device. The shading device in the room was initially controlled by a centralised system which was de-activated for the needs of the second prototype testing. During the summer period the centralised on-off venetian blind control, based on global solar irradiance, was activated while the rest of the year the system remained entirely under local manual control. The electric light installation of the office consisted of three luminaires with simple on-off manual control.

Position sensors and control signals

As identified above, the two important limitations of the second installation was the inability of the already installed motors to report back to the system about the current status of the shading device and the coupling of the control signals concerning the tilt angle of the slats. Additionally, unlike the case of the first installation where a universal actuator was installed for the exact adjustment of the height and the tilt angle of the venetian blinds, both signals sent to the shading device were applied through a common switch differentiating only as to their duration.
The first problem was addressed by installing a laser distance sensor and an inclination sensor for the monitoring of the blind configuration. The laser distance sensor was fixed at the top of the window and an aluminum plate was fixed at the lowest slat (Figure 3.7). A laser beam was emitted downwards from the sensor and was

FIGURE 3.6: The real-life office hosting the second prototype installation

reflected diffusely frem the plate at the bottom of the system. The position of the received light spot defined the received angle which corresponded to the distance of the reflection point. By measuring the produced voltage, the exact position of the venetian blinds was calculated as a linear function of the output current of the sensor in mA in relation to the distance. For the calibration of the sensor, measurements at different positions were carried out and the conversion formula was calculated with the least square method, as shown in Figure 3.8.

For the measurement of the tilt angle an inclination sensor (Figure 3.9) was placed under one of the top slats. The sensor itself did not affect the position of the slat due to its small size and light weight. Additionally, by placing the sensor on the side of the slat the connection cable did not interfere with the blind movement. The output of the sensor was given in Volts and was converted to degrees according to the following formula (3.3) provided by the manufacturer:

$$angle = arcsin(\frac{V_{out} - Offset}{Sensitivity}) \tag{3.3}$$

Where: offset refers to the output of the device at 0° inclination and sensitivity refers to the sensitivity of the device in V/°.
Possible deviations at the positioning of the slats were not corrected at the same time-step to avoid frequent movements of the blinds. However, the actual position would be updated at the beginning of every new controller action in order to avoid mistakes in the following calculations due to any previous time-step deviations.
Both the tilt angle and the height were adjusted using the same switch. The two signals were differentiated based on the duration of the manual pressure applied on the up and down buttons; with short, discrete pushes re-adjusting the tilt angle and prolonged pressure moving the blinds up and down. To imitate the short duration of the manual signals, two time relays were used, one for each direction. The duration of the signal was shortened to the smallest interval possible; 0.1 second. Due to the short time of every signal and the very small resolution of the angle changes, the uncertainty of slat tilting was rather large. To approximate the average tilt angle the

FIGURE 3.7: The top (up) and the bottom (down) part of the laser position sensor.

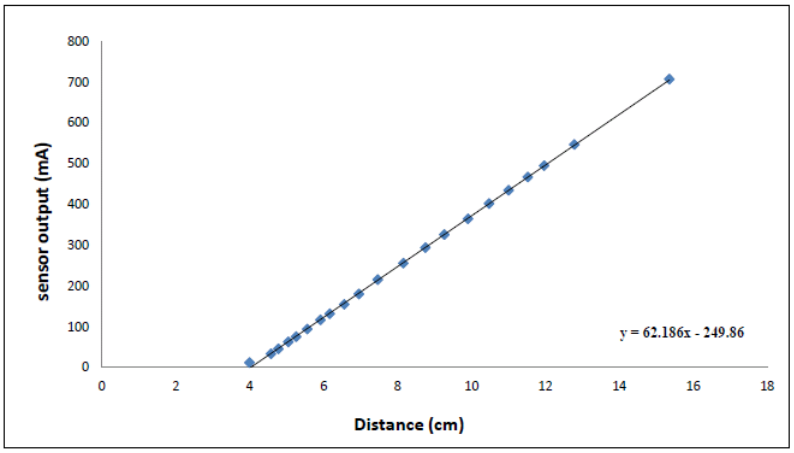

FIGURE 3.8: Correlation between measurements of current output of the laser distance sensor in mA and measured distance in cm.

blinds were tilted from vertical to horizontal position repeatedly and the tilt steps were measured. The measured angles at each adjustment varied between 6 and 13 degrees with larger deviations observed near the extreme positions. The average value of all tilt angle measurements at the course of a full movement of the blind between open and closed position was found for all cases between 9° and 10°. According to that, the minimum angle step defined in the controller was 10° under the notion that a positioning error of up to 30% could occur.
To set the shading device at a specific height, the time required for lowering or retracting the blinds to discrete intervals was repeatedly measured. By limiting the

FIGURE 3.9: The inclination sensor

signal duration to eight seconds with a short shell script, the blinds would move by 30 cm step at the top and bottom partitions of the window and a 25 cm step at the intermediate heights.

Inputs

Similar to the first installation, a temperature sensor was installed in the room to monitor the interior temperature and force the sensor to take additional measures in the case of overheating. A Pt100 was connected directly at the controller's electric installation box and was placed next to the door on the room's thermostat. Additionally, a presence sensor was installed next to the door and parallel to the working stations in order to monitor the room occupation. As soon as the user entered the room, the controller was forced to take action outside its prescribed time intervals in order to readjust the room conditions according to the new occupation status.
The weather input necessary for the controller was downloaded from the same weather station at Fraunhofer ISE which was considered the best choice due to its proximity to the second installation site across the street. Although the data acquisition was characterised by a small time delay of a few seconds, the irradiance values were averaged over a three-minute period compensating for the delay, any missing values or any sudden changes in the irradiance levels such as passing clouds. The measurement data used was the same as in the case of the first prototype with the addition of the measured wind speed. Since the shading device of the second prototype was external, an alert signal would retract it in the case of strong winds exceeding 13.5 m/s.

Hardware set-up

The second prototype installation was created over an already existing system the characteristics of which were explained above. Since the signals of the original installation were based in principle on the signals introduced manually by the user, the controller hardware was installed over the existing switches in order to override the existing system's signals and at the same time allow manual interactions. The electric installation was enclosed in a box for aesthetic and safety reasons (Figure 3.11) and the switches were moved forward over the installation box. Within this box all the components composing the second prototype were assembled.

As in the case of the first prototype, a fieldbus was used as a communication link and all the input and output modules were connected to it. Unlike the first installation, no special actuators were used for the shading device or for the lights. Instead, a combination of digital inputs and outputs was used to change the position of the venetian blinds and to register any user interactions. A simple digital input was used for the electric lights which in this case were just on-off; switching on automatically when the light in the occupied room was insufficient.

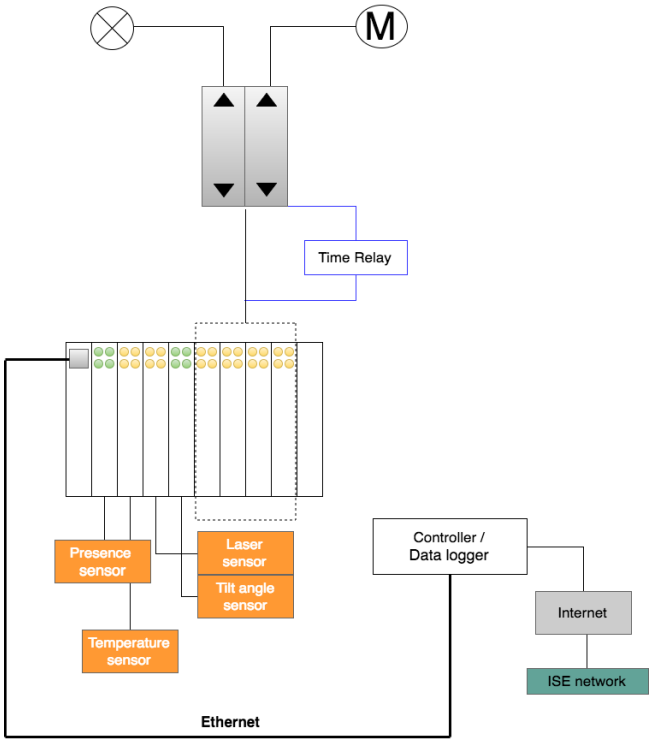

FIGURE 3.10: Schematic representation of the component set-up of the second prototype installed in a real life office

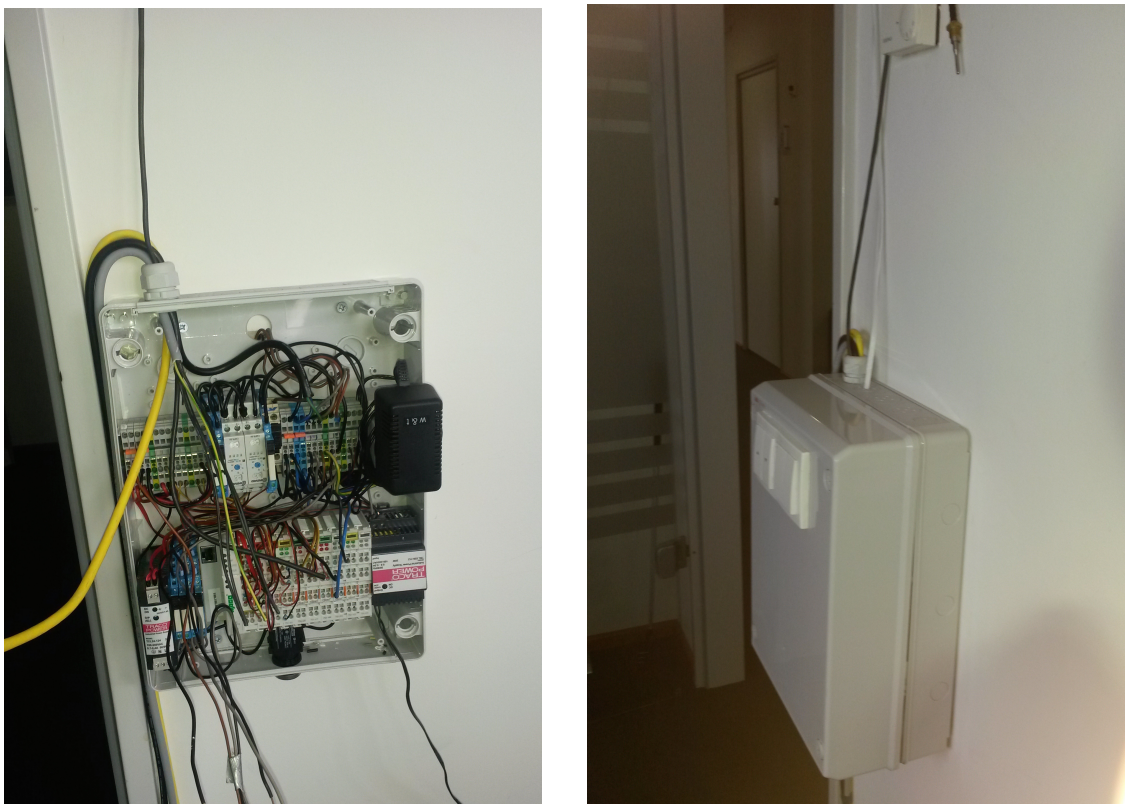

(a) (b)

FIGURE 3.11: The box containing the controller's electric installation, open (a), closed (b)

3.3 Monitoring

In order to keep track of the controller process and to remotely monitor both systems, a large amount of information was written at every second in files generated daily and stored for future reference. For both installations, the monitoring process was very similar. The stored data was separated in three major categories; measurements, controller outputs and hardware signals. The hardware signals refer to the feedback sent back from the controlled devices and to the registered user interactions. The measurements and hardware signals were synchronised and saved in the same file with a single second time step. On the other hand, the controller outputs were updated every time the controller was activated. The activation time was set to intervals of few minutes except for the case of manual input when the controller went to a sleep mode for 40 minutes to avoid interfering with the user's interaction. Since at the beginning of the testing period the control time-step was set to 20 minutes, the sleep mode was set to double the time-step period and remained unchanged for the rest of the time. The sleep mode was renewed every time the user interacted with the switches.
In the case of the first installation, the actuator of the venetian blinds and the electric light dimmer sent back information about the height of the blinds and the status of the luminaires and the user interactions were also stored. The tilt angle changes were given in the form of independent stepped signals allowing to calculate the final tilting position of the slats.
In the case of the second prototype, the position of the blinds was measured at every second by the position sensors and the only information extracted from the switches was the time and the duration of the interaction. The controller outputs were resumed every time the controller was activated and consisted of the applied shading configuration, the calculated solar angles, the simulated maximum vertical and average horizontal illuminance at the work plane, the internally calculated average global and diffused irradiance, the internally calculated average 24-hour outdoor temperature, the calculated direct radiation on the facade and the adaptable fuzzy function and electric light variables.

Chapter 4

Experimental Evaluation

4.1 Measuerment set-up

In order to assess the capability of the daylight simulations to replace the illuminance sensors in the room, the agreement between the simulated and the measured illuminance values was investigated. For this purpose, a number of illuminance sensors was installed at the measurement room of the Daylight laboratory. It must be noted that the vertical and horizontal illuminance values measured on the work station were used only for monitoring and validation purposes and they were not used by the controller.
The work station at the centre of the measurement room was identical with the one in the test room and it held a measurement set-up for the horizontal and the vertical illuminance at positions of high interest. Under the assumption that the user could be sitting on either side of the working station, the horizontal illuminance measurements were carried out by an array of six sensors facing upwards, distributed evenly on the work surface, 0.8 meters above the floor.
For the vertical illuminance measurements, six sensors were used in pairs facing at opposite directions parallel to the window. The pairs were placed on three wooden constructions, positioned in a row in the middle of the table and perpendicular to the window, with distances 2, 2.5 and 3 meters from it. Each construction had a height of 0.4 meters keeping the sensors at a total height of 1.1 meter above the floor. In Figure 4.1, a diagram of the sensor positions on the work surface is presented including the distances of the sensors from each other and from the wall. In Figure 4.2, an actual picture of the measurement set-up is given.
The measurements of the illuminance sensors were taken at a five second step throughout the entire day and they were stored in the data logger for monitoring purposes. The aggregated measurements are used in the following sections represented by the mean value in the case of the horizontal illuminance and by the maximum value in the case of the vertical illuminance.

4.2 Simulation set-up

The simulation set-up is considered to be the most important step in the system's function since the effectiveness of the controller depends entirely on the accuracy of the simulation model definition. For setting up the simulation model, the geometry of the room, the work surface and the building surroundings were reproduced in a *Radiance* formalism. All the surfaces included in the simulation model, including walls, ceiling and floor, external surfaces and work surface, were investigated in order to determine the optical properties of their materials which were used for the material definition in *Radiance*.

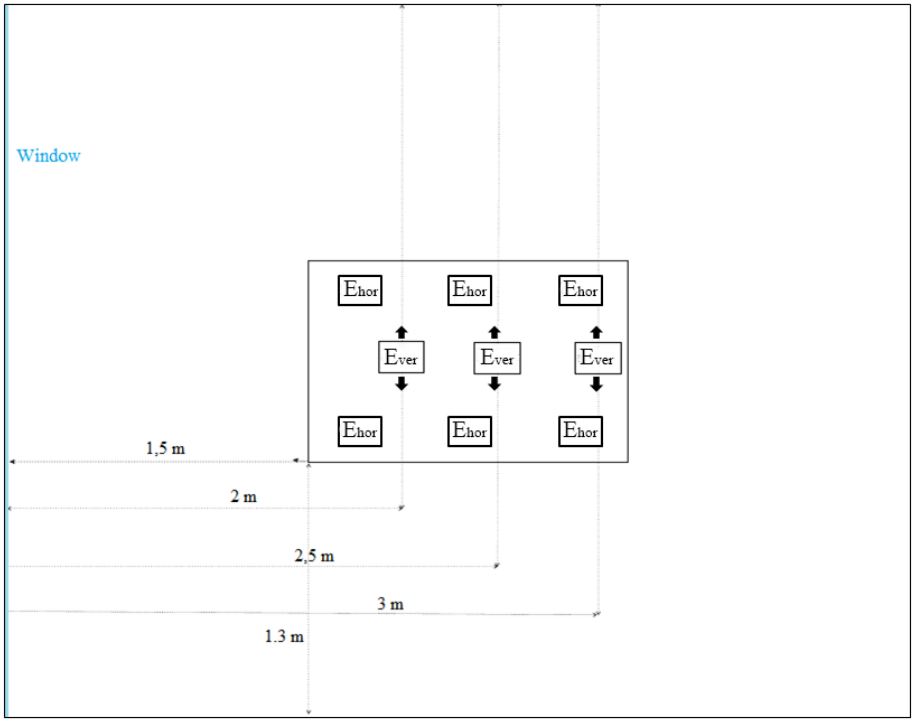

FIGURE 4.1: Positions of the illuminance sensors for measurement of horizontal and vertical illuminance on the work station in the measurement room

To calculate the reflectance of each material, the illuminance received by a surface was measured simultaneously with the luminance reflected from it. According to its definition, the luminance (L_V) is the illuminance (E_V) per solid angle . Based on this and under the assumption that the investigated surfaces were Lambertian and therefore their luminance was isotropic, the reflectance (R) was calculated using Equation 4.1. The luminance was measured with a portable luminance meter (MINOLTA LS-110) and the illuminance was measured with a portable illuminance meter (MINOLTA T-1H). This procedure was repeated for all simulated surfaces at every commissioning process carried out throughout this project. The reflectances of all surfaces within the daylight laboratory, including the external obstruction, are summarized in Table 4.1.

$$R = \pi \frac{L_V}{E_V} \tag{4.1}$$

For the description of the light transfer through the fenestration system including the venetian blinds, a BSDF was generated with the *Radiance* ray-tracing tool, genBSDF [51]. To model the venetian blinds, a single slat was modelled using its vertical section expressed as a set of x-y coordinates and extended at a prescribed length at the z-axis. The single slat was rotated to the given tilt angle and multiplied over the entire window height. The glazing was generated as a polygon in front or behind the blinds depending on whether the shades were internal or external. The entire system was saved in a *Radiance* geometry file and was used for the BSDF generation.

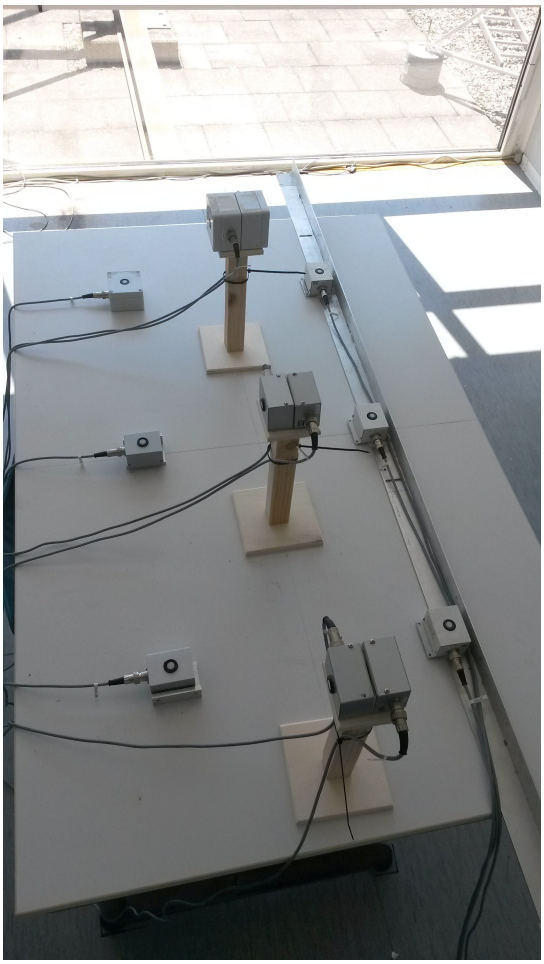

FIGURE 4.2: Measurement set-up

The optical properties of the venetian blind material were provided by the manufacturer and they were included within a *Radiance* material definition. The specifications of the glazing were also provided by the manufacturer; however, to simulate its angular dependent optical properties, the Roos model [52] was used. The model was introduced to the *Radiance* material definition via a function file along with the values of visual and solar transmittance of the glazing at normal incidence, its front and back reflectance, the number of panes and the calibration coefficient of the Roos model (q), depending on the coatings of the glazing unit.

Surface	Reflectance
Walls	0.521
Ceiling	0.800
Floor	0.223
Table	0.601
Venetian blind	0.810
External obstruction	0.546

TABLE 4.1: List of reflectances corresponding to the surfaces included in the simulation model used at the first prototype in the daylight laboratory at Fraunhofer ISE, in Freiburg

4.3 Results

Evaluation for static blinds

In order to evaluate the ability of the simulation model to predict the daylight conditions in the room, measurements were carried out for several days and for different positions of the venetian blinds. Using the weather data collected during the measurement days, the horizontal and the vertical illuminance at the sensor positions on the work surface were simulated for the corresponding window configuration and they were compared with the measured values. As explained in Chapter 2, the controller does not address each sensor independently since the shade configuration aims at improving the overall visual comfort in the room. Therefore, instead of comparing the values at each individual sensor, the average horizontal and maximum vertical illuminance were used to better represent the optimisation factors.
Figure 4.3 shows the comparison between simulations and measurements for four different configurations of the facade system: no solar control (blinds retracted), fully closed blinds, and extended blinds at two intermediate tilted positions. Although the actual measurements had a five second time-step, in the following graphs they have been averaged over five minutes. To correspond to the averaged measurements, the simulated values were calculated using measured horizontal global and diffuse irradiance, also averaged over five minutes. The simulations were performed for the time between 06:00 and 20:00 to cover all daylight hours in a day. A first look at the graphic comparison between the measurements and the simulations reveals a general agreement of the datasets and no large deviations occur.
Table 4.2 shows the Mean Bias Error (MBE), the Root Mean Square Error (RMSE) and their relative values as well as the average values of each measurement over all daylight hours. RMSE and MBE are commonly used in the daylighting literature in order to evaluate the agreement between two data series. The RMSE provides information on the deviation between the data series and the MBE indicates to which extend one data series tends to be larger or smaller than another. In this case, the two statistical quantities are used to evaluate the errors between the simulated and actual illuminance values.
According to Reinhart and Breton [53], the results of a simulation can be considered reliable if the MBErel remains below 15% and the RMSErel remains below 35%. Based on this definition, the accuracy of the daylight calculations used in the controller can be considered acceptable since the RMSErel remains below 25% for three out of four cases and in no case exceeds 27%, while the largest calculated MBErel is 14%. At a more detailed analysis, the highest values of the RMSErel are observed for the case of the fully tilt angles which can be also attributed to the overall lower illuminance values. The highest MBErel value is observed for the unshaded window on a cloudy day in March. In this case, the daylight simulations appear to over-predict both horizontal and vertical illuminance. However, since both positive and negative MBErel values appear Table 4.2 no systematic error is observed.
For the case of fully tilted blinds, the mismatch between the measurements and the simulations is more evident. Although the configuration was investigated over different days, both overcast and sunny, and small variations of one degree of the simulated tilt angle were tested to eliminate the possibility of positioning errors, there was no apparent improvement. To explain these discrepancies different assumptions are made. To begin with, the edge effects of the venetian blinds might become more prominent for large tilt angles significantly blocking the solar radiation. Additionally, the error margin always existing between simulations and reality due to

small irregularities of the actual material or geometry could lead to errors in large tilt angles. Moreover, the tilting of the blinds is not in reality as uniform as in the simulation model. Individual slats might be deviating from the defined tilt angle. To verify this claim, the angle of a sample of 10 slats was measured after a fully tilt angle was applied on the system and their average deviation from the prescribed angle was found $\pm 5^{\circ}$. In the cases of direct sunlight on the facade, small errors in positioning could allow direct radiation in the room and result to more noticeable discrepancies.
In general, the overall agreement between simulations and measurements is satisfactory leading to the conclusion that the simulation model is in fact able to replace the illuminance sensors or luminance cameras which are normally necessary to predict the visual conditions in the room.

Configuration (Illuminance)	MBE (lux)	RMSE (lux)	RMSErel (%)	MBErel (%)	Mean (lux)
Glazing (Horizontal)	-58.39	78.37	20	-14	355.74
Glazing (Vertical)	-30.55	52.93	19	-8.4	332.97
5° tilt (Horizontal)	-8	137.27	21.8	-1.3	633.36
5° tilt (Vertical)	52.21	154.41	24	8	693.86
40° tilt (Horizontal)	-3.25	27.04	8	-1.5	210.40
40° tilt (Vertical)	-15.80	31.54	9.7	7.3	233.23
70° tilt (Horizontal)	-24.66	59.82	26	-10	214.00
70° tilt (Vertical)	10.10	57.88	27	4.8	219.22

TABLE 4.2: Statistical errors for the comparison of simulated and measured illuminance values over an entire day, for different window configurations

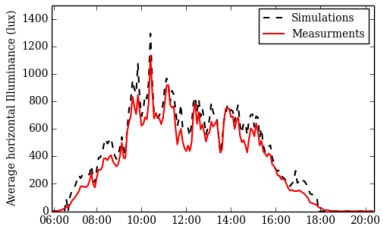

(a)

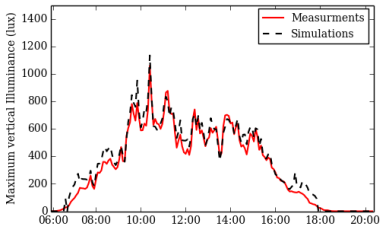

(b)

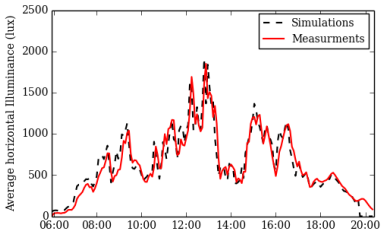

(c)

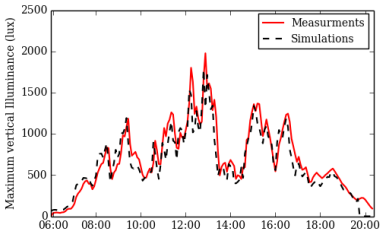

(d)

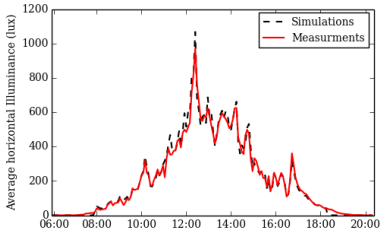

(e)

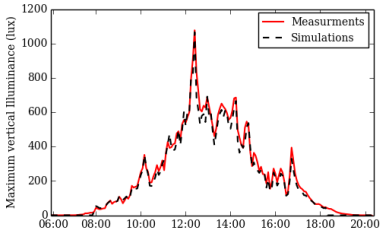

(f)

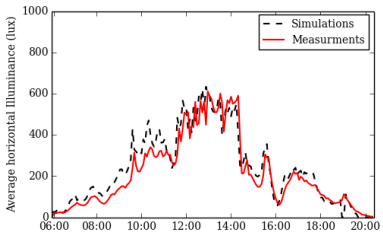

(g)

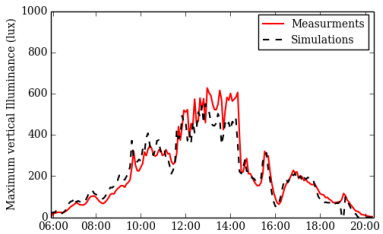

(h)

FIGURE 4.3: Comparison of simulations and measurements for a constant window configuration in relation to the global horizontal illuminance. (a) Average horizontal illuminance for uncovered window (25 March), (b) Maximum vertical illuminance for uncovered window (25 March), (c) Average horizontal illuminance for 5° tilt angle (14 June), (d) Maximum vertical illuminance for 5° tilt angle (14 June), (e) Average horizontal illuminance for 40° tilt angle (1 April), (f) Maximum vertical illuminance for 40° tilt angle (1 April), (g) Average horizontal illuminance for fully tilt angle (18 June), (h) Maximum vertical illuminance for fully tilt angle (18 June)

Evaluation for dynamically changing tilt angles

It has been shown already that the simulation model is able to satisfactorily predict the daylight conditions in the room for slat positions that are static over time. However, during the dynamic operation of the controller the positioning of the shading system relies only on the accuracy of the actuator since the received feedback functions correctively for the initial position of the blind at the beginning of the following time step. For the installed shading system, the adjustment of the height is very precise due to the use of the SMI motors; however, the tilting of the slats appears to be influenced by the weight of the suspended system. For the same applied signal, the average actuated angle when the shades are fully extended has been found to be up to 20% smaller than the average actuated tilt angle for half-way extended shades. Such errors in the positioning of the blinds become more prominent in the case of older shading systems and they affect the accuracy of the daylight simulations. Although such positioning errors can be in general mitigated with the use of newer and better calibrated shading systems, they cannot be entirely corrected and they require a substantial effort to be included in the simulation model. However, by tuning the fuzzy functions of the optimisation method accordingly, the influence of systematic positioning errors can be reduced without a significant impact on the controller's operation.
In this section the dynamic performance of the controller is evaluated under the assumption that the positioning of the venetian blinds might not be as accurate as in the static case. For this purpose, the ongoing illuminance measurements were compared with the simulated values that the controller anticipated after the setting of the optimum shading configuration. The default set-points of the fuzzy functions given in Chapter 2 were applied during the testing period.
In Figure 4.4, the comparison between measurements and simulations is presented for five days of sunny weather in summer and for five sunny days in winter. The days represented in the graphs are not consequent but are all within a short period of time. This is done to exclude overcast days with low solar radiation when the blinds remain retracted. The individual values calculated by the controller every 10 minutes in summer and 8 minutes in winter are represented by green dots while the blue line represents the continuous illuminance measurements in the room. The controller time-step was set to 8 minutes in winter due to the generally rapidly changing weather conditions. In summer, for continuously sunny weather conditions, a slightly longer time-step was applied to reduce the disturbance of the frequent blind movements.
As mentioned above, the controller was activated every few minutes and took corrective measures when the calculated illuminance values in the room did not comply with the visual comfort criteria. A visually comfortable situation, as defined in Chapter 2, was achieved when both the horizontal and the vertical illuminance values were found under the comfortable area of the corresponding membership functions. Since a range of values for both vertical and horizontal illuminance could fulfil the comfort condition, statistical errors such as MBE and RMSE were not considered relevant for the evaluation of the controllers operation. Instead, its main focus moved to the overall controller performance rather than the simulation accuracy. To evaluate the controller performance, two aspects need to be investigated; to which extend the positioning errors influence the the ability of the controller to estimate the visual conditions in the room, and what is the actual visual comfort offered by the controller. The first point is addressed by calculating the amount of time during

which the simulated illuminance values are at the same comfort level as the corresponding measurements. The second point is addressed by calculating the amount of time when the controller fails to prevent glare or to provide sufficient daylight in the room.
The fuzzy functions of the controller optimization correspond to the three areas separated by the red lines in each graph of Figure 4.4. The continuous red lines represent the $x_{V,uncomf}$ in the case of maximum vertical illuminance and the $x_{H,sp}$ in the case of the average horizontal illuminance. The dotted lines, in turn, represent the $x_{H,comf}$ for the horizontal illuminance and the $x_{V,sp}$ for the vertical. The degree of comfort declines as the horizontal illuminance values become smaller while the other way round applies in the case of vertical illuminance.
In summer, the simulated values and the measurements of the horizontal illuminance are found at the same comfort areas as defined by the fuzzy set-points at 88% of the occupied time. The corresponding percentage for the vertical illuminance is 79%. In winter, the illuminance measurements are found at the same comfort area as the simulated values at 78% of the occupied time in the case of the average horizontal illuminance and at 80% in the case of the maximum vertical illuminance. By examining the overall performance, one can see that the measured vertical illuminance remains within the acceptable limits for 98% of the controller actions in summer and for over 80% in winter. Additionally, the daylight provision is satisfactory throughout the entire day.
In the winter graphs, intense peaks at both the horizontal and the vertical illuminance values occur in the middle of the day. These peaks correspond to the periods when the user is absent and the controller retracts the blinds completely. As soon as no occupant is detected in the room, the controller prioritises energy efficiency and fully accepts the solar heat gains to reduce the heating demand. The opposite case applies in summer when during the user's absence the window remains fully shaded to maintain the room cooler.
By closely examining the graphs corresponding to summer measurements, the reader can observe a systematic under-prediction of both the horizontal and vertical illuminance, mainly during the afternoon hours. By examining the data collected during these days, it can be concluded that due to the elevated interior temperature, the control algorithm, in an attempt to avoid overheating, lowers the blinds fully varying only the tilt angle. As previously mentioned, the extension height of the blind can affect the applied tilt angle which tends to be smaller for fully extended blinds. Therefore, the slats remain in reality less tilted than the controller assumes resulting to a systematic under-prediction of the interior illuminance.
Another behaviour observed in the graphs for the winter measurements is that in the afternoon, after the horizontal illuminance values decrease below comfort level, they present an even increase for a short time. These values correspond to the automatic response of the electric light which is switched on when the daylight is insufficient and illuminates the room for the remaining work hours.

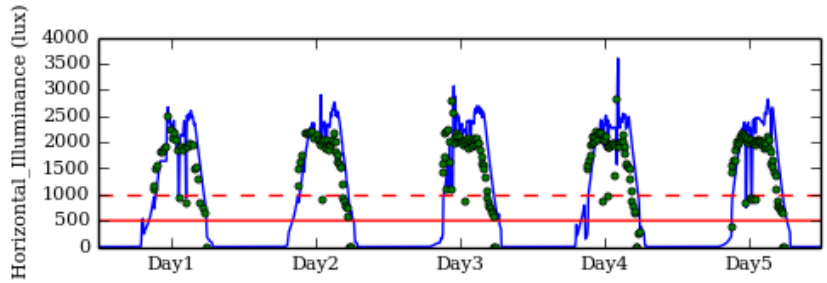

(a)

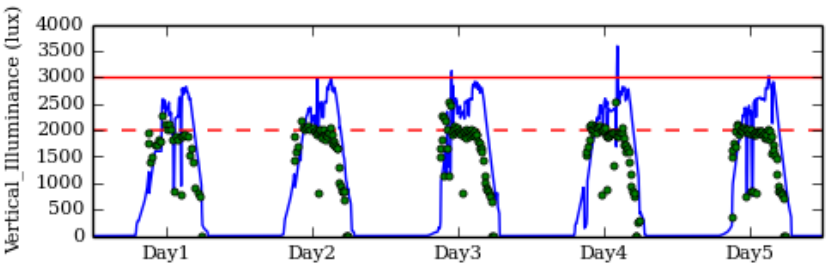

(b)

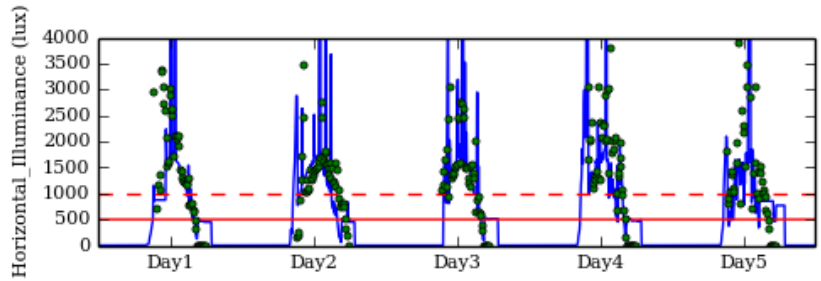

(c)

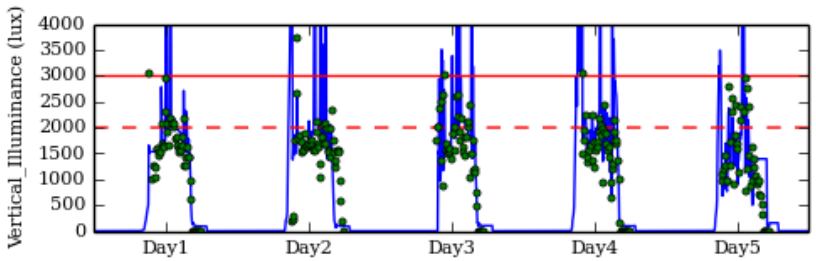

(d)

FIGURE 4.4: Comparison between simulations and measurements for dynamic movement of the Venetian blinds. The blue line represents the measured illuminance values and the green dots represent the simulated illuminance at every control action. The continuous red lines represent the $x_{V,uncomf}$ in the case of maximum vertical illuminance and $x_{H,sp}$ for the case of the average horizontal illuminance. The dotted red lines represent $x_{H,comf}$ for the horizontal illuminance and $x_{V,sp}$ for the vertical. (a) Average horizontal illuminance for five days between September 7 and September 13, (b) Maximum vertical illuminance for five days September 7 and September 13, (c) Average horizontal illuminance for five days between November 29 and December 8, (b) Maximum vertical illuminance for five days between November 29 and December 8

4.4 Test of the adaptation function in laboratory settings

After evaluating the simulation model and the decision process of the system, the adaptation function of the controller was tested in laboratory conditions. For the needs of the testing, the results of the two possible interactions (opening or closing the blinds) were tested separately under predefined and controlled scenarios. By testing the two situations separately, the adaptation results are evaluated based on the anticipated values. As it has already been explained in the algorithm description, user actions resulting to more open window configurations are perceived as attempts to increase daylight in the room leading to increased horizontal and vertical illuminance set-points. In this way, view out is also indirectly addressed. Under this assumption, the two scenarios defined in order to simulate the effects of the users' interactions with the system; hereafter referred to as *user profiles*, are summarized in the following basic situations; need for additional daylight and glare sensitivity.
To simulate the user profiles, a researcher; hereafter referred to as a *test user*, occupied the room at normal office hours interacting with the system in a prescribed manner according to the current illuminance measurements. Each user profile was tested over a two-weeks period and each profile testing period started with the default controller values. During those periods the test user readjusted the venetian blinds to adapt the visual conditions according to the tested profiles. The adaptation of the electric light was also tested, without applying any specific profile.

User Profile 1: User sensitive to glare

According to the first scenario, a user with high sensitivity to glare is expected to increase the window occlusion in order to create a more shaded environment. Following this principle, the test user tended to lower the blinds in order to reduce the vertical illuminance without compromising the daylight in the room.
As the test user had access to the illuminance measurements taken in the measurement room of the daylight laboratory at all times, the adaptation results could be evaluated based on the visual conditions that the test user applied in the room. Under this assumption, the test user took action as soon as the maximum vertical illuminance exceeded 2000 lux and adjusted the blinds in order to reduce the vertical illuminance while maintaining the average horizontal illuminance above 500 lux.
As can be seen in Figure 4.5, the vertical illuminance set-point decreases slowly for five days before saturating at 1300 lux. During the rest of the adaptation period, small fluctuations of maximum 50 lux occur without any significant changes. The weekends are not included in the graph since they do not contribute to the adaptation. The horizontal illuminance graph is not included since the set-point values present no change throughout the entire period. This is a reasonable situation since the controller did not identify any interaction as an attempt to receive additional daylight and the test user preserved the horizontal illuminance levels above 500 lux. The results of both adaptation profiles are summarised in Table 4.3 in comparison to the initial fuzzy logic set-points.

User Profile 2: User requiring additional daylight

This scenario refers to a users who prefers to frequently open the blinds. Although the controller cannot evaluate whether this action is taken in order to allow more light or more view to the outside, the adaptation of the fuzzy function set-points to

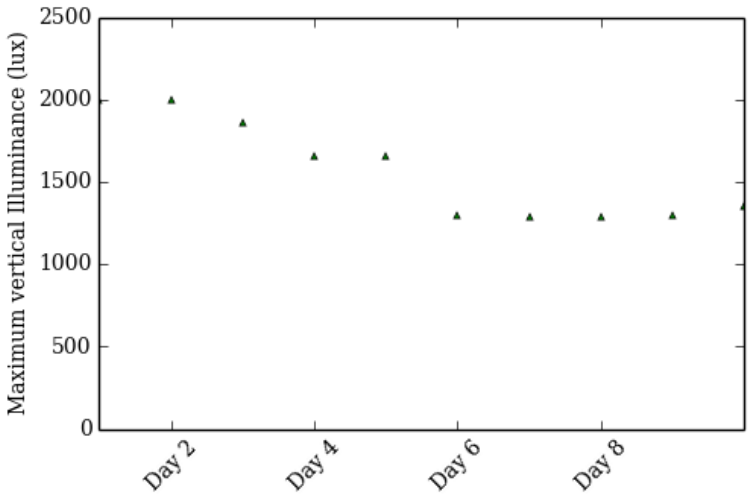

FIGURE 4.5: Adaptated $x_{V,sp}$ for a user sensitive to glare (User Profile: 1)

higher values is assumed to increase the uncovered window, addressing both situations.
In this case, the test user reacted by retracting the blinds as soon as the average horizontal illuminance measured by the sensors of the test installation dropped below 1000 lux and the maximum vertical illuminance did not exceed the 3000 lux after the adjustment. As before, the weekends were omitted from the graphs since no adaptation took place during these days. The new set-points are also summarized in Table 4.3. In Figures 4.6 and 4.7, the adapted values of both vertical and horizontal illuminance are presented. In the case of the vertical illuminance, the set-point increases slowly and after 5 days saturates at 3000 lux which is the highest value allowed. The horizontal illuminance set-point also increases for 6 days before also getting saturated at 1000 lux which is also the highest adaptation point possible.
The saturation at the highest set-points of horizontal and vertical illuminance is an anticipated outcome for the case of a user who, in general, tends to retract the shades. It must be noted that the upper limits applied on the adapted values are a necessary restriction in order to avoid extreme scenarios and ensure visual comfort. For example, the adaptation of the horizontal illuminance set-point to a very large value would prevent the algorithm from realistically evaluating the visual comfort and would result to situations of high glare in an attempt to increase the daylight in the room to the desired levels.

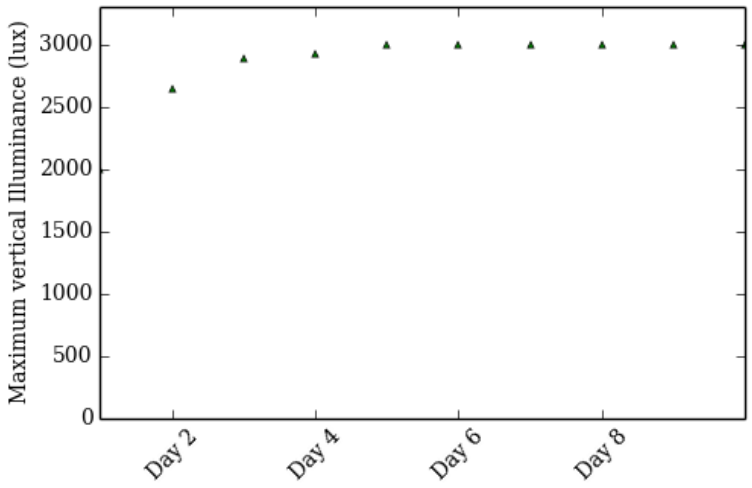

FIGURE 4.6: Adaptated $x_{V,sp}$ for user requiring more daylight (User Profile :2)

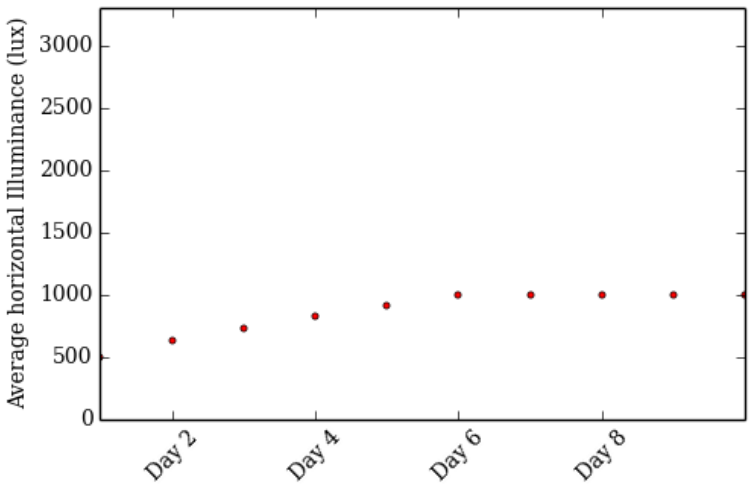

FIGURE 4.7: Adaptated $x_{H,sp}$ for user requiring more daylight (User Profile: 2)

	Variable	Default Value	Adapted Values User Profile 1	Adapted Values User Profile 2
Vertical Illuminance	$x_{V,comf}(lux)$	0	0	0
	$x_{V,sp}(lux)$	2000	1359	3000
	$x_{V,uncomf}(lux)$	3000	3000	3000
Horizontal Illuminance	$x_{H,uncomf}(lux)$	0	0	0
	$x_{H,sp}(lux)$	500	500	1000
	$x_{H,comf}(lux)$	1000	1000	1000

TABLE 4.3: Adapted horizontal and vertical illuminance set-points for the two user profiles. The Default values refer to the initial set-points of the fuzzy functions of the controller and the Adapted values of the two user profiles refer to the set-points at the end of the adaptation period.

Electric light adaptation

As mentioned above, for the evaluation of the light adaptation no specific user profile was used, as the adaptation process of the electric lights is not based on fuzzy logic like in the case of the shades. The test user interacted freely with the system to increase the *switch on set-point* and the *required illuminance level*. The adaptation process for each of the two adjustable variables can be investigated in detail for each individual interaction.
As before, the test user interacted with the system based on actual illuminance measurements in the room. The default values used for the light control, as given in Chapter 2, were; 100 lux for the *switch-on point* and 500 lux for the *desired illuminance level*. It must be reminded that the *desired illuminance level* corresponds to the average horizontal illuminance due to both natural and artificial light on the workplane.
For the evaluation of the dimming control, four adaptation days were examined for a single user action per day. For each action, a detail account of all parameters is presented. The four day pattern is summarized bellow:

- Day 1: The user switches on the lights before the controller takes action and dims the lights to the level considered comfortable.
- Day 2: The lights are switched on automatically when the average horizontal illuminance falls below the new set-point and some moments later the user reacts to increase the dim level
- Day 3: Similar as Day 2
- Day 4: The user switches the lights on before the controller takes action and adjusts them to the desirable level.

In Table 4.4 the adaptation for each day is represented by six different values; two referring to the values the controller used at the specific day annotated with *current*, the test-user actions annotated with *user* and the values after the adaptation annotated with *adapt*. The values involved are presented in detail demonstrating that although the user dimmed the lights to a high level, the controller adjusted the set points in small steps. This is due to the fact that the system avoids to learn random wishes that will potentially lead to unnecessarily high energy consumption

	Switch-on level (current) (lux)	Dim level (current) (lux)	Switch-on level (user) (lux)	Dim level (user) (lux)	Switch-on level (adapt) (lux)	Dim level (adapt) (lux)
Day 1	100	500	193	1099	193	625
Day 2	193	625	-	1222	193	781
Day 3	193	781	-	1189	193	976
Day 4	193	976	414	1050	414	1000

TABLE 4.4: Artificial light adaptation. The first column refers to the day of adaptation, the second and third column to the variables used by the controller that day, the fourth and fifth column to the values requested by the user and the two last columns refer to the adapted values

4.5 Evaluation of real office installation

In the previous section, the core elements of the controller such as the simulations and the algorithm were evaluated in a laboratory environment. In the current section, the results of the testing of the second prototype are presented. The second installation was built in a real life office in order to evaluate the acceptance of users unfamiliar to the control algorithm and to identify problems occurring during normal operation that hadn't been identified at the testing period. Based on the assumption that the simulations can predict the illuminance levels satisfactorily and due to many similarities between the two installations, no illuminance measurements were carried out. By not installing any illuminance sensors on the user's working surface, any further disturbance in the working environment was avoided.
The user input was received in both written form and through a series of short interviews. Two questionnaires were filled out by the user; one at the beginning of the testing period, to identify the problems the user was facing due to the previously installed control system and to understand the user's expectations of the prototype controller, and one at the end of the testing period, to evaluate the overall system performance. The interviews were carried out every two weeks in order to locate mistakes or problems at the system, fine-tune the controller variables and ensure the overall good function of the installation.
The testing of the second installation was carried out from May to October covering the entire summer and early fall. By monitoring the system and the user interactions with it, several conclusions about the performance of the controller could be drawn. The frequency of the user's interactions as well as the deviations from the system defined configurations allowed an estimation of the user satisfaction. Frequent interactions leading to radical shading position changes functioned as indicators of function errors or system crashes. Finally, the adapted set-points of the horizontal and vertical illuminance as well as the electric light were used to evaluate the adaptation process under real-life conditions and for a real-life user.
It must be noted that the office was only occasionally occupied by two people. For this reason only the regular user contributed to the evaluation through questionnaires.

User questionnaire at the beginning of the testing

At the beginning of the testing period, the occupant of the second installation was asked to describe his expectations of the newly installed controller and the problems he faced with the existing centralised shading control. The user appeared rather dissatisfied with the existing system due to delays in the system reactions which did not always correspond to the current solar conditions. The reasons for the actions of the system were not always clear to the user and the visual conditions were often considered uncomfortable mainly due to poor glare control. On the other hand, the daylight levels as well as the solar heat gain control were considered appropriate. When asked about his expectations of the prototype system the user stated that he expected more efficient glare protection as well as quick system reactions against increasing solar radiation. The entire questionnaire is included in Appendix C.1.

Error and problems arising during the testing period

The bugs and errors of the system were discovered through the user's input provided through frequent discussions and by investigating the corresponding monitoring data saved at the data logger. These problems can be mainly categorized under; software bugs, hardware problems and tuning issues.
Although at the time the controller software had already been tested in the daylight laboratory, some bugs mainly relevant to thermal comfort had gone unnoticed during the testing period and became more prominent during the hot summer months leading to issues related with the overheating prevention. These issues were identified when the controller failed to provide comfortable conditions and the monitored system behaviour did not agree with the function principles of the controller.
Concerning the tuning of the controller variables, the time allocated between the controller actions became an issue during the testing period. During the first weeks of the installation the user stated that in the early morning of sunny days the 20-minute time-step originally set between the controller's actions was very long. That would prevent the controller from sufficiently blocking the direct radiation between the actions and as a result uncomfortable visual conditions occurred. A shorter period of 10 minutes was tested for two more weeks without completely solving the problem. After communication with the user, the controller reaction time was set to 5 minutes for a testing period of three weeks. At the end of this period, the user reported that although in the early morning the glare protection was indeed improved, the disturbance due to such frequent movements during the rest of the day was substantial. For lack of a better solution in the current time, a compromise was reached when the time step was set to 8 minutes.
Hardware problems were observed since the second prototype installation had some fundamental differences from the first one. These differences were a result of the various limitations imposed at the installation site, strongly connected to the already existing components and to restrictions related to any invasive procedures in the building. A number of changes made to the original set-up concerned the switches, the position sensors and the location of the occupancy sensor. These changes led to some malfunctions during the testing period. However, such issues were fairly straightforward and easy to correct as soon as they were reported.
Finally, one of the major problems that compromised the function of the system was the unstable internet connection that inhibited the timely reception of weather data as well as the accessibility of the system remotely. This problem occurred at a frequency of about once per week causing discomfort to the users and preventing the controller's smooth function, despite the fact that the communication between the weather station and the controller was in general recovered quickly due to the easy access to the installation site. The communications were improved during the last weeks of testing by introducing an independent and more stable internet connection.
It is evident that the communication between the controller and any available source of weather data is of the highest importance to the installation and requires extensive planning to guarantee a reliable and quick connection.

User adaptation

As a significant amount of time during the second prototype testing period was dedicated in beta-testing and fine-tuning of the system, it was not until the final

weeks that the adaptation was tested. As in the case of the prototype, the testing period addressed both the shading system and the electric light control. The default set-points, as defined in Chapter 2, were also set as starting values for the controller; however, the electric light adaptation concerned only the switch-on set-point since the existing luminaires supported no light dimming.

Shade control

In the days of the adaptation period, the illuminance set-points were adjusted according to the user preferences. By a closer look at the adapted values, it can be inferred that the user's behaviour matches better the profile of a user sensitive to glare since the vertical illuminance set-point is eventually reduced with only some minor fluctuations. More specifically, the vertical illuminance set-point decreases to about 1400 lux and then after very small fluctuations increases to around 1600 lux (Figure 4.8). The horizontal illuminance set-point also presents a gradual increase of more than 100 lux due to these fluctuations (Figure 4.9).

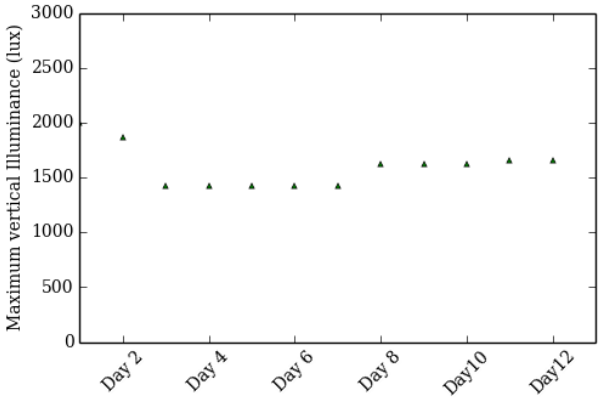

FIGURE 4.8: Adapted $x_{V,sp}$ after a three week testing period of the real office installation

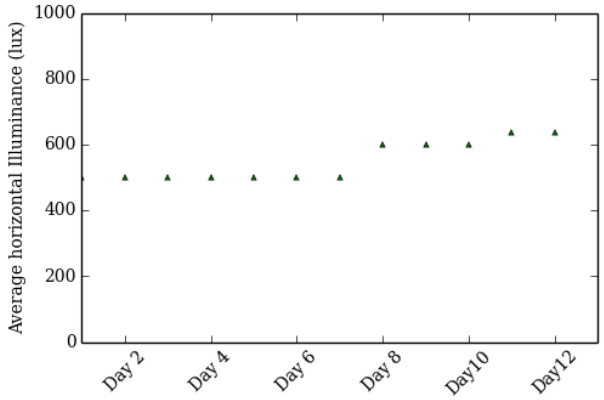

FIGURE 4.9: Adapted $x_{H,sp}$ after a three week testing period of the real office installation

Light control

The adaptation of the *switch-on set-point* of the electric light was considered less successful due to the following reasons. Since the controller's reaction to the change of occupancy status required a few seconds, the occupant did not allow the necessary time for the system to react according to the *switch-on set-point* upon arrival at the office very early in the morning. Instead, if the illuminance was low, he would immediately switch on the light upon entering the room resulting to irregular adaptation values (Figure 4.10).
The real-life testing of the electric light control and its adaptation algorithm revealed two weak points of the controller. To begin with, the long reaction time of the decision making and actualisation reduces the effectiveness of the controller especially when the user enters the space at hours of low daylight. The second issue lies at the adaptation process itself. As can be seen at the adapted values, the *switch-on set-point* adapts directly to higher or lower values depending on the user's action on the previous day instead of adapting for only increasing illuminance values in order to avoid irregular fluctuations.

Final user evaluation

At the end of the testing period the user was asked to fill out a second questionnaire (Appendix C.2), similar with the first one but oriented exclusively to the evaluation of the simulation-based control system. According to that, the user stated a general satisfaction with the prototype controller which was considered an improvement in relation to the previous centralized control system. The glare control was rather satisfying; however, it was noted that further room for improvement existed concerning the reaction time of the system. No big changes were observed concerning the thermal comfort since no complaints were formed for the previous system either. Finally, no comments were formed concerning the electric control, the function of which went mainly unnoticed by the user.

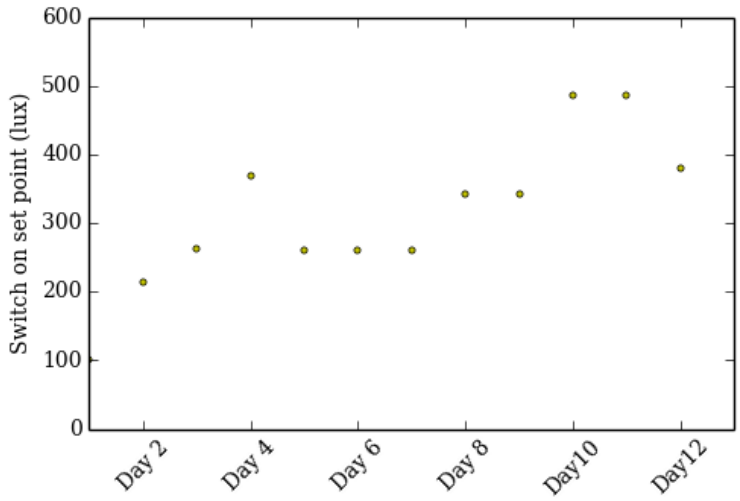

FIGURE 4.10: Adapted switch-on set point for the electric light after three weeks of testing of the real office installation

4.6 Discussion

From the evaluation of the two prototypes certain conclusions can be drawn. To begin with, the first indications suggest potential benefits due to the use of the controller concerning both visual comfort and energy savings from the electric light consumption. Additionally, the overall positive behaviour of the second prototype supports the claim that the system can be actually combined with already installed devices.

On the other hand, one must keep in mind that both prototypes were built for testing purposes. First of all, certain flexibility in the amount of sensors installed for the monitoring of the controller's operation was allowed. Specifically, although the use of position sensors allowed a very detailed understanding of the blind movement, it also created the impression of a test facility. At commercial installations, a large number of measurement devices can cause the discomfort of the user and eventually lead to poor acceptance. However, the use of sensors should be considered during the commissioning process for both modelling accuracy and error detection. In the current study, the two installations shared many similarities, therefore the validation of the simulations was only carried out for the first prototype. Nevertheless, a validation procedure could be established in future projects. The use of an industrial type installation was also preferred for testing purposes; however, any future version of the controller should be designed based on standard commercial components to fully take advantage of any already installed components in office buildings and reduce the communication time between the controller and the actuators. Finally, as far as the user evaluation is concerned, it is evident that further system assessment is necessary in order to acquire a clearer picture concerning the user acceptance and improve the controller performance.

Some points of the controller require further investigation and several issues not yet addressed are worth mentioned for future reference. The reaction time of the

controller, currently set to specific time intervals, should be further investigated especially for hours of high risk depending on the facade orientation. Moreover, the efficiency of the system concerning the reduction of energy consumption as well as the energy consumption of the system itself, neither included in this thesis, should be investigated. Finally, the development of a user interface could provide a significant improvement in future testing installations since it would help the user to accept the system easier and potentially provide real time feedback.

Chapter 5

Case study: Energetic and comfort potential

In the previous chapters, the controller was evaluated as to its algorithm and function. In this chapter, the performance of the controller is assessed as to its energy saving and visual comfort potential through a number of annual simulations and is compared with two common shade control strategies. Moreover, a sensitivity analysis of the daylight simulations of the controller is presented to investigate the influence of the exterior scene on the system's performance.

5.1 The case study

The building model

The annual simulations were carried out on the **Fener** simulation platform for a deep shoebox space with one external wall. A single window covered around 50% of the facade and was positioned 0.9 meters over the floor. The shading device used was the white venetian blind of the test installation described in Chapter 3 which could move between 0° and 65° by angle steps of 5°. Additionally, the lighting system assumed was also modelled according to the system described in Chapter 3. A rendering of the building is presented in Figure 5.1 and the input parameters of the simulations are summarised in Table 5.1.
Two facade orientations were investigated, south and south-west. The annual weather data used in the simulations was acquired from Meteonorm 7 and was based on 20-year measurements (from 1991 to 2010) for the area of Freiburg, Germany. The occupancy of the room was defined as extended office hours from 08:00 to 18:00 and from Monday to Friday. The default set-points of the fuzzy logic functions defined in Chapter 2 were used for the simulation-based control.
The surroundings of the building varied according to the needs of the simulations. For the comparison of the three systems, no obstructions were considered. Instead, only the surrounding ground with an albedo of 0.2 was included. To examine the response of the three systems to an obstruction near the building, an exterior construction was generated in front of the south-oriented facade. This construction served as an obstructing building, a floor higher than the investigated office. The adjacent building was located on the other side of a two lane street at a distance of 10 meters, shifted 1 meter to the east in relation to the office's west wall. Its walls were made of grey concrete with a reflectance of 0.35 and no windows were included. The total width of the building was 7.6 meters and its height was 6.5 meters in order to approximate an additional floor in relation to the room of the case study.

To investigate the sensitivity of the controller simulations to changes of the surroundings, a number of variations was applied at the scenery. Firstly, the effect of a snow covered ground to the simulated illuminance was investigated by increasing the ground albedo from 0.2 to 0.85. Furthermore, the influence of model inaccuracies of the surroundings was assessed by comparing different variations of the obstructions' size and material. These changes focused on three parameters; the obstruction height, the distance between the obstruction and the building, and the obstruction reflectance.

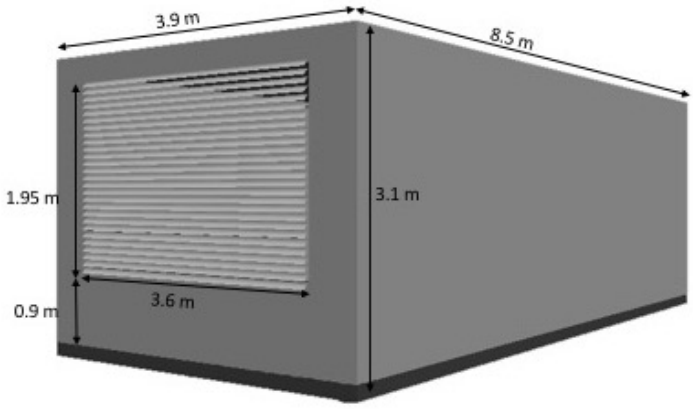

FIGURE 5.1: Illustration of the shoebox building used in the simulations

Daylight and thermal simulations

For all daylight simulations two sensor grids were defined; one for the calculation of the horizontal and one for the calculation of the vertical illuminance. The horizontal illuminance was allocated 32 sensors, distributed evenly over the entire room at a height of 0.8 meters over the floor and a distance of 0.5 meters from each wall. For the vertical illuminance, six sensors divided in three pairs were defined at a height of 1.2 meters over the floor. The sensor pairs were located in a row in the middle of the room, at distances of 1, 1.5 and 2 meters away from the window, each facing at opposite orientations parallel to it (Figure 5.2).
For the assessment of the annual cooling and heating energy demand, the thermal model of **Fener** was used [39]. According to this model, a sensible heat balance at the indoor air was solved. The heat balance was composed by the convective heat flux from indoor surfaces, the convective fraction of the internal heat gains, and the infiltration and ventilation sensible heat flux when the air was at the set-point temperature. The energy balances of the internal and external surfaces were also solved providing the boundary conditions of the conduction equation at every time step. Additionally, the thermal calculations concerning the fenestration systems in **Fener** were based on Directional Heat Gain Coefficients (DHGC), or directional g-values, and on BSDF to better describe the thermal impact of the three dimensional structures such as venetian blinds [54].

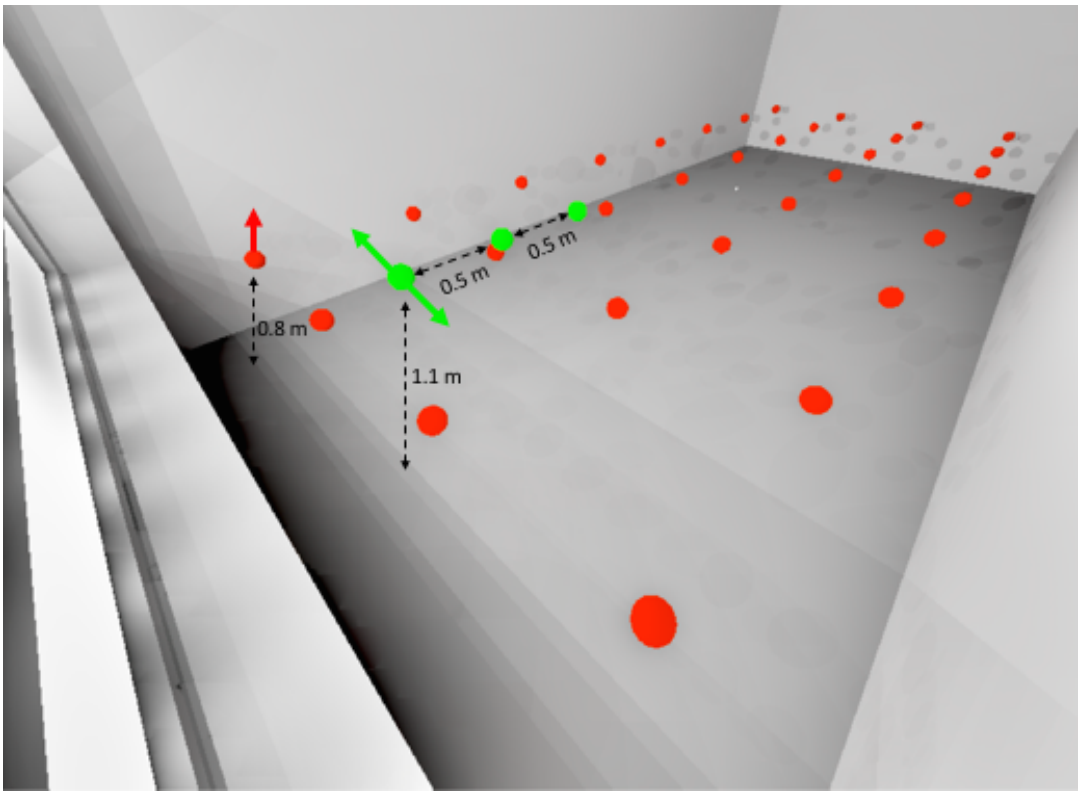

FIGURE 5.2: Sensor positions inside the shoebox geometry. The red dots correspond to the position of the horizontal illuminance sensors, 0.8 m over the floor. The green dots correspond to the positions of the vertical illuminance sensors. The arrows on the front vertical and horizontal illuminance sensors are indicative of the view directions of all corresponding measurements.

For the calculation of the lighting energy demand, according to the occupancy schedule mentioned above, the electric light dimming curve of Chapter 3 was used. In the case of the simulation-based control, the light was activated based on the average horizontal illuminance in the room. For the light control used with two other systems, the readings of an illuminance sensor at the centre of the room were used instead. For all three systems, the switch-on set point coincided with the required dim level and was set to 500 lux in order to fulfil the EN-12464-1 standard [17]. Both electric light controls allowed for a continuous dimming in order to adjust the light output. It must be noted that, according to the light dimming Equation (eq. 3.1), for an illuminance output of 500 lux the electric light did not function to its full power.
The two solar control strategies compared with the simulation-based control are the solar-tracking (or cut-off) strategy (see 5.2.1) and the radiation on the facade control strategy (see 5.2.2). Both systems took the occupation status of the room into account and reacted to accept or reject solar heat gains when the room was unoccupied based on the season to decrease the total energy demand for heating and cooling. Additionally, two different sets of heating and cooling set-points have been assigned; one for the working hours and one for the no-occupancy time.
The time step of all simulations was set to one hour.

Room width (interior)	3.6 m
Room length (interior)	8.05 m
Room height (interior)	2.8 m
Sky view factor	0.5
Ground albedo	0.2
Wall reflectance	0.5
Ceiling reflectance	0.7
Floor reflectance	0.2
Worktime schedule	8-18 LT
Infiltration/ventilation	0.5 ACH
Equipment heat gain	8.0 W m^{-2} (worktime)
Occupation	1 person (worktime)
People radiant fraction	0.5
Sensible activity level	63.72 W $person^{-1}$
Light installed power	10.1 W m^{-2}
Light radiant fraction	0.72
Illuminance set-point	500 lux
Heating thermostat set-point (according to DIN 18599)	20 C° (worktime) 15 C° (rest)
Cooling thermostat set-point (according to DIN 18599)	26 C° (worktime) 30 C° (rest)
Opaque surface construction	Exterior finish (1 cm) $\lambda = 0.25\ Wm^{-1}$ K^{-1} Insulation (5cm) $\lambda = 0.03\ Wm^{-1}$ K^{-1} Massive material (8 cm) $\lambda = 2.3\ Wm^{-1}$ K^{-1} $\rho_c = 2.3\ e^6$ J m^{-3} K^{-1} Interior finish (1cm) $\lambda = 0.25\ Wm^{-1}$ K^{-1}
Window dimentions	3.6 m x 1.95 m
Window U-value	1.1 W m^{-2} K^{-1}
Window SHGC (without shading device)	0.29
Window visible transmittance (without shading device)	0.54
Shading device	External white Venetian blinds Width of the slats: 80 mm Distance between the slats: 72 mm Reflectance: 0.8

TABLE 5.1: Input parameters for the annual simulations

5.2 Reference systems

Cut-off control

During occupation time, the cut-off control system extended the venetian blinds over the entire window and tilted the slats to an angle which was re-calculated at every time step according to the solar altitude, azimuth and building orientation in order to block the direct solar radiation (see Appendix A). The system benefit in this case was that the blinds only blocked the direct radiation component, which is mainly responsible for glare and overheating, while it allowed the diffuse radiation to increase the daylight in the room.
To avoid high shading configurations that would penalise daylight in the room, the system recognised overcast conditions by the global horizontal irradiance values and adjusted its operation accordingly. That would simulate a situation where a pyranometer was installed at the roof of the building. The irradiance threshold was set to 200 W/m^2 and the values were extracted directly from the weather file to be used as a weather indication, independently from the building orientation. Under the assumption that the average solar radiation on a summer mid-day in Germany is 1000 W/m^2, the threshold of 200 W/m^2 has been prescribed to address overcast days in summer and in winter.
If such a controller is combined with venetian blind systems that allow the slats to rotate around 180°, the solar-tracking algorithm can also address the negative calculated cut-off angles improving the visual conditions further. Different variations of the solar-tracking control are available in the market; however, little information concerning the source code of commercial control algorithms is available. For this reason, a simple version was used instead combined with a very common venetian blind system which allowed the slats to move from 0° to 65 ° with a tilt angle step of 5 °. In the case of negative cut-off angles, the slats were set to the horizontal position serving as the closest tilt angle available.
As commercial systems offer the option to program predefined reactions to specified situations, seasonal variations are possible in the control systems often separated into two seasons; heating and cooling. The switching between the two modes is commonly applied manually based on the user's perception of the seasons. Since such an experiential response is difficult to simulate, the average 24-hour external temperature was used as an indicator of the season and the set-point was set to 18 °C, as explained in Chapter 2. For the winter period the shading device was fully retracted to accept all the available solar heat gains; whereas, for the summer period the window remained fully covered during the entire day for the opposite reason.

Direct radiation control

The direct radiation control was structured as an on-off system that fully extended the shading device when the total solar irradiance on the window exceeded 150 W/m^2, leaving the window uncovered the rest of the time. The threshold of 150 W/m^2 has been defined according to previous studies such as the work of Wienold [48].
Although such strategies tend to significantly block the view contact to the outside and to often penalise the daylight admission due to the drastic movements of the system, they are widely used commercially as they only require a single sensor on the facade and they prevent glare effectively. Depending on the system, the tilt angle of the activated venetian blinds might vary. In the current case study, the extreme

case of totally closed blinds was chosen to demonstrate a scenario of high glare protection and reduced daylight. As in the case of the cut-off control, the direct radiation control was only applied when the room was occupied and for the rest of the time the blinds remained extended or retracted according to the season as explained above.

Behaviour of the compared systems for unoccupied room

To provide a clear overview for the comparison of all three systems for the case of no occupancy, the conditions and reactions of each system are summarised in a concise matrix in Table 5.2.

Case	Occup.	Day.	Temp. out. >18 °C	Temp. out. <8 °C	Indoor air temp.	Pos.
Controller 1	0	0	1	0	Any	Open
Controller 2	0	0	0	1	Any	Closed
Controller 3	0	0	0	0	>25°C	Open
Controller 4	0	0	0	0	<25°C	Closed
Controller 5	0	1	1	0	Any	Closed
Controller 6	0	1	0	1	Any	Open
Controller 7	0	1	0	0	>25°C	Closed
Controller 8	0	0	0	0	<25°C	Open
Cut-off control 1	0	0	1	-	Any	Closed
Cut-off control 2	0	0	0	-	Any	Open
Radiation control 1	0	0	1	-	Any	Closed
Radiation control 2	0	0	0	-	Any	Open

TABLE 5.2: Decision matrix for an unoccupied room for the simulation based control (Controller), the Cut-off control and the Radiation control. The first column indicates a numbered situations under a specific control strategy, the second column refers to the occupancy status of the room, the third column to whether it is daytime or not, the fourth and fifth to the average 24-hour outdoor temperature which when higher than 18 °C corresponds to the summer and when lower than 8 °C to winter, the sixth column refers to the current indoor air temperature and the last column refers to the position of the blinds. From columns 2 to 5, the indication 0 corresponds to NOT TRUE situations, the indication 1 corresponds to TRUE situations and the indication - means that the option in question is irrelevant. The indications in the sixth column refer to the indoor temperatures and the indications Open and Closed in the last column refer to fully open or fully closed venetian blinds at the entire window surface.

5.3 Simulation results

In the comparison of the three control systems the visual comfort is evaluated through two criteria; daylight admission and glare protection. The daylight admission in the room is expressed by the Daylight Autonomy (DA). DA refers to the spatial distribution of the annual percentage of daylight that exceeds 300 lux during occupied time. Three different values of DA are calculated; the maximum value, referring to the front of the room which is closest to the window, the minimum value, referring to the back of the room and the average value referring to the distribution over the

entire room.
The glare protection, expressed by the simplified DGP (DGPs), is investigated over the entire year calculated at every time step of the simulation. The DGPs is introduced for the presentation of this case study due to its dependence on the maximum vertical illuminance at eye level and at the computer screen which is used by the simulation-based control. Its purpose is to offer a comprehensible means of comparison for the three different scenarios, although it is not used within the actual control algorithm. The DGPs can be used instead of the full DGP in the case of venetian blinds since their agreement is good and their RMSErel is 8% [48]. To better interpret the DGPs values during occupation hours in the room, two important values are calculated; the 95 percentile, referring to the value below which the DGPs remains during 95% of the time and the total time in a year during which the DGPs exceeds 0.45 indicating high probability of disturbing glare [55].
By examining the estimated DA values (Table 5.3), the controller exhibits the highest maximum DA value in comparison to all three systems at both orientations due to its ability to control the height to which the shading device is extended. By allowing the lowest window area to remain uncovered, the light contribution at the area of the room closest to the window is higher in the case of the controller. As far as the south-west orientation is concerned, the mean DA of the cut-off control outperforms the controller by 8% absolute difference and the radiation control by 11%. The minimum DA referring to the back of the room remains below 10% for all three cases with very similar values for the controller and the radiation control while the corresponding value for the cut-off control is roughly double in relation to the other two systems. At the south orientation, the DA values of the simulation-based control and the cut-off control present only small deviations from one another with the cut-off control exhibiting slightly higher values. Both systems appear to perform significantly better than the radiation control.
The evaluation of the annual glare levels in the room requires a more careful investigation since the results might be highly divergent depending on the investigated sensor position and view direction. Although for both orientations a quick overview of all the sensor positions is included, the temporal map and the presented results concern only the sensor position which is most affected by glare. This sensor corresponds to the position of maximum vertical illuminance used in the controller algorithm.
In the case of the south-west orientation, five out of six sensors present low glare within the acceptable levels. No hours of DGPs higher than 0.45 are observed and the 95 percentile of annual DGPs remains bellow 0.35 for all three systems. However, the sensor located at a distance of 2 meters away from the window, with a view direction parallel to the window and towards south-east appears to be highly affected by glare leading to very different results. By closer investigation of this particular position, the controller performs better than the other two systems with a 95 percentile of 0.36 and no hours of disturbing glare. The radiation control performs slightly worse with a 95 percentile of 0.41 and 65 hours annually when the DGPs exceeds 0.45 corresponding to 3% of the total occupied time. Finally, the performance of the cut-off control for the south-west orientation is rather lower with a 95 percentile of 0.59 and the percentage of occupied hours when disturbing glare occurs for the specific illuminance sensor being 25% of the total time. For the south orientation, the glare levels are lower for all three systems with lower 95 percentile values and significantly less hours of disturbing glare. The sensor most affected by glare is in this case located one meter away from the window and has a view direction parallel to the window, towards east. The lowest 95 percentile value is observed for the case

of the radiation control with a value of 0.26 and no hours of disturbing glare while the controller follows with also no hours of disturbing glare and a 95 percentile of 0.30, remaining within the visual comfort standards. For the cut-off control, the corresponding value is 0.32 and only 3 hours of disturbing glare is anticipated annually (Table 5.4). By carefully examining these results, the correlation between the DGPs values and the previously reported DA values is evident; with a positive relationship observed between improved daylight in the room and increased glare levels.

	Simulation-based control	Cut-off control	Radiation control
$DA_{max}(SW)$	88.7%	84.6%	86.8%
$DA_{mean}(SW)$	36.0%	43.07%	32.1%
$DA_{min}(SW)$	3.2%	7.0%	3.6%
$DA_{max}(S)$	87.8%	87.5%	86.9%
$DA_{mean}(S)$	44.0%	46.9%	29.9%
$DA_{min}(S)$	2.8%	6.1%	5.9%

TABLE 5.3: DA results for the three compared control systems: simulation-based control, cut-off control, radiation control, for south and south-west orientation

	Simulation-based control	Cut-off control	Radiation control
$DGPs_{95percentile}(SW)$	0.36	0.59	0.41
DGPs > 0.45 (hours/year) (SW)	0	664	65
$DGPs_{95percentile}(S)$	0.30	0.32	0.26
DGPs > 0.45 (hours/year) (S)	0	3	0

TABLE 5.4: DGP results for three compared control systems: simulation-based control, cut-off control, radiation control, for south and south-west orientation

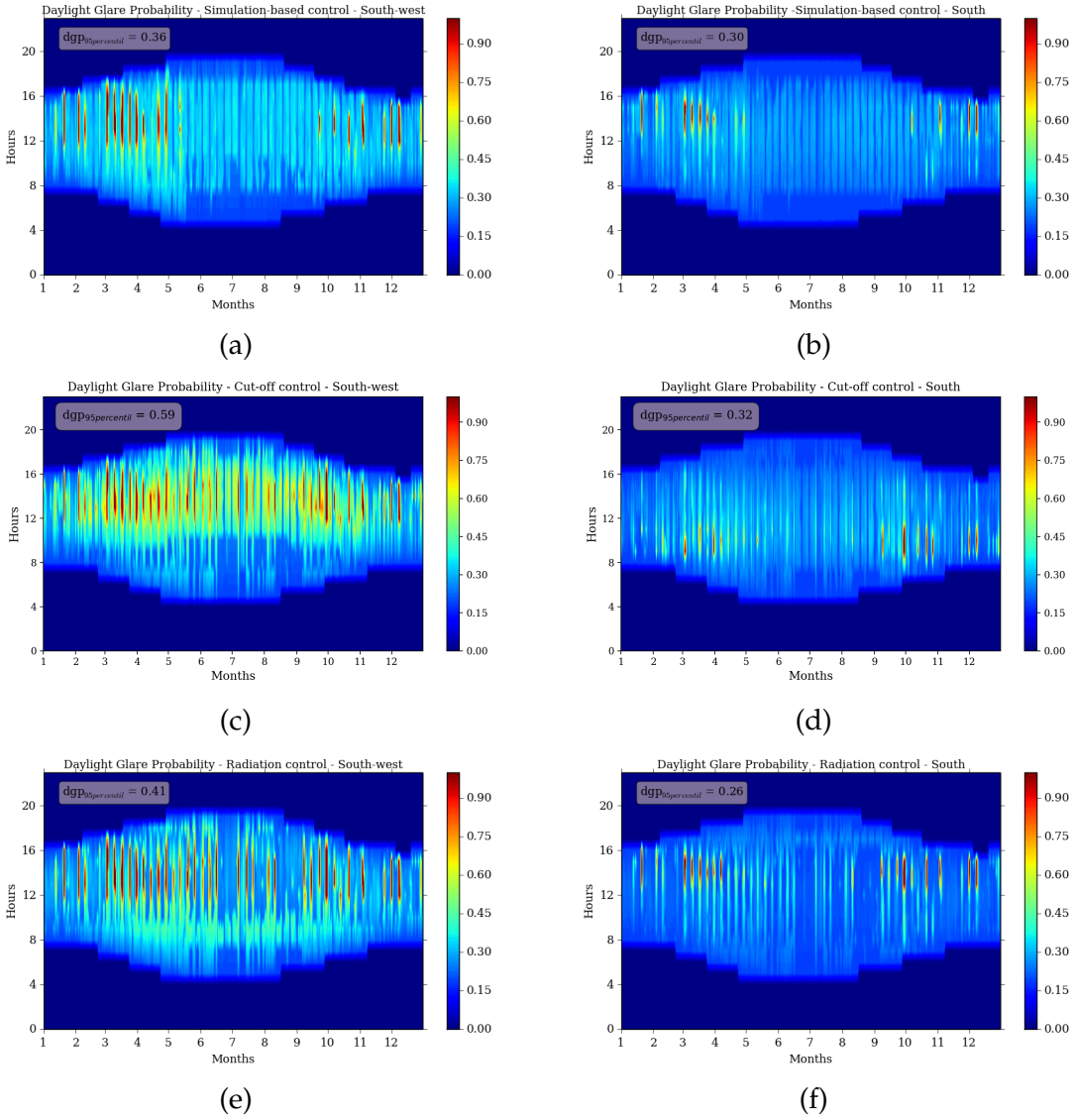

FIGURE 5.3: Temporal map of DGPs. (a) Simulation-based control (South-west orientation), (b) Simulation-based control (South orientation)), (c) Cut-off control (South-west orientation), (d) Cut-off control (South orientation),(e) Direct radiation control (South-west orientation), (f) Direct radiation control (South orientation)

In terms of the annual energy demand, it is evident that the controller performs better than the other two systems regardless of the building orientation (Figure 5.4). In general, at the south orientation the total energy demand appears reduced for all three systems over the south-west orientation. More specifically, at the south-west orientation the simulation-based control presents a total energy demand 10% lower than the cut-off control and 13% lower than the radiation control while the corresponding values for the south orientation are 17% and 24%. By looking at the two orientations in more detail the reader can observe that, despite the similar values of the three systems, the heating energy demand for the south-west orientation is slightly higher for the case of the simulation-based control. This is a result of the reduced admission of solar radiation in order to improve the glare protection in the

room. This increase in heating energy demand is compensated by a substantial reduction of the cooling energy demand in comparison to the other two systems. This reduction of the cooling energy demand for the controller depends strongly on the cooling activated during the no-occupancy period, combined with the selective rejection of solar heat gains in the mid-season.
The radiation control follows second and the cut-off control exhibits the highest cooling energy demand. Finally, the lighting energy demand presents only a minor difference between the controller and the cut-off control and a roughly 35% reduction over the radiation control. At the south orientation, the energy demand of the three systems follow a very similar distribution over heating, cooling and lighting energy, with the controller outperforming the other two systems. The energy demand values are summarised in Table 5.5.

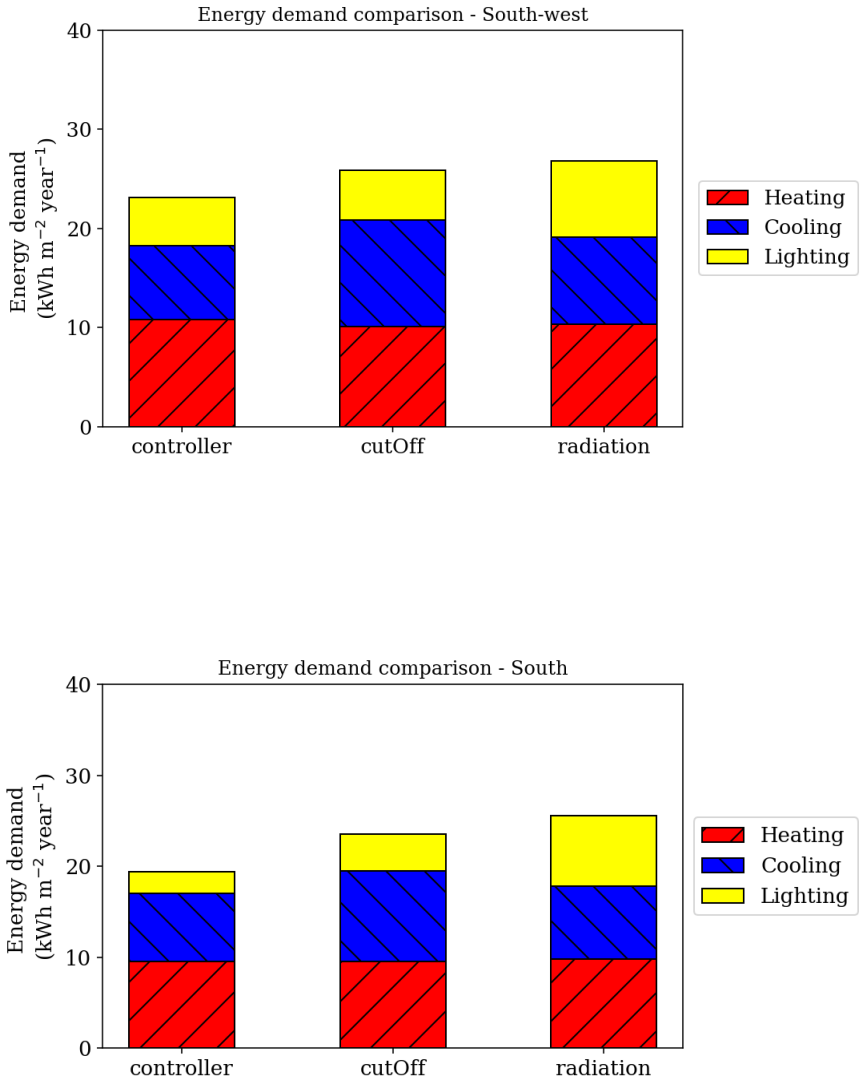

FIGURE 5.4: Energy demand comparison for the three control systems. (up) South-west orientation, (down) South orientation

As far as the view out is concerned, the calculated window occlusion is used for lack of a better expression. The window occlusion is the percentage of the geometrically calculated projection of the blinds on the window over the entire window area as given in Equation 5.1; where A refers to the covered area, θ refers to the tilt angle of the blind, x_{slat} refers to the width of the slat, N refers to the number of released slats and h_{window} refers to the total height of the window.

$$occlusion = \frac{\sum_{i}^{N} x_{slat} \cdot sin(\theta_i)}{h_{window}} \tag{5.1}$$

For the visual representation of the comparison, six temporal maps for the entire

	Simulation-based control	Cut-off control	Radiation control
South-west orientation			
Heating (kW $m^{-2}year^{-1}$)	10.8	10.1	10.3
Cooling (kW $m^{-2}year^{-1}$)	7.5	10.7	8.8
Lighting (kW $m^{-2}year^{-1}$)	4.9	5.0	7.6
Total	23.2	25.8	26.7
South orientation			
Heating (kW $m^{-2}year^{-1}$)	9.6	9.5	9.8
Cooling (kW $m^{-2}year^{-1}$)	7.5	10.0	8.1
Lighting (kW $m^{-2}year^{-1}$)	2.4	4.1	7.8
Total	19.5	23.6	25.7

TABLE 5.5: Energy demand for three compared control systems

year are included, one for each system and orientation, illustrating the geometrically calculated occlusion percentage of the window and taking into account the height and tilt angle of the blinds (Figure 5.5). To illustrate the behaviour of the control systems during the occupied hours more clearly, the occlusion percentages during no-occupancy periods are not taken into account in these graphs. For further interpretation, the mean occlusion percentages were calculated for all the occupied hours in a year and were narrowed down further for two seasons, summer (May-September) and winter (October-April) and for the morning and afternoon working hours at each season. In this way, the behaviour of the two systems can be investigated under different insolation conditions. All the calculated values are summarised in Table 5.6.

For the south-west orientation, as expected by the results referring to the DA and the glare control, the mean annual occlusion for the controller appears to be higher than the cut-off control by an absolute difference of 15% and lower than the radiation control by 6%. Through a closer examination of the calculated values of window occlusion, the simulation-based control appears to cover in general a slightly larger window aperture in relation to the cut-off control systems. The radiation control presents the highest occlusion of all three cases. The differences between the simulation-based and the cut-off control become especially prominent during the afternoon hours for both the winter and the summer months when the occlusion due to the cut-off control is very low as one can also observe in Figure 5.4. During the afternoon hours, the average covered window aperture due to radiation control remains above 50% in both winter and summer months; exceeding the other two systems at all times. The average window occlusion is rather even for all three systems during the morning hours in the winter with absolute differences within a 10% range. Finally, one can observe that during the morning hours in summer the lowest average occlusion corresponds to the radiation control without significant deviations from the other two systems.

Looking at the south orientation, the average uncovered window apertures for the case of the controller and the cut-off control present only minor absolute differences of 1-2% and slightly more (6% absolute difference) during the morning hours in the summer months, with the cut-off control always presenting slightly lower values. On the other hand, the radiation control presents at all times throughout the year a substantially higher average window occlusion than the other two systems, especially in the case of the summer months.

To address the feature of the controller to vary the extension length of the shading

system, the average uncovered aperture at the lower part of the window at both orientations does not exceed 10% corresponding to an area of about 0.3 meters height. Since the window is located at less than one meter over the floor, the uncovered lower part of the window is positioned around the eye level of the user and therefore contributes only to the small degree at the unobstructed visual contact to the outside.

	Simulation-based control	Cut-off control	Radiation control
South-west orientation			
Average annual occlusion	42%	27%	48%
Average winter occlusion	33%	23%	40%
Average winter height occlusion	90%	100%	100%
Average winter occlusion (morning)	24%	20%	30%
Average winter occlusion (afternoon)	42%	26%	50%
Average summer occlusion	56%	33%	60%
Average summer height occlusion	93%	100%	100%
Average summer occlusion (morning)	51%	49%	44%
Average summer occlusion (afternoon)	61%	17%	75%
South orientation			
Average annual occlusion	20%	19%	56%
Average winter occlusion	22%	21%	54%
Average winter height occlusion	82%	100%	100%
Average winter occlusion (morning)	22%	21%	49%
Average winter occlusion (afternoon)	23%	21%	44%
Average summer occlusion	17%	14%	68%
Average summer height occlusion	89%	100%	100%
Average summer occlusion (morning)	17%	11%	78%
Average summer occlusion (afternoon)	16%	17%	59%

TABLE 5.6: Geometrically calculated percentage of window occlusion during occupation hours for the simulation-based control, the cut-off control and the radiation control

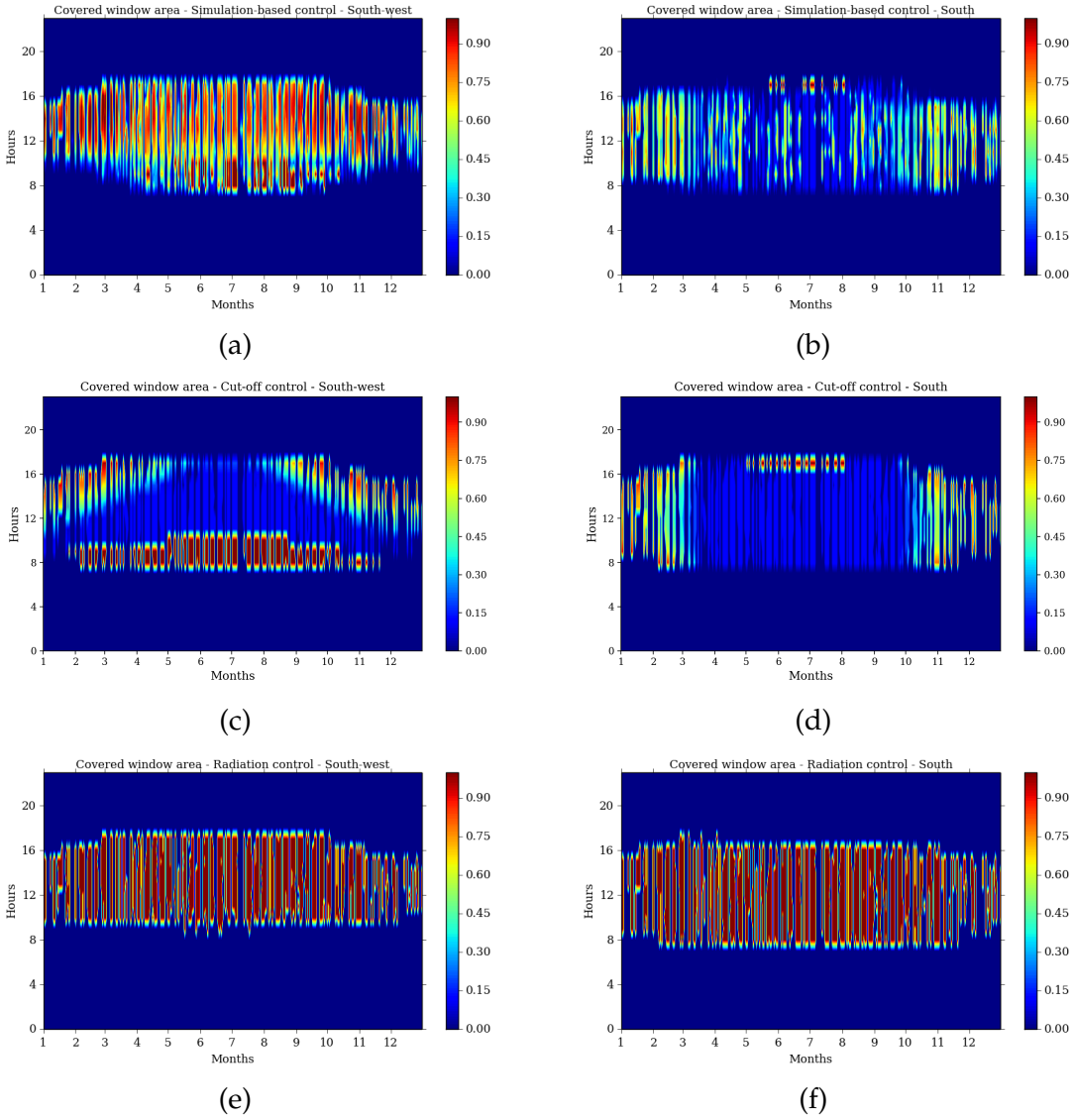

FIGURE 5.5: Average window occlusion. (a) Simulation-based control (South-west orientation), (b) Simulation-based control (South orientation),(c) Cut-off control (South-west orientation), (d) Cut-off control (South orientation),(e) Radiation control (South-west orientation), (f) Radiation control (South orientation). The occlusion percentages during no-occupancy periods are not taken into account in these graphs.

Finally, the performance of the three systems in the presence of an obstruction at the area adjacent to the south-oriented building is compared in a similar manner. As expected, the average annual occlusion due to the simulation-based control decreases by 4% absolute difference by including the building surroundings in the simulation model. The radiation control also presents a very similar reduction since its function depends on the values of the total irradiance on the facade which accounts for changes in the building surroundings. On the other hand, the cut-off control's reactions remain unaltered since the tilt angle applied by the system depends only on the solar position.
Although no significant changes are observed in the glare conditions of the room for any of the three systems, the DA presents a higher reduction for the cut-off control

	Simulation-based control	Cut-off control	Radiation control
Average annual occlusion	16%	19%	52%
Maximum DA	87.8%	87.2%	85.2%
Mean DA	38.7%	38%	26.6%
Minimum DA	0.2%	0.2%	0.2%
Heating energy demand (kW $m^{-2}year^{-1}$)	10.7	10.6	10.5
Cooling energy demand (kW $m^{-2}year^{-1}$)	7.0	9.2	7.9
Lighting energy demand (kW $m^{-2}year^{-1}$)	2.7	5.1	8.5
Total	20.4	24.9	26.9

TABLE 5.7: Summarized performance results for the simulation-based control, the cut-off control and the radiation control, at south orientation with the addition of an obstructing building.

in comparison to the corresponding effects of the simulation-based control and the radiation control. Despite the fact that only minimal changes occur in the maximum DA of all three systems, as far as the mean DA is concerned, a reduction of about 9% is observed for the cut-off control; whereas the corresponding reduction for the other two systems is calculated to around 5% for the simulation-based control and 3% for the radiation control. Finally, no useful conclusions can be drawn for the minimum DA value since a strong reduction is observed for all three systems, whose value falls below 1%.

As far as the energy demand is concerned, the results are quite similar for all three systems. A small increase of the total energy demand is observed and the controller outperforms the other two systems, like in the previous cases. At a closer look, the total energy demand increase corresponds to a small increase of the heating energy demand, a reduction of the cooling energy demand and another small increase of the lighting energy demand. The results for the three systems under comparison are summarised in Table 5.7.

Based on this comparison, it can be inferred that by including the building surroundings within the simulation model of the controller the visual comfort is improved not only by maintaining the daylight levels in the room higher but also by avoiding unnecessary window occlusion. These visual comfort benefits of the controller can eventually lead to an improvement of the user acceptance in comparison to systems such as the ones described. Finally, regarding the comparison of the energy demand for the three systems, the changes occurring, although in agreement with the reduced radiation reaching the building, do not reveal any additional advantage of the controller over the other two systems that can be specifically attributed to the implementation of the building surroundings in the simulation model. However, it is reasonable to assume that in cases of large scale installations the energetic effects due to the implementation of the simulation-based control could potentially sum up leading to more prominent differences.

5.4 Sensitivity of the simulation to the building surroundings

The assessment of the influence that the different parameters describing the surroundings of the model geometry have on the daylight simulations is necessary to identify the controller's susceptibility to commissioning errors or unexpected changes of scenery. The parameters investigated within this work are; the ground albedo, the distance between an obstruction and the facade, the height and the material reflectance of the obstruction. The effect of the changes in the height and the reflectance is further investigated in relation to the obstruction's distance from the simulated building. The building model used was the south-oriented geometry with the model parameters of Table 5.1 and the corresponding vertical and horizontal illuminance sensor grid described in the previous section. No shade control was used in the simulations to directly evaluate the effect of the investigated parameters.
In the case of the ground reflectance, no obstruction was included in the simulation. The reference value of 0.2 corresponding to the average ground albedo at a residential area was compared with the case of the ground being covered with fresh snow, corresponding to an albedo value of 0.85. In the remaining cases, a construction directly in front of the building's facade, very similar to the one used in the previous section, was included in the simulation model. The construction represented an obstructing building, longer and a floor higher than the simulation building, with no windows included. Two reference cases, denominated Reference A and Reference B, were defined to address the different comparison scenarios of an obstruction at 10 and at 5 meters from the building's facade respectively. Reference A construction was used to evaluate the effect of a variable distance between the facade and the obstruction and for the comparison of variable obstruction heights and reflectances. Reference B was used to further examine the correlation of the effects of the obstruction's height and reflectance with its distance from the facade. The parameters of the reference obstructions are included in Table 5.8. In Table 5.9 the different cases under investigation are summarized.

	Reference A	**Reference B**
Floor Dimentions	8.5 m x 7 m	8.5 m x 7 m
Height	6.5 m	6.5 m
Reflectance	0.35	0.35 m
Distance from the building	10 m	5 m

TABLE 5.8: Parameters of the reference constructions obstructing the south facade.

Parameter	**Value**
Distance from the building	• $8\ m$ • $12\ m$
Height	• $4.5\ m$ • $8.5\ m$
Reflectance	• 0.5 • 0.65

TABLE 5.9: Parameter variations of the construction obstructing the south facade.

To evaluate the effect that the parameters describing the obstruction have on the controller's daylight simulation, the horizontal and the vertical illuminance of each case was calculated. As before, the average horizontal and the maximum vertical illuminance were used instead of the values from individual illuminance sensors to better represent the controller operation. Their deviations from the reference case are expressed in terms of RMSErel and MBErel which are summarised in Table 5.10 for the case of variable ground albedo and in Table 5.11 for the cases where an obstruction is included in the simulation model. The results in Table 5.10 correspond to a sunny day in the beginning of February, while the results in Table 5.11 correspond to sunny day in late May.

Upon close examination of the results concerning the ground albedo, a substantial increase is observed in both the average horizontal and the maximum vertical illuminance. As the RMSErel and MBErel values indicate, the snow coverage of the building surroundings can result to an increase of almost 15% of the calculated vertical illuminance in the room and an even higher value of the average horizontal illuminance. Although situations of such intensity are normally limited to a few days per year, depending on the climate, the impact of the ground albedo on the daylight simulations must be taken into consideration during the commissioning process.

In the presence of an obstruction in front of the facade, small changes in the modelling parameters seem to also have a strong influence on the daylight simulations. To begin with, by reducing the distance between the obstruction and the facade by two meters, a reduction of over 18% is observed in the calculated illuminances. On the other hand, by increasing the distance of the reference case by the same interval the observed illuminance is increased at a lower rate, by 13% for the horizontal illuminance and slightly over 10% for the vertical. The obstruction height appears to have the strongest influence on the daylight simulations. By reducing the obstruction height by two meters, the impact on the horizontal illuminance is substantially higher than on the vertical illuminance. Additionally, no strong correlation between

the effect of the obstruction height and the distance between the facade and the obstruction is observed. When increasing the obstruction height by two meters, the effect on the illuminance values is significantly lower; however, the average horizontal illuminance presents a larger reduction than the maximum vertical illuminance. As before, no correlation with the distance of the obstruction from the building is observed.
The calculated illuminances appear to increase with the material reflectance, although its impact is smaller than the impact of the geometrical characteristics. However, a strong relation with the distance from the obstruction is observed. More specifically, a 15% increase of the reflectance in absolute value results to a three times higher increase of the calculated illuminance when the distance between the obstruction and the facade is reduced to half. It must be noted that the investigated material was assumed to be a Lambertian diffuser and no specularity was taken into account.

	Horizontal Illuminance	*Vertical Illuminance*
RMSErel	16.9 %	14.7 %
MBErel	-10.6 %	-9%

TABLE 5.10: Statistical difference of the average horizontal and the maximum vertical illuminances for a ground albedo of 0.2 and a ground albedo of 0.85.

		Horizontal Illuminance		*Vertical Illuminance*	
Parameter	**Reference case**	**RMSErel**	**MBErel**	**RMSErel**	**MBErel**
Distance (8 m)	Reference A	18.5%	20.5%	18.9%	18.3%
Distance (12 m)	Reference A	13.0%	-15.8%	10.4%	-10.8%
Height (4.5 m) & Distance (10 m)	Reference A	25.3%	-33.4%	14.9%	-15.5%
Height (4.5 m) & Distance (5 m)	Reference B	28.5%	-32.1%	10.9%	-9.9%
Height (8.5 m) & Distance (10 m)	Reference A	14.8%	16.9%	4.7%	4.4%
Height (8.5 m) & Distance (5 m)	Reference B	14,6%	15,3%	3.7%	3.8%
Reflectance (0.5) & Distance (10 m)	Reference A	1.9%	-1.5%	1.1%	-0.8%
Reflectance (0.5) & Distance (5 m)	Reference B	6.4%	-5.5%	2.2%	-1.9%
Reflectance (0.65) & Distance (10 m)	Reference A	3.6%	-2.6%	1.2%	-0.7%
Reflectance (0.65) & Distance (5 m)	Reference B	12.1%	-10.6%	4.8%	-4.0%

TABLE 5.11: Statistical differences of the average horizontal illuminances and the maximum vertical illuminances between the reference cases and cases where one model parameter has been changed. The variable parameter is given in the first column and the reference case for the specific comparison is defined in the second one.

5.5 Discussion

Looking at the comparison of the simulation-based control with the other two reference systems, it can be concluded that significant benefits are to be expected by its implementation regarding both the visual comfort and the building energy performance. It must be noted that the versions of the two reference systems used for the comparison are not very elaborated but are representative of older control systems that are commonly found in commercial buildings. The set-points defined for the operation of both reference systems in the case study were selected according to literature references; however, their exact impact on the performance of the corresponding systems was not further investigated within this work.
The performance of the controller appeared slightly lower in comparison to the cut-off control when the aspects of daylight and window occlusion were independently examined but exceeded the performance of the radiation control in both situations. The controller performed substantially better than the cut-off control regarding glare protection despite the tilt angle limitations (no negative angles) of the assumed venetian blind system. Additionally, the overall energy demand in the case of the controller presented a substantial reduction over the two reference systems at both orientations. At large, each aspect presented a promising performance with daylight admission remaining within the standards of commonly used shading controls, reliable glare protection and energy efficiency. Another benefit of the controller was its ability to maintain its high performance independently of the obstructions surrounding the installation site. That was achieved by including them in the simulation model to adjust the controller operation accordingly, without unnecessarily penalising the energy demand and daylighting of the space.
By examining the effect that different modelling parameters of the building surroundings have on the controller's simulations, the geometrical characteristics of the nearby obstructions were found to have the strongest influence. The impact of the obstruction's optical properties was increased with their proximity to the building facade. Additionally, radical changes in the ground albedo were found to also have a strong impact on the simulated illuminance in the room. This analysis was carried out by assuming no specular reflections in the surroundings that could eventually compromise the controller operation. A closer look at the results suggests that the average horizontal illuminance tended to be more susceptible to changes in the building surroundings. It is worth noting that although the values of individual illuminance sensors might present larger deviations, only the average horizontal and maximum vertical illuminances are relevant for the controller. Additionally, small deviations as an effect of model inaccuracies can be mitigated with the use of the fuzzy logic optimisation.
Closing, the simulation-based comparison can only offer a rough estimation of the performance of the three systems. Despite the uncertainty related to simulation models that leads to rather unrealistic comparison results (due to the assumption of ideal conditions and perfectly operating systems), it can be still assumed that the real-life performance of the developed system remains promising. It is therefore reasonable to conclude that the controller concept can not only enhance energy efficiency but also improve the visual conditions with minimum disturbance to the working space due to the reduced use of sensors for the visual conditions.

Chapter 6

Theoretical basis and evaluation of the developed glare control

According to the control algorithm description in Chapter 2, the glare protection is designed based on two aspects; the prevention of direct radiation on the work surface and the control of the vertical illuminance values on the computer screen and at the eyes of the observer. The developed method is inspired by the DGPs which strongly depends on the vertical illuminance (E_V) at the eye level. In order to investigate the reliability and the limitations of this glare control method, the DGPs was calculated over an entire year and the results during occupation hours were compared with the calculated Enhanced simplified DGP. The comparison was carried out for two shading systems; the simple white, aluminum venetian blind used in Chapter 5 and a grey, perforated venetian blind system.

6.1 Theoretical background

The Simplified DGP and the Enhanced simplified DGP

According to the definition by Wienold and Christoffersen [55], the DGP function consists of two terms; one referring to the vertical eye illuminance (*Term 1*) and the other to individual glare sources (*Term 2*), according to the Equation 6.1.

$$DGP = \underbrace{c_1 \cdot E_V}_{\text{Term 1}} + \underbrace{c_2 \cdot log(1 + \sum_i \frac{L_{s,i}^2 \cdot \omega_{s,i}}{E_V^{c_4} \cdot P_i^2}) + c_3}_{\text{Term 2}} \tag{6.1}$$

$$\begin{aligned} \text{Where:} \quad & c_1 = 5.87 \cdot 10^{-5} \\ & c_2 = 9.18 \cdot 10^{-2} \\ & c_3 = 0.16 \\ & c_4 = 1.87 \end{aligned}$$

Where: E_V refers to the vertical illuminance, $L_{s,i}$ to the luminance of the individual sources, ω_s to the solid angle of the source and P to the position index.

To calculate the DGP value within the current framework, a picture of the scene under investigation is generated for a specific moment and view direction, and is evaluated using Evalglare [56]. To reduce the long computational time required for the picture generation, the Enhanced simplified DGP can be used instead. In this simplified variation, only a simplified image is generated taking into account the

contribution of the main individual glare sources without calculating the exact luminance distribution within the room by reducing the ambient calculations in *Radiance*. The largest calculation time reductions can be achieved by leaving the ambient calculation completely out by setting the -ab option to 0. Although this option can be applied to non-scattering materials, such as venetian blinds, it might create complications for scattering materials such as fabrics [48].
The DGPs, which functions as the basis of the developed glare control strategy, reduces the computational time further by completely omitting the image generation and take only the vertical illuminance contribution into account. The simplified metric can be applied on each virtual sensor positioned at a view point of interest, provided that no direct radiation or specular reflections of sunlight reach the sensor (Equation 6.2).
In the case of the controller, all sensors are positioned on the working surface. According to the control algorithm, all direct radiation is prevented from reaching the work surface and specular reflections from the floor or other surfaces in the room are neglected. Although the simplified version of the DGP works satisfactorily on normal venetian blinds, it might fail in the case of more complicated systems such as specular or perforated blinds which cannot block the direct radiation or its specular reflections entirely.

$$\text{DGPs} = 6.22 \cdot 10^{-5} \cdot E_V + 0.184 \tag{6.2}$$

6.2 The simulation set-up

The shading systems

In the current comparison two shading systems have been used; a plain white venetian blind, modelled after the shading system described in Chapter 5, and a grey perforated venetian blind. The first system has already been extensively tested theoretically and experimentally and has performed satisfactorily under the simulation-based control. The perforated system, although similar as to the shape and the size of the slats, presents a more challenging subject. Due to the perforations the direct radiation is not entirely blocked coming into conflict with the *"no-direct-radiation"* condition necessary for the effectiveness of the glare control.
For the calculation of the DGPs for each shading system, a set of BSDFs for the entire fenestration system including the glazing was generated. Each set consisted of fourteen BSDFs, one per tilt angle from 0° to 65° with an angle step of 5°, plus one additional BSDF for the uncovered window. The BSDFs were generated using genBSDF as explained in Chapter 4. For generating the images necessary for the calculation of the Enhanced simplified DGP a set of *Radiance* geometries was generated, each representing the entire fenestration system for a specific tilt angle. Since the slat geometry of the two shading systems was the same, the only change made for the simulation of the Enhanced simplified DGP of the two systems was the *Radiance* material definition.
The material used for the white venetian blind was the same as described in the previous chapters. The perforated material of the second shading system was modelled with a *Radiance mixfunc* material as a mixture of *air* and *Radiance plastic*. The perforations were described by their dimensions, diameter and material thickness, and by the density of their distribution on the slat surface. The inter-reflections within the material depended on the ratio of the material thickness to the perforation diameter; however, for the described material the ratio was equal to one and the

Width (mm)	80
Thickness (mm)	0.05
Color	grey
Reflectance	0.62
Specularity	0.02
Perforated area (%)	8
Perforation diameter (mm)	0.05

TABLE 6.1: Perforated venetian blind parameters

inter-reflections were neglected. The angular dependency of the light transmission through the perforations was calculated trigonometrically taking into account the angle of incidence with a .cal file used within the material definition. The material properties of the perforated blinds are summarised in Table 6.1.

The simplified images used for the calculation of the Enhanced simplified DGP were generated with the *rpict* command in Radiance. The rendering parameters used are summarised in Table 6.2. Since the effect of excluding the ambient calculation was not clear in the case of the perforated venetian blinds, the influence of two different values of the -ab rendering parameter was investigated. The annual values of the Enhanced simplified DGP were calculated on the one hand using simplified images generated with no ambient calculation and on the other hand using images generated with the -ab value set to 1. The simulation model used the south-oriented shoebox geometry of Chapter 5 and a single virtual sensor in the middle of the room and 2 meters away for the window, positioned 1.2 meters over the floor, with view direction oriented towards south-west. The simulation time-step was set to one hour. The calculated Enhanced simplified DGP values for the two cases presented negligible differences for six time-steps over an entire year. Since no significant impact was observed by increased ambient bounces, -ab 0 was also used for the calculations related to the perforated venetian blinds.

Ambient bounces (-ab)	0
Direct jitter (-dj)	0
Relays for secondary sources (-dr)	2
Limit reflection (-lr)	4
Limit weight (-lw)	0.000001
Specular threshold (-st)	0.15
Pixel sample spacing (-ps)	0
Pixel sample jitter (-pj)	0
View type (-vt)	*a* (angular fisheye view)
View vertical size (-vv)	180
View horizontal size (-vh)	180
View up vector (-vu)	0 0 1
View shift (-vs)	0
View lift (-vl)	0

TABLE 6.2: Rendering parameters for the picture generation used for the calculation of the Enhanced simplified DGP calculation

The simulation model

As mentioned above, the simulation model used for this comparison is the same as the model described in Chapter 5. The building facade was south oriented and no surroundings were taken into account. No furniture was included in the room model. The view point was positioned in the middle of the room, 2 meters away from the window and 1.2 meters over the floor. For this view point, four different view directions were defined; two parallel to the window facing east and west and two more at 45° degrees towards the window facing south-east and south-west. The four view directions were used for the calculation of the vertical illuminance and for the generation of the 180° - HDR image.
For the calculation of the vertical illuminance two annual simulations were carried out; one for each shading system under the simulations parameters defined in Chapter 5. Based on the calculated vertical illuminances, the DGPs of each view direction was calculated for every time-step over the entire year. The corresponding Enhanced simplified DGP values were calculated using the vertical illuminance values of each view direction. The *Radiance* geometry used for the generation of the simplified images was defined by the controller at each time-step.

6.3 Simulation results

For the interpretation of the simulation results, the calculated values of the four virtual sensors representing the four assigned view directions are analysed for both shading systems in a way similar to the comparison of glare protection in Chapter 5. In this case, the values above the limit of 0.35 are additionally included, addressing the threshold of noticeable glare in order to express the differences between the values of the Enhanced simplified DGP and the DGPs in more detail. In Table 6.3 the total occupied hours annually that both metrics exceed 0.35 and 0.45 are summarised for both systems.
The 95 percentile used in Chapter 5 is calculated again for the evaluation of the occurring glare situations. However, it is used as the value of the enhanced simplified DGP and DGPs exceeded 5% of the time. The point of this is to underline the situations where the direct solar component is not properly blocked and the glare control fails. Such cases are mostly anticipated for the perforated venetian blind system which occasionally allows direct radiation to enter the room through the perforations. To better understand how the two shading systems affect the performance of the controller, the results of the two metrics are summarised in Table 6.4 for the four defined view directions
By a closer look at the results of both shading systems a number of observations concerning the set-up and the performance of the two systems is made. In Figure 6.1 and in Figure 6.2 the graphs present the comparison of the annual DGPs and Enhanced simplified DGP for the two most affected view directions, South-east and South-west, for the two investigated shading devices. It is evident that the performance of the controller is substantially better when the white venetian blinds are used. In this case, the percentage of occupied hours annually when the Enhanced simplified DGP values exceed 0.35 is 3% for the East and West oriented view sensors and increases by about 10% absolute value for the South-east and South-west view directions. The percentage of occupied hours affected by disturbing glare, or the Enhanced simplified DGP values exceeding 0.45, remains at a maximum of 4% at all view directions.

White venetian blinds				
	East	West	South-east	South-West
Simplified DGP ≥ 0.35	0%	0%	9%	9%
Simplified DGP ≥ 0.45	0%	0%	0%	0%
Enhanced simplified DGP ≥ 0.35	3%	2%	12%	13%
Enhanced simplified DGP ≥ 0.45	2.5%	2%	4%	4%
Perforated venetian blinds				
	East	West	South-east	South-West
Simplified DGP ≥ 0.35	0%	0%	15%	15%
Simplified DGP ≥ 0.45	0%	0%	0%	0%
Enhanced simplified DGP ≥ 0.35	14%	13%	44%	44%
Enhanced simplified DGP ≥ 0.45	8%	7%	21%	22%

TABLE 6.3: Percentage of occupation hours annually when the calculated Enhanced simplified DGP exceeds 0.35 and 0.45 for white venetian blinds and for perforated venetian blinds. The view sensor is positioned in the middle of the room, 2 meters away from the window and the four view directions are oriented towards East, West, South-east and South-west.

White venetian blinds				
	East	West	South-east	South-West
Enhanced simplified DGP exceeded 5% of the time	0.25	0.25	0.38	0.37
Simplified DGP exceeded 5% of the occupation time	0.25	0.24	0.38	0.37
Perforated venetian blinds				
	East	West	South-east	South-West
Enhanced simplified DGP exceeded 5% of the occupation time	0.49	0.48	0.61	0.59
Simplified DGP exceeded 5% of the occupation time	0.25	0.25	0.38	0.37

TABLE 6.4: Values of Enhanced simplified DGP and DGPs exceeded during 5% of the occupancy hours, for white venetian blinds and perforated venetian blinds. The view sensor is positioned in the middle of the room, 2 m away from the window and the four view directions are oriented towards East, West, South-east and South-west.

For the perforated blinds the controller performance is lower with substantially more hours of Enhanced simplified DGP values exceeding 0.35; 13% of the total occupation time at the least affected view directions and up to 44% for the South-east and South-west oriented sensors. Although these percentages drop to half for Enhanced simplified DGP values exceeding 0.45 at all orientations, they remain significantly higher than the corresponding values under the white venetian blind system. As far as the South-east and South-west oriented view directions are concerned, the results suggest that by using perforated blinds disturbing glare conditions are expected in the room for more than 20% of the occupied time.
By directly comparing the values in Table 6.4 corresponding to the highest 5% range of the DGPs and Enhanced simplified DGP, a large mismatch is observed in the case of the perforated blinds. This deviation is significant since it indicates that the controller fails to perceive situations of disturbing glare where the Enhanced simplified DGP exceeds the disturbing glare threshold of 0.45. In these situations, the corresponding DGPs values are only 0.25. On the other hand, the values of the DGPs and the Enhanced simplified DGP agree very well for the white venetian blinds.

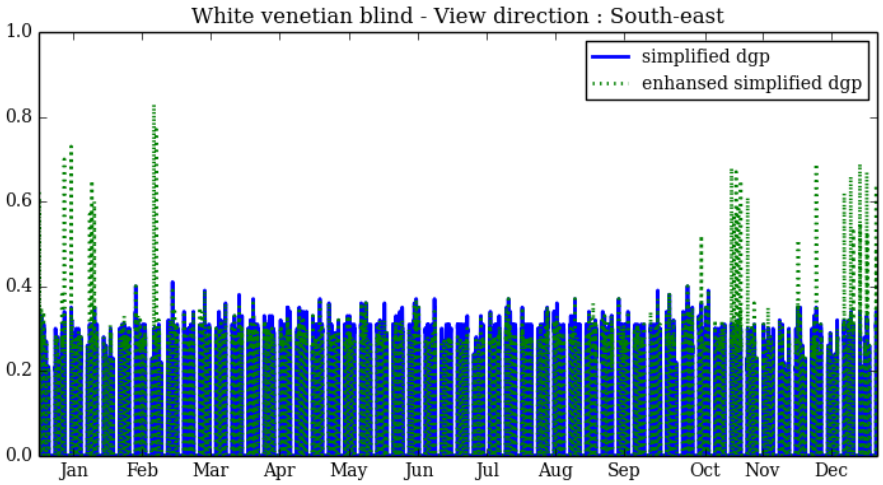

(a)

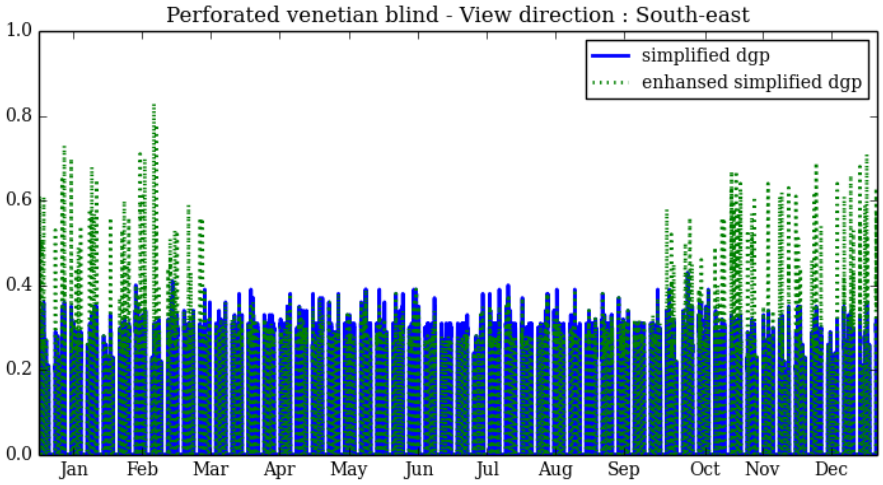

(b)

FIGURE 6.1: Comparison of DGPs and Enhanced simplified DGP for a virtual sensor located in the middle of the room and 2 m away from the window and view direction towards South-east for (a) a white venetian blind and (b) a grey perforated blind

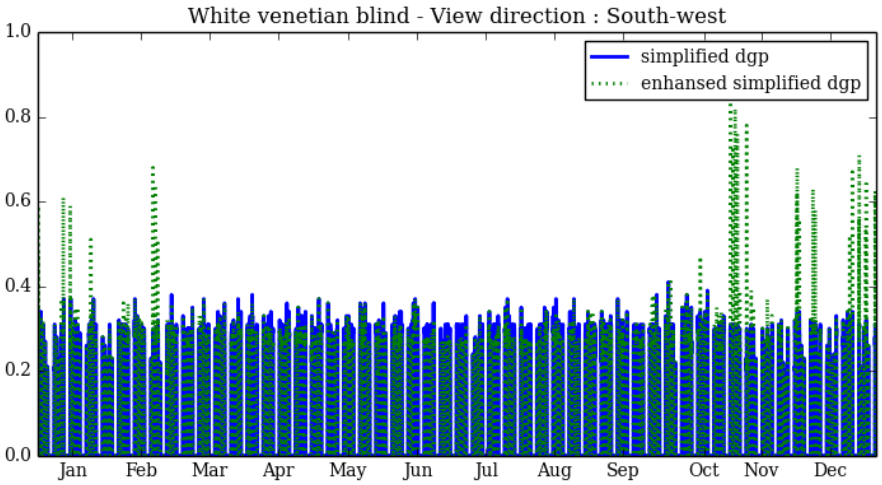

(a)

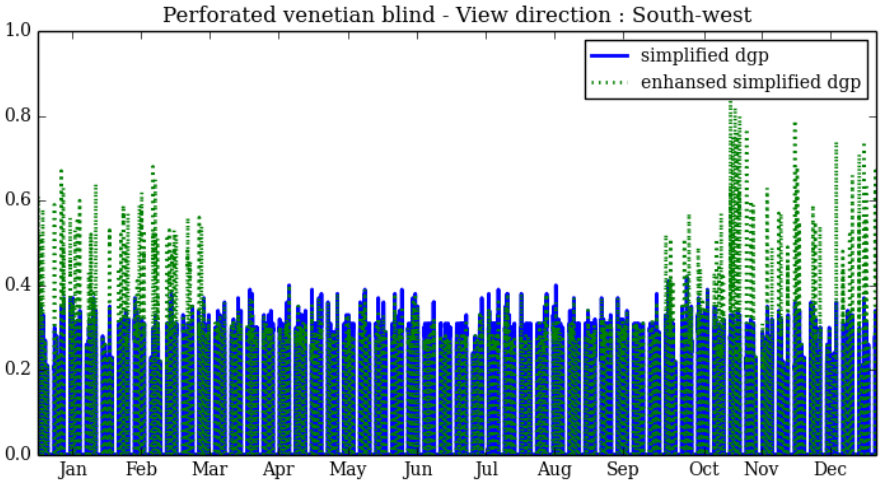

(b)

FIGURE 6.2: Comparison of DGPs and Enhanced simplified DGP for a virtual sensor located in the middle of the room and 2 m away from the window and view direction towards South-west for (a) a white venetian blind and (b) a grey perforated blind

6.4 Discussion

According to the simulation results, it can be concluded that the DGPs can sufficiently predict the glare conditions in the room when simple blinds are used. On the other hand, in the case of the perforated blinds a substantial mismatch between the Enhanced simplified DGP and the DGPs is observed, with the DGPs significantly under-predicting the glare conditions in the room. These deviations are a result of the inability of the DGPs to accurately predict the glare conditions when direct sun is found in the field of view since it only takes vertical illuminance into account. This assumption is in order with the findings of Konstantzos et al. [24] who, as mentioned in Chapter 1, investigated the correlation between DGP and vertical illuminance along with the applicability of DGP and DGPs for different shading devices. As they state in their work, the probability of glare occurring under the influence of even small amounts of direct radiation is high even for low vertical illuminance values due to the contrast term of DGP which substantially increases in the presence of glare sources such as the sun. As the DGPs is directly correlated to the vertical illuminance, the glare protection method designed for the controller is expected to fail for a perforated system.
For more common shading devices such as venetian blinds, the agreement between the DGPs and the Enhanced simplified DGP is very satisfactory. The results presented above suggest that the metric developed for the glare control algorithm of the controller is very promising for maintaining a comfortable visual environment within the room, with the DGP values remaining within the acceptable limits.
Closing, it is worth mentioning that the applicability of less common designs of shading devices is a rather complex matter that often requires individual photogoniometric measurements to investigate the light scattering properties of the device in question. Therefore, it is difficult to apply a general rule at this stage leaving open questions for further research.

Chapter 7

Conclusions

7.1 Overview

A simulation-based controller for venetian blinds and electric lights, adaptive to the user wishes was developed to address daylighting, glare protection and energy efficiency. Considerations such as thermal comfort and flexibility of the commissioning process were taken into account and the need of the user to maintain view contact to the outside and to influence the system's function was addressed. In this way, the controller aimed at providing solutions for the identified weaknesses of the existing control systems and at increasing the overall user acceptance. The structure of the system was designed to remain transparent in order to facilitate the monitoring and updating of the control process.
The daylight simulations were evaluated experimentally with a first prototype under laboratory conditions. The evaluation included situations of blinds at fixed tilt angles and of blinds at dynamically changing positions where both the system's extension length and tilt angle was adjusted during the controller's normal operation. In the first case, the agreement between the simulated and the measured illuminance for four different shade configurations was satisfactory according to the standards defined in literature, with the relative RMSE values remaining below 26% for the horizontal illuminance and 27% for the vertical. In the second case, five days in summer and five days in winter were examined. The agreement between the simulation results and the measurements was less accurate mainly due to imprecisions of the positioning of the venetian blinds resulting from the installed shading system. Nevertheless, the measured and the calculated values were found around 80% of the testing time within the same fuzzy areas defined in the optimisation process. Through this qualitative interpretation, the results were considered satisfactory for a first prototype operation. This analysis was considered more appropriate for the evaluation of comfort, the ambiguous nature of which can not be clearly expressed through absolute values. The deviations observed during the dynamic controller operation could be mitigated by using a newer and more accurate shading system.
A second prototype of the controller was installed at a real life office over an existing installation. The system was tested by a user uninvolved in the controller's development in order to provide an unbiased assessment. At the final evaluation questionnaire the user offered a positive feedback noting that the system was an improvement in comparison to the previously installed control system. However, it was stated that further improvements were possible in particular regarding the management of the activation time of the controller.
The potential benefits of the simulation-based control were investigated through its comparison with two popular shading control strategies. The comparison was based on annual simulations of a shoebox office in Germany operating as a typical office

in mid-European climate. Two orientations of high interest for this location were investigated; south and south-west. According to the simulation results, the controller performed better regarding glare protection at both orientations in comparison to the other two systems having only a small impact on the daylight admission. The view out was evaluated by comparing the geometrically-calculated window occlusion under different seasons of the year and times of the day. The average window occlusion was found slightly higher for the controller in comparison to the cut-off control, with the difference remaining in general below 5% at the south orientation and slightly higher at the south west. Larger deviations were only observed during the afternoon hours in the summer months. Regarding the energy demand, the controller presented a small increase of heating energy demand over the two other systems compensating with an important reduction of cooling and lighting energy demand. As a result, an overall reduction of the total annual energy demand was observed for the controller.
The three systems were further investigated in the presence of an obstruction in front of the building's facade assuming that the simulation model of the controller included the site surroundings. The simulation-based control and the radiation control reacted to the existence of the obstruction by reducing the window occlusion. As a result, both systems improved their daylight admission as opposing to the cut-off control that did not account for the obstruction.
To identify how the different model parameters describing the building surroundings impact the calculated illuminance in the building, an additional study was carried out for the south oriented facade. The horizontal and the vertical illuminance in the room were calculated under different parameter variations referring to the ground albedo, the obstruction geometry and position, and the obstruction reflectance. According to the difference between the resulting illuminance values and the reference case, the impact of the ground albedo on the daylight simulations was substantial and strongly dependent on the site and the climate of the simulated building. The geometry of the obstruction as well as its distance from the facade were found to have the highest influence on the calculated illuminance values. The influence of the optical properties of the obstruction was highly dependent on the obstruction's distance from the facade increasing rapidly with the proximity.
Finally, to evaluate the developed glare control method and to identify its limitations, the DGPs and the Enhanced simplified DGP for two shading devices were calculated and compared. The DGPs was used as an indicator of the controller-calculated glare conditions based on the vertical illuminance at a view point. The Enhanced simplified DGP acted as a reference case to identify the situations where the DGPs failed. According to this comparison, the developed glare control strategy worked reliably for simple venetian blinds but failed to adequately block glare for a perforated device. Therefore, it was concluded that the controller failed to prevent glare in the cases when the direct solar radiation was allowed in the field of view since its function took only vertical illuminance into account.

7.2 Potential of an optimised system

Shortly before closing, it is worth discussing the possible impact of the implementation of an optimised simulation-based control in commercial buildings. As presented in Chapter 5, for a central European climate the reduction of heating, cooling and lighting energy demand due to the controller in comparison to a cut-off and a radiation control strategy could reach up to 10% annually depending on the facade

orientation. Additionally, the ability of the simulation-based control to include the building surroundings and obstructions in the simulation model allowed it to adjust its operation and maintain its advantage over other control strategies as far as the visual comfort and the reduced energy demand were concerned. Although within the scope of this work only a single room with simplified surroundings and a single obstruction was investigated, one can estimate the corresponding effects of the controller applied on a larger scale at similar climatic conditions.
As an example, let us assume a multi-storey building with several offices in different orientations which encounter different surroundings, with a varying number of obstructions depending on the floor they are. Since the controller reactions are designed to apply individualised signals to every room, the shading configurations will differ depending on the orientation and the surroundings of the rooms to incorporate the corresponding effects. In this way, the overall solar heat gains and daylight are expected to be utilised in full at every part of the building increasing its overall efficiency.
For large scale applications, the installation of small weather stations providing weather data fast and reliably in real time for the entire building can significantly simplify the system commissioning. Since no additional sensors are required at the exterior of the building, an important material and cost reduction can be promised and any cabling interacting with the facade aesthetics can be avoided. As a direct result of the above, the maintenance of the installed system can be significantly simplified since all the sensors are localised at the weather station and only commonly used measurement devices remain inside the building.
It must be emphasised that the calculated energy corresponds to the demand of the controlled space and not to the energy consumption itself. It is therefore important to combine the simulation-based control with a HVAC control system in order to take full advantage of the offered energy reductions. As this assumption is only based on the case study carried out for a specific climate, one needs to further investigate the corresponding effects under different environmental conditions to fully understand the influence of the proposed system to the total energy demand.
Finally, the improved comfort conditions that the system promises due to the controller's adaptation, glare protection and improved view contact to the outside, even in the presence of external obstructions, is an important contribution to any application independently of its size. The significance of improving the indoor light conditions and personalising the controller's function to correspond to the user preferences is great since it enhances the user satisfaction. The satisfaction of the occupants reflects on their health and productivity and can be practically observed on the frequency and nature of their interaction with the system; satisfied users are less likely to deactivate or override the system.

7.3 Limitations

Having discussed about the benefits of the developed controller, it is necessary to also mention the limitations of the system. A major issue identified lies on the assumptions of the glare control which takes into account only the vertical illuminance at the eye level of the user and on the computer screen, under the condition that no direct sunlight or its specular reflections enter the view field. Although this assumption functions very well with simple venetian blinds, an incompatibility with a number of complex shading devices may occur if they fail to meet the *no-direct-light*

condition. For example, as has been shown in Chapter 6, by using a perforated venetian blind system the direct light at the view point can not be completely eliminated. Although for normally shaped slats the controller would act in the prescribed way, the effectiveness of the system would be compromised by the perforations of the material. Similar problems would be expected for blinds with redirecting properties when a specular surface is included. In this case, the controller algorithm would react incorrectly due to the inability of the system to include specular reflections within the field of view and evaluate glare accurately. Moreover, any light redirection properties of the system would not be taken into account leading to reduced daylight admission.
The answer to the question *"At which systems can the controller be applied?"* is rather complicated since it largely depends on the characteristics of each system. Therefore, to specify these limitations in a more definite way, further testing based on actual shading devices is necessary. It must be noted that using complex shading devices requires an accurate representation of the light transmission in the form of a BSDF which should be acquired through careful modelling or by the photogoniometric measurement of the system.
Another limitation of the system is the user adaptation which would be significantly complicated by increasing the number of interacting users. The exact number limitation can not be immediately specified due to the lack of testing references and the large number of parameters involved. Although the complexity introduced by multiple users might be reduced when their preferences converge, one should remain cautious when dealing with prediction of human behaviour.
Moreover, the applicability of the controller as a centralised system in large scale installations remains an open question. That limitation lies on the fact that the effectiveness of the controller depends on the accuracy of the model created for each individual space. Although the simulation set-up can be scaled up to account for open-plane offices with multiple windows, the uniform applicability of the simulation-based control on multiple spaces is opposing to its operation principles.
Last but not least, the inability of the system to detect operation errors due to the lack of light sensors in the room must be considered. As shown within this work, by building an accurate and detailed simulation model the daylight simulations can sufficiently predict the illuminance in the room providing a comfortable visual environment. However, possible changes of the installation site and its surroundings along with the degradation of the shading system after a long operation period have been also found to substantially affect the simulation accuracy. Therefore, in the absence of any light sensors in the room, calculation errors can not be detected compromising the system's effectiveness and raising a maintenance issue.

7.4 Discussion

The basic objectives of this thesis, as defined in Chapter 1, have been fulfilled. A simulation-based control algorithm was developed and assessed. The glare control was addressed in a simple, flexible and effective way taking into account both glare at the eyes of the user and haze at the computer screen. This method was proven adequate for simple venetian blinds; however, more complex shading systems require further investigation. The applicability of the system in real life was demonstrated by two prototype installations and its potential over existing systems was presented through a case study. The sensitivity, limitations and weaknesses of the system were identified, creating a solid theoretical background for future follow-ups.

Closing, it is important to mention a number of open questions regarding the improvement of the control algorithm and installation that would be worth investigating in the future. To begin with, while the visual comfort has been assessed in detail within this doctoral thesis, the thermal effects of the controller have not yet been addressed. The concept of overheating prevention included in the control algorithm should be investigated in comparison to other rooms with different shading control strategies in order to realistically assess the assumed benefits. Additionally, the energy efficiency potential of the controller during low occupancy periods must be assessed in combination with the monitoring of the lighting energy consumption and the consumption of the system itself throughout a year.
As stated by the test user of the second prototype, the current system can be further improved especially regarding its prescribed activation time during hours when the daylight conditions change rapidly, such as early morning and afternoon hours around sunset. To address this issue, hours of higher occurrence could be defined during which a different activation time-step or a more conservative tilt angle could be applied in advance to act preventively to the evolution of the solar position. Finally, the user adaptation requires further testing since there is no evidence that the user preferences would remain constant over different seasons. It would be interesting to observe whether the glare acceptance of the user is affected by the seasonal variations and in such a case, to consider the establishment of two separate sets of fuzzy set-points alternating between the winter and the summer period.
It is important to mention that a wider user assessment is necessary including users from different age ranges and backgrounds in order to investigate how different influences might affect the assessment of the system. A necessary condition for a large scale testing is the re-designing and standardisation of the electric installation. Such an installation should include widely available commercial components to increase its compatibility with any already installed systems. Moreover, a validation method applied during the commissioning process should be developed combined with an error detection scheme for the long term use of the system. Regarding the user acceptance, the development of a user friendly interface would be an important contribution to the system making the user interactions easier and act as a two-way communication to provide instant feedback of the user preferences.
Finally, an interesting possibility is to investigate the controller's behaviour in cases of large rooms or open plane offices. Such a test case would provide the opportunity to evaluate the assumption of a flexible illuminance sensor grid definition and identify its limitations. Moreover, by installing the controller in open plane spaces the independent control over different windows for the optimisation of the visual conditions could be also tested.
It is evident that this work is only the first step on a very interesting and promising application of daylight simulations. Much work still remains to be done and only extensive testing through longer time periods can answer the open questions formulated above. Nevertheless, this work functions as a proof of concept providing a theoretical background for the implementation of daylight simulations in a real-time controller and an alternative approach of glare control and visual comfort. Therefore, this work can function as a stepping stone in the future aiming at the development of a commercial building automation.

Appendix A

Venetian blind position based on the solar angles

A.1 Cut-off angle

Both the simulation-based control and the cut-off control introduced in Chapter 5 are using the *cut-off angle* to define the tilt angle of the venetian blind; although, in the case of the simulation-based control the tilt angle might be afterwards re-adjusted to improve the visual comfort in the room. The idea behind the cut-off control is to calculate the minimum tilting of the slats depending on the solar azimuth and altitude to only block the direct solar radiation from entering the room (Figure A.1).

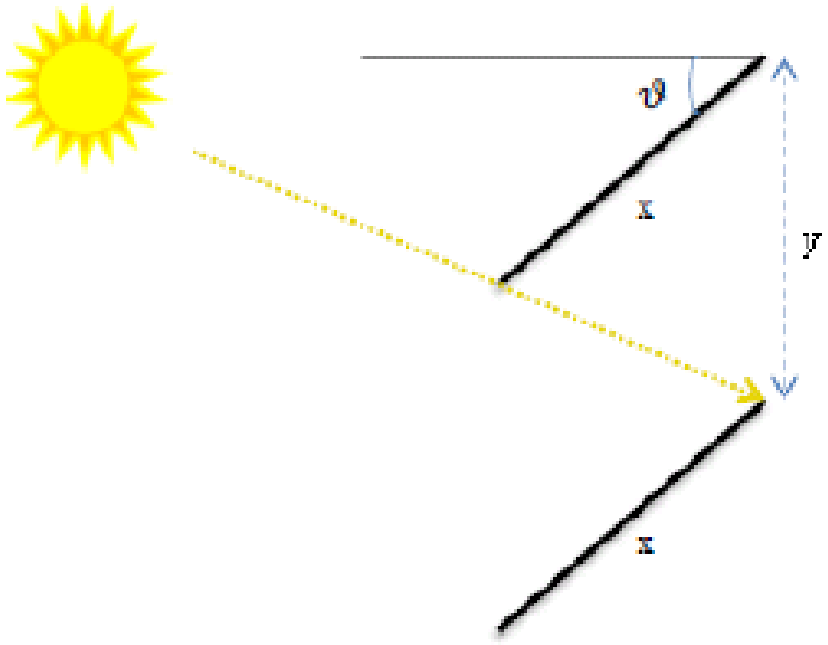

FIGURE A.1: Side view of two slats tilted at the cut-off angle.

The cut-off angle of the slats depends at a specific moment in time on the solar profile angle. The profile angle is defined as the angular difference between the horizontal plane perpendicular to the window and the plane tilted about the horizontal axis in order to include the sun (Figure A.2). The profile angle (β) is calculated through the Equation A.1.

$$\beta = \arctan(\frac{\tan\alpha}{\cos(\gamma - \delta)}) \tag{A.1}$$

Where: α refers to the solar altitude, γ to the solar azimuth and δ to the surface azimuth angle.

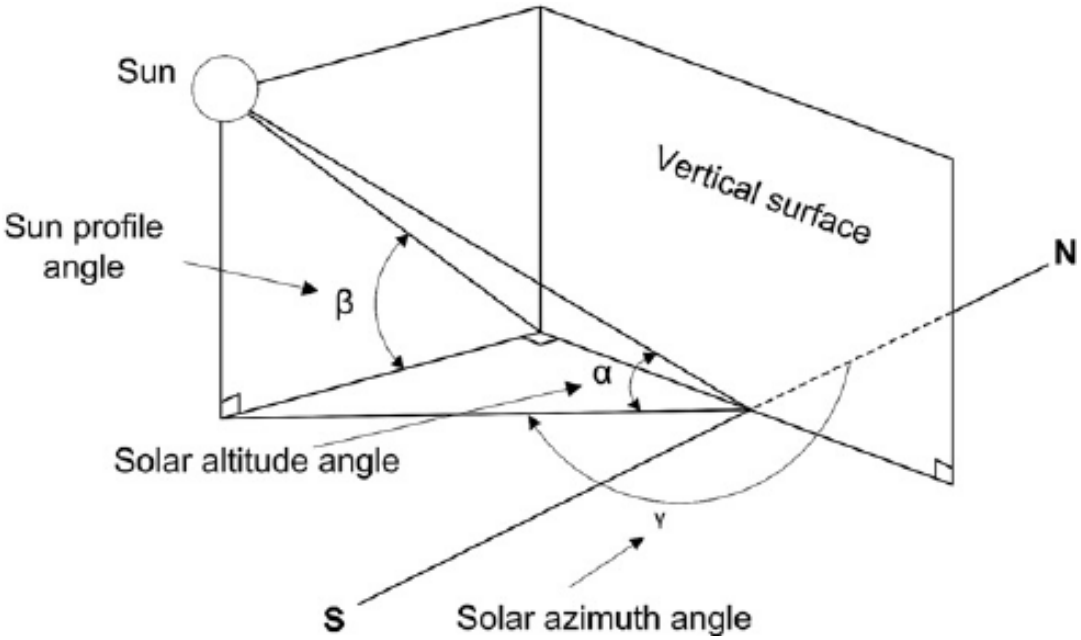

FIGURE A.2: Representation of solar angles in respect to a vertical surface with a south orientation

The cut-off angle (θ) is calculated as a function of the blind width, the distance between two blinds and the solar profile through Equation A.2:

$$\theta = \arcsin(y \cdot \frac{cos\beta}{x}) - \beta \tag{A.2}$$

Where: y is the distance between two blinds, x is the width of the slats and β is the solar profile angle as calculated in Equation A.1.

A.2 Minimum height shading device

The minimum height of the shading device refers to the distance to which the device must be extended to prevent any direct radiation from reaching the work surface (Figure A.3). To calculate this distance, a simple geometric formula is extracted based on the room and furniture characteristics and on the solar profile angle. In the following expression (Equation A.3), H refers to the height the blind needs to be extended, h_{window} to the height of the window, h_{wall} to the height of the window over the floor, h_{ws} to the height of the working surface over the floor, l to the distance of the working surface from the window and β to the profile angle calculated above.

$$H = h_{wall} + h_{window} - h_{ws} - l \cdot tan\beta \tag{A.3}$$

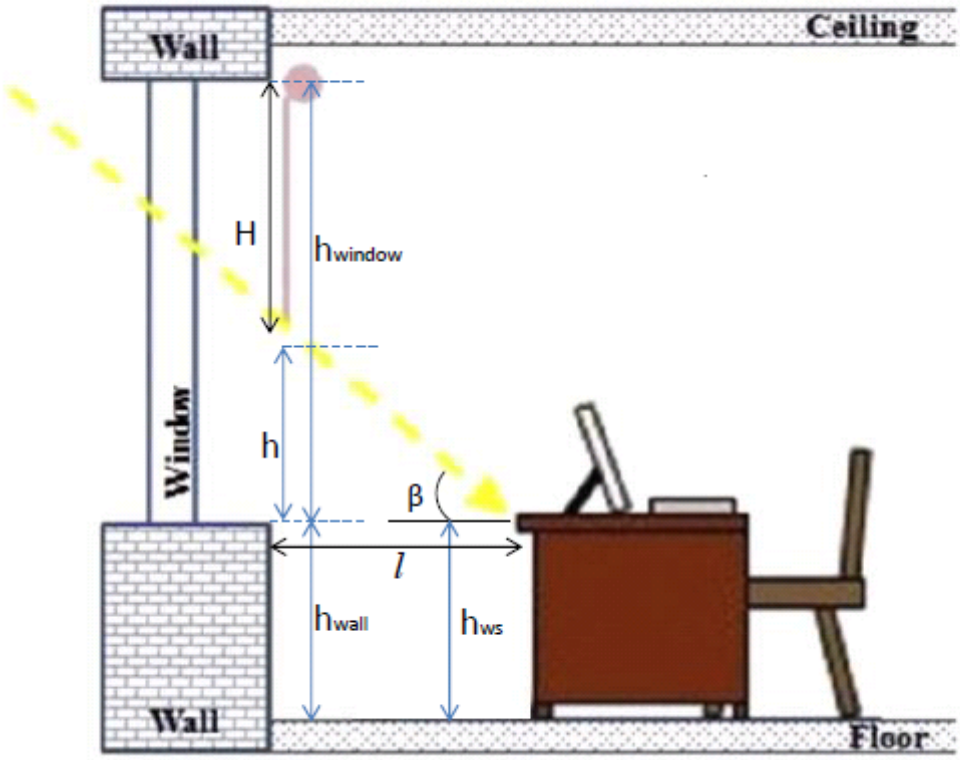

FIGURE A.3: Minimum distance that the shading device must be extended to prevent direct radiation from reaching the working surface

Appendix B

Rule-based algorithm matrix

Case	Occupancy	Daytime	Ext. temp. >18 °C	Ext. temp. <8 °C	Indoor temp.	Global rad. >500 W/m^2	Pos.
1	1	0	1	0	Any	0	Open
2	1	0	0	1	Any	0	Open
3	1	0	0	0	Any	0	Open
4	1	1	1	0	< 24°C	Either	Tilt blinds Variable height
5	1	1	1	0	> 24°C	0	Tilt blinds Variable height
6	1	1	1	0	> 24°C	1	Tilt blinds Fully extended
7	1	1	0	Either	> 26°C	1	Tilt blinds Fully extended
8	1	1	0	Either	> 26°C	0	Tilt blinds Variable height
9	1	1	0	Either	< 26°C	Either	Tilt blinds Variable height
10	0	0	1	0	Any	0	Open
11	0	0	0	1	Any	0	Closed
12	0	0	0	0	> 25°C	0	Open
13	0	0	0	0	< 25°C	0	Closed
14	0	1	1	0	Any	Either	Closed
15	0	1	0	1	Any	Either	Open
16	0	1	0	0	> 25°C	Either	Closed
17	0	1	0	0	< 25°C	Either	Open

TABLE B.1: Control algorithm decision matrix

Appendix C

User Questionnaires

C.1 First questionnaire - Beginning of the testing period

1. **How satisfied are you from the current shading control in your office?**

   ☐ Very satisfied
   ☐ Somewhat satisfied
   ☐ Neutral
   ☐ Somewhat dissatisfied
   ☐ Very dissatisfied

2. **In case of dissatisfaction, could you give specific reasons?**

3. **How satisfied were you by the daylight in the room due to the current shading control?**

   ☐ Very satisfied
   ☐ Somewhat satisfied
   ☐ Neutral
   ☐ Somewhat dissatisfied
   ☐ Very dissatisfied

4. **How satisfied were you by the glare protection due to the current shading control?**

   ☐ Very satisfied
   ☐ Somewhat satisfied
   ☐ Neutral
   ☐ Somewhat dissatisfied

- ☐ Very dissatisfied

5. **Do you consider the room temperature uncomfortably high during summer?**
   - ☐ No
   - ☐ Yes
6. **How would you characterize the frequency the current control adjusts the shading device?**
   - ☐ Too often
   - ☐ Just fine
   - ☐ Not often enough
7. **When the current control adjusts the shading system, is the reason obvious to you?**
   - ☐ Yes
   - ☐ Sometimes
   - ☐ Not at all
8. **Do you believe that the actions of the current control contribute to the improvement of the conditions in the room?**
   - ☐ Yes
   - ☐ Sometimes
   - ☐ Not at all
9. **What would you expect from the prototype controller?**

C.2 Second questionnaire - End of the testing period

1. **How satisfied were you by the daylight in the room due to the prototype shading control?**

   ☐ Very satisfied
   ☐ Somewhat satisfied
   ☐ Neutral
   ☐ Somewhat dissatisfied
   ☐ Very dissatisfied

2. **How satisfied were you by the glare protection due to the prototype shading control?**

   ☐ Very satisfied
   ☐ Somewhat satisfied
   ☐ Neutral
   ☐ Somewhat dissatisfied
   ☐ Very dissatisfied

3. **How satisfied were you by the thermal comfort due to the prototype shading control?**

   ☐ Very satisfied
   ☐ Somewhat satisfied
   ☐ Neutral
   ☐ Somewhat dissatisfied
   ☐ Very dissatisfied

4. **Do you consider the room temperature uncomfortably high during summer?**

   ☐ No
   ☐ Yes

5. **How would you characterize the frequency the prototype controller adjusts the shading device?**

   ☐ Too often
   ☐ Just fine
   ☐ Not often enough

6. **How would you characterize the performance of the prototype controller in comparison to the previous system?**

   ☐ Better
   ☐ Same
   ☐ Worse

7. **Which improvements of the prototype system would you propose?**

Bibliography

[1] D.Arnold. "The evolution of modern office buildings and air conditioning". In: *ASHRAE Journal* (June 1999), pp. 40–54.

[2] *www.ec.europa.eu*.

[3] E.Ne'eman, W. Light, and R.G.Hopkinson. "Recomendations for the admission and control of sunlight in buildings". In: *Building and Environment* 11 (1976), pp. 99–101.

[4] D.R.G. Hunt. "The use of artificial lighting in relation to daylight levels and occupancy". In: *Building and Environment* 14 (1979), pp. 21–33.

[5] U.S.Choi, R.Johnson, and S.Selkowitz. "The impact of daylighting on peak electrical demand". In: *Energy and Buildings* 6.4 (1984), pp. 387–399.

[6] P.T.Stone. "The effects of environmental illumination on melatonin, bodily rythms and mood states". In: *Lighting Research and Technology* 31.3 (2000), pp. 71–79.

[7] L.Heshcong. "Daylight and human performance". In: *ASHRAE Journal* (June 2002), pp. 65–67.

[8] P.Boyce, C.Hunter, and O.Howlett. "The benefits of daylight through windows". In: *Troy, NY:Rensselaer Polytechnic Institute* (Sept. 2003).

[9] J.Choi, L.O.Beltran, and H.Kim. "Impacts of indoor daylight environments on patient average length of stay (ALOS) in a health care facility". In: *Building and Environment* 50 (2012), pp. 65–75.

[10] M. Velds. "Assessment of lighting quality in office rooms with daylighting systems". PhD thesis. Technical University Delft, Jan. 2000.

[11] M.S.Rea. "Window blind occlusion: A pilot study". In: *Building and Environmentnvironment* 19.2 (1984), pp. 133–137.

[12] M.Foster and T.Oreszczyn. "Occupant control of passive systems: the use of Venetian". In: *Building and Environment* 36 (2001), pp. 149–155.

[13] P.C.deSilva, V.Leal, and M.Andersen. "Occupants interaction with electric lighting and shading systems in real single-occupied offices: Results from a monitoring campaign". In: *Building and Environment* 64 (2013), pp. 152–168.

[14] S. Coldicutt and T.Williamson. "Concepts of solar energy use for climate control in buildings". In: *Energy Policy* 20.9 (Sept. 1992), pp. 825–835.

[15] M.Santamouris et al. "Energy characteristics and savings potential in office buildings". In: *Solar Energy* 52.1 (1994), pp. 59–66.

[16] T.E.Kuhn, C.Bühler, and W.J.Platzer. "Evaluation of overheating protection with sun-shading systems". In: *Solar Energy* 69.1 (2000), pp. 59–74.

[17] T.Inoue et al. "The development of an optimal control system for window shading devices based on investigations in office buildings". In: *ASHRAE Trans* 94 (1988), pp. 1034–1049.

[18] S.Zhang and D.Birru. "An open-loop venetian blind control to avoid direct sunlight and enhance daylight utilization". In: *Solar Energy* 86 (2012), pp. 860–866.

[19] S.Y.Koo, M.S.Yeo, and K.W.Kim. "Automated blind control to maximize the benefits of daylight in buildings". In: *Building and Environment* 45 (2010), pp. 1508–1520.

[20] E.S.Lee, D.L.DiBartolomeo, and S.E.Selkowitz. "Thermal and daylighting performance of an automated venetian blind and lighting system in a full-scale private office". In: *Energy and Buildings* 29 (1998), pp. 47–63.

[21] E.S.Lee and S.E.Selkowitz. "The New York Times Headquarters daylighting mockup: Monitored performance of the daylight control system". In: *Energy and Buildings* 38 (2006), pp. 914–929.

[22] E.S.Lee et al. *Commissioning and verification procedures for the automated roller shade system at The New York Times Headquarters, New York*. Tech. rep. Laurence Berkley National Laboratory, May 2007.

[23] M.H.Oh, K.H.Lee, and J.H.Yoon. "Automated control strategies of inside slat-type blind considering visual comfort and building energy performance". In: *Energy and Buildings* 55 (2012), pp. 728–737.

[24] I.Konstantzos, A.Tzempelikos, and Y.C.Chan. "Experimental and simulation analysis of daylight glare probability in offices with dynamic window shades". In: *Building and Environment* 87 (2015), pp. 244–254.

[25] M.T.Lah et al. "Daylight illuminance control with fuzzy logic". In: *Solar Energy* 80 (2006), pp. 307–321.

[26] V.Čongradac et al. "Algorithm for blinds control based on the optimization of blind tilt angle using a genetic algorithm and fuzzy logic". In: *Solar Energy* 86 (2012), pp. 2762–2770.

[27] A.I.Dounis et al. "Design of a fuzzy set environment comfort system". In: *Energy and Buildings* 22 (1995), pp. 81–87.

[28] D.Daum and N.Morel. "Identifying important state variables for a blind controller". In: *Building and Environment* 45 (2010), pp. 887–900.

[29] D.Kolokotsa. "Comparison of the performance of fuzzy controllers for the management of the indoor environment". In: *Building and Environment* 38 (2003), pp. 1439–1450.

[30] Y.C.Chan and A.Tzempelikos. "Efficient venetian blind control strategies considering daylight utilization and glare protection". In: *Solar Energy* 98 (2013), pp. 241–254.

[31] J.Xiong and A.Tzempelikos. "Model-based shading and lighting controls considering visual comfort and energy use". In: *Solar Energy* 134 (2016), pp. 416–428.

[32] E.Vine et al. "Office worker response to an automated venetian blind and electric lighting system: a pilot study". In: *Energy and Buildings* 28 (1998), pp. 205–218.

[33] L.G.Bakker et al. "User satisfaction and interaction with automated dynamic facades: A pilot study". In: *Building and Environment* 78 (2014), pp. 44–52.

[34] A.Guillemin and S.Molteni. "An energy-efficient controller for shading devices self-adapting to the user wishes". In: *Building and Environment* 37 (2002), pp. 1091–1097.

[35] H.B. Gunay et al. “Development and implementation of an adaptive lighting and blinds control algorithm”. In: *Building and Environment* 113 (2017), pp. 185–199.

[36] David Lindelöf. “Bayesian optimization of visual comfort”. PhD thesis. École Polytechnique Fédérale de Lausanne (EPFL), Nov. 2007.

[37] C.Schierz, C.Vandahl, and P.W.Schmits. *Evaluation zur Störung der Anzeigen von LCD-Bildschirmen durch die Beleucthung*. Tech. rep. Gesetzliche Unfallversicherung VBG, Mar. 2012.

[38] DIN Deutsches Institut für Normung e.V. “DIN V 18599, Energy Efficiency of Buildings - Calculation of the Net, Final and Primary Energy Demand for Heating, Cooling, Ventilation, Domestic Hot Water and Lighting.” In: *Beuth Verlag* Parts 1-10 (2007-02-01 edition).

[39] B.Bueno et al. “Fener: A Radiance-based modelling approach to assess the thermal and daylighting performance of complex fenestration systems in office spaces”. In: *Energy and Buildings* 94 (2015), pp. 10–20.

[40] A.McNeil and E.Lee. “A validation of the Radiance three-phase simulation method for modeling annual daylight performance of optically-complex fenestration systems”. In: *Journal of Building Performance Simulation* (2012), pp. 1–14.

[41] J.H. Klems. “A new method for predicting the solar heat gain of complex fenestration systems:I.Overview and derivation of the matrix layer calculation”. In: *ASHRAE Trans* 100.1 (1994a), pp. 1065–1072.

[42] J.H. Klems. “A new method for predicting the solar heat gain of complex fenestration systems:II. Detailed description of the matrix layer calculation”. In: *ASHRAE Trans* 100.1 (1994b), pp. 1073–1086.

[43] G.Ward et al. “Simulating the daylight performance of complex fenestration systems using bi-directional scattering distribution functions within Radiance”. In: *Leukos, Journal of the Illuminating Engineering Society of North America* 7.4 (Apr. 2011), pp. 241–261.

[44] R.Perez, R.Seals, and J.Michalsky. “All weather model for sky luminance distribution-Preliminary configuration and validation”. In: *Solar Energy* 50.3 (1993), pp. 235–245.

[45] C. Reinhart and O. Walkenhorst. “Dynamic RADIANCE-based daylight simulations for a full-scale test office with outer venetian blinds”. In: *Energy and Buildings* 33.7 (2001), pp. 683–697.

[46] G.Ward and R.Shakespeare. *Rendering with Radiance: The Art and Science of Lighting Visualisation*. San Francisco: Morgan Kaufmann, 1998.

[47] L.A.Zadeh. “Fuzzy Sets”. In: *Information and Control* 8 (1965), pp. 338–353.

[48] J. Wienold. “Daylight glare in offices”. PhD thesis. University of Karlsruhe (TH), July 2009.

[49] DIN-EN:12464-1. *”Licht und Beleuchtung-Beleuchtung von Arbeitsstätten”, Teil1: ”Arbeitsstätten in Innenräumen”*. Norm. Aug. 2011.

[50] S.H.A. Begemann, G.J. van den Beld, and A.D.Tenner. “Daylight, artificial light and people in office environment overview of visual and biological responses”. In: *International Journal of Industrial Ergonomics* 20 (1997), pp. 231–239.

[51] A.McNeil et al. "A validation of a ray-tracing tool used to generate bi-directional scattering distribution function for complex fenestration systems". In: *Solar Energy* 98 (2013), pp. 404–414.

[52] A. Roos et al. "Angular dependent optical properties of low-e and solar control windows simulations versus measurements". In: *Solar Energy* 69.Supplement 6 (2001), pp. 15–26.

[53] C.F. Reinhart and P.F. Breton. "Experimental validation of 'Autodesk 3ds Max Design 2009 and Daysim 3.0." In: *Leukos, Journal of the Illuminating Engineering Society of North America* 6.1 (2009), pp. 7–35.

[54] B.Bueno, J.M. Cejudo-Lopez, and T.E.Kuhn. "A general model to evaluate the thermal impact of complex fenestration systems in building zones". In: *Energy and Buildings* 155 (2017), pp. 43–53.

[55] J.Wienold and J.Chritoffersen. "Evaluation methods and development of a new glare prediction model for daylight environments with the use of CCD cameras". In: *Energy and Buildings* 38 (2006), pp. 743–757.

[56] J. Wienold. *Evalglare: a new RADIANCE-based tool to evaluate glare in office spaces*. 3rd International Radiance Workshop, Fribourg, CH. 2004.